NTNU – Trondheim
Norwegian University of
Science and Technology

DC/DC Converters for Multi-terminal HVDC system for Integrating Offshore Wind Farms

Shihabudheen Kavungal Kolparambath

Wind Energy
Submission date: July 2015
Supervisor: Elisabetta Tedeschi, ELKRAFT
Co-supervisor: Pavol Bauer, Delft University of Technology
Jon Are Suul, SINTEF Energy Research

Norwegian University of Science and Technology
Department of Electric Power Engineering

Master Thesis of Science

DC/DC Converters in Multi-terminal HVDC System for Integrating Offshore Wind Farms

Shihabudheen Kavungal Kolparambath

22.07.2015

European Wind Energy Master - EWEM- Electrical Power system Track

DC/DC Converters in Multi-terminal HVDC System for Integrating Offshore Wind Farms

Master of Science Thesis

For obtaining the degree of Master of Science in Electrical Engineering at Delft University of Technology and in Technology-Wind Energy at Norwegian University of Science and Technology.

Shihabudheen Kavungal Kolparambath

22.07.2015

European Wind Energy Master - EWEM
Norwegian University of Science and Technology
Delft University of Technology

European Wind Energy Master - EWEM
Of
Electrical Power system Track

The undersigned hereby certify that they have read and recommend to the European Wind Energy Master - EWEM for acceptance a thesis entitled **"DC/DC Converters in Multi-terminal HVDC System for Integrating Offshore Wind Farms"** by **Shihabudheen Kavungal Kolparambath** in partial fulfillment of the requirements for the degree of **Master of Science**.

Dated: 22.07.2015

Supervisor: _____
Prof. dr. ir. Pavol Bauer of TU Delft

Supervisor: _____
Prof. Elisabetta Tedeschi of NTNU Trondheim

Reader: _____
dr. ir. Henk Polinder of TU Delft

Abstract

The development of far-offshore wind farms and other large-scale renewable energy sources, together with the increasing needs for long distance power transmission is resulting in more HVDC systems being integrated into the traditional AC power network. Due to the capability for operation in isolated AC grids, VSCs are becoming the preferred technology for HVDC systems. Additionally, VSC HVDC allows for more flexible power control within a network than the conventional LCC systems. Moreover, the need for flexible transmission capacity to balance fluctuating power generation from renewable sources over wide geographical areas combined with the corresponding potential benefits in a deregulated power market is expected to favour the concept of VSC based Multi-terminal HVDC system (MTDC).

MTDC provides enhanced reliability and functionality and reduces the cost and conversion losses. However, most HVDC transmission schemes are currently constructed as point-to point connections, and there is not yet any clear standardization of voltage levels. Thus, DC/DC converters will become necessary if existing or emerging HVDC links operating with different voltages and different configurations. i.e. monopolar and bipolar should later be interconnected into MTDC configurations. DC/DC converters might also be needed for power flow control in meshed MTDC grids.

The goal of this thesis is to summarize the requirements for DC/DC converters in HVDC applications and focus on the modelling and control of DC/DC converters for various applications. The modelling includes both switching and average models. Four types of DC/DC converters intended for different applications are modelled using MATLAB/ Simulink® platform. The functionality of the developed models are demonstrated by simulations in MTDC grid based on the CIGRÉ B4 DC grid test system.

Acknowledgements

First and foremost, praises and thanks to the God, the Almighty, for His showers of blessings throughout my studies and thesis work to complete it successfully.

My deepest gratitude goes to my supervisors, Prof. Elisabetta Tedeschi, NTNU Trondheim and Prof. Pavol Bauer, TU Delft. It is an honour and a pleasure for me to have these great people as my supervisors. I am grateful for their generosity to share their deep understanding on scientific work.

It is also a privilege for me to have Dr. Jon Are Suul, as my co-supervisor. You have laid the foundation and supported me in uncertain times, and been there for me when I had questions. My acknowledgement also goes to Dr. G Bergna-Diaz, employee at SINTEF Energy, who provided me with the necessary simulation models and always been available for explanations of difficult questions.

I express my sincere gratitude to EWEM-EPS coordinators, Dr. ir. Henk Polinder, TU Delft and Prof. Olav B. Fosso, NTNU Trondeim for helping and supporting me in my entire master studies at 3 universities. A big thanks to Ms. Linda Gaffel and Ms. Zarah Glaap, who answered all my queries related to the studies. I wouldn't have ended up here without the Erasmus EWEM programme. Special thanks to European Union for providing me all the financial assistance through the Erasmus Mundus Scholarship.

Last but not the least, I owe more than thanks to my EWEM friends and my family members, including my parents and my girl Ms. Rouzana aka Malutty, without them, this would have been impossible.

Trondheim, Norway
22.07.2015

Shihabudheen Kavungal Kolparambath

Contents

List of Figures

List of Tables

List of Acronyms

AC	Alternating Current
AVM	Average Value Models
CIGRÉ	Conseil International des Grands Réseaux Électriques
DC	Direct Current
GTO	Gate Turn-Off
HVAC	High Voltage Alternating Current
HVDC	High Voltage Direct Current
IGBT	Insulated Gate Bipolar Transistor
LCC	Line Commutated Converter
MMC	Modular Multi-level Converter
MTDC	Multi-terminal Direct Current
PI	Proportional-Integral
PLL	Phase Locked Loop
PWM	Pulse Width Modulation
VSC	Voltage Source Converter
2Q	Two Quadrant
4Q	Four Quadrant

Chapter 1

Introduction

This chapter describes the background and motivation for the thesis. The objectives and the contributions, as well as the thesis outline are also presented.

1.1 Background

Utilization of energy from renewable sources like hydro, wind and solar is the only sustainable solution for meeting the increasing energy demand of a growing population while facing the challenges of global climatic changes. Wind energy is one among the most promising renewable energy and more focus is moving towards offshore wind farms. Recent energy statistics show a rapidly increasing utilisation of offshore wind. The annual and cumulative offshore wind farm installation for the period 1993-2014 for Europe is shown in the Fig. 1.1 [1].

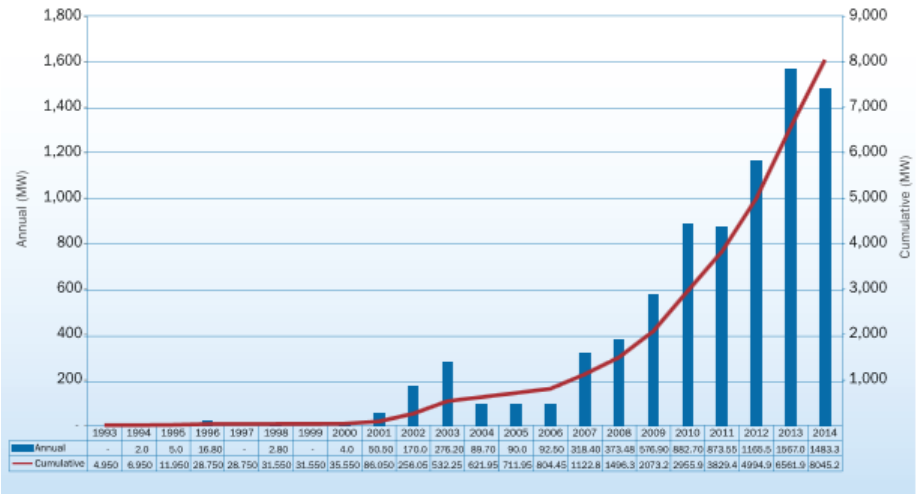

Figure 1.1: *Cumulative and Annual offshore wind farm installation(MW)[1]*

As evident from the Fig. 1.1, until 2014, nearly 8 GW of installed capacity was achieved in Europe, but the total installations are expected to increase in a dramatic way to around 40 GW by 2020 [2]. However, traditional HVAC transmission between offshore generation and onshore load centres is not suitable in case of long distances and wind farms located far offshore, due to the high cable charging capacitance, which reduces the active current capability of long ac cables. Thus, long distance HVAC transmission through subsea cables will lead to high cable losses and requirements for reactive power compensation [3]. These challenges can be avoided by HVDC systems, which can ensure higher transmission capacity, reduced losses and improved local system stability with no problem of reactive power control. For the same power transmission, previous studies show that the DC cable losses are nearly 30-50% less as compared to three phase AC system [4], although the losses and cost of the converter stations need to be taken into account when assessing the overall transmission scheme.

VSC based HVDC systems can operate in weak and islanded AC systems and allow for DC power flow reversal without changing voltage polarity. Thus, VSC HVDC is a more flexible solution than conventional LCC based HVDC and is seen as the enabling technology for the implementation of multi-terminal HVDC grids. In this perspective, a future European Supergrid is envisioned as a VSC-based HVDC grid, interconnecting various European countries and neighbouring regions, while providing power corridors for North Sea wind power generation, solar power plants in North Africa and hydro generation in Norway. Such a HVDC transmission system will consist of a meshed DC grid with many connections between AC and DC systems [5].

Suitable converter topologies for interconnecting AC and DC systems, with various corresponding control philosophies, have already been analyzed [6] - [7]. However, a future HVDC grid is expected to emerge through a gradual development where point-to-point connections can later be connected into multi-terminal, meshed, configurations. If independent HVDC links operating with different voltage levels and/or different configurations should be connected, high power high voltage DC/DC conversion systems are required. Additionally, the need for power flow control when there is a risk of cable overloading in specific network sections, require the introduction of DC/DC converters. Such DC/DC converters for HVDC applications are not as mature as for low voltage applications where a wide range of topologies are well established for suiting different voltage ratios and power ratings. Furthermore, the interconnection of HVDC systems, operating at different voltages with variable configurations cannot rely on a single DC/DC converter topology.

1.2 Objective

With the above background, this work focuses on detailed analysis of high voltage DC/DC converters for various applications. The main objectives of the thesis are

- Investigate the significance of DC/DC converters in MTDC grids.
- Review various DC/DC converter topologies for HVDC applications.

- Design, modelling and control of DC/DC converters suitable for power flow control in an MTDC grid.
- Design, modelling and control of DC/DC converter suitable for interconnecting independent HVDC systems into MTDC grid.
- Implementation of DC/DC Converters into the CIGRÉ B4 DC grid test system [8] and verification of overall system performance.

In addition to switching model of the converters, the modelling includes average model also for reducing the simulation time of large systems and for design of controllers.

1.3 Contributions

The thesis aims to provide an extensive idea on significance of DC/DC converters in future MTDC grids. The major contribution of the work is revising various topologies of high voltages DC/DC converters for such application including design, modelling and control of two classes of DC/DC converters for different scopes. Furthermore, the work also involved modelling of an MTDC grid composed of AC networks, DC networks with both monopolar and bipolar configurations, AC/DC converters and DC/DC converters.

1.4 Thesis Structure

The chapters of thesis are organised as follows.

- **Chapter 2** presents the general introduction about HVDC systems starting with a comparison of HVDC with HVAC system and then giving general description on various converter technologies used in HVDC and various HVDC configurations. It further discusses the significance of MTDC system and common configurations of MTDC system. The chapter ends with the presentation of DC/DC converter concept and its importance in an MTDC system.
- **Chapter 3** investigates the first class of DC/DC converters, i.e, DC/DC without galvanic separation. A general overview on DC/DC converters discussed in the literature is presented before particular attention is dedicated to two types of converters i.e, 4Q converter and Front-to-front DC/AC/DC converters. Both the converters are analysed in detail including design, modelling and control. The switching and average model of the converters are also discussed and implemented. The chapter ends with the results obtained from simulation.
- **Chapter 4** discusses the second class of DC/DC converters, i.e, galvanically separated DC/DC converters. Converters suitable for interconnecting DC systems with different voltages and dissimilar configurations are separately addressed. This includes modelling, control strategy, design of coupling transformer and transformer connections. The results with both switching and average models are reported at the end of the chapter.

- **Chapter 5** demonstrates the functionality of all the converters discussed in the previous chapters on CIGRÉ B4 HVDC Grid System, an MTDC system composed of AC and DC grids. A detailed description of CIGRÉ B4 HVDC Grid System is presented before introducing the developed converters into the system.
- **Chapter 6** presents the conclusion and proposal for future work.

Chapter 2

HVDC System

This chapter presents general aspects of HVDC transmission. Firstly, a comparison between HVDC and HVAC transmission systems is presented. Two major HVDC technologies, i.e., LCC based and VSC based HVDC transmission are described in addition to the different HVDC configurations. The chapter also discusses general overview on Multi-terminal HVDC system and need of DC/DC converters in MTDC system

2.1 Introduction

The history of transmission of electricity started way back in 1882, when a 57 kM long, 1.4kV DC transmission line from Miesbach to Munich was constructed [9]. However, the DC system developed during this period was operating with the same voltage from generation till consumption due to the lack of a device which could transform the DC voltage. This resulted in using very costly huge conductors even for distribution, thus forcing to build generating stations near to the load centres. With the development of AC transformer during the late 1880, transmission through DC lost interest as AC power now could be transmitted over long distances at a high voltage, thereby reducing the transmission losses and then can be stepped down to a level suitable for the consumer loads.

In spite of the use of AC system for transmission of electric power, there were many focus towards DC transmission in the early 20^{th} century [10]. Ever since the first mercury arc based HVDC system with a capacity of 20MW, operating at 100kV DC was built in 1945, there was a steady increase in HVDC schemes commissioned worldwide. The recent developments in the power electronics industry has changed the way the transmission is going to be in the future with HVDC system.

2.2 HVDC Vs HVAC System

Transmission through HVDC has many distinct advantages over HVAC scheme [11]. Some of them are listed below.

- ✓ For the similar insulation level and cross sectional area, DC lines can carry $\sqrt{2}$ times more power than AC.
- ✓ Right of way requirement for carrying electric power using DC lines are smaller than AC for the same power. In other way, for the same right of way, more power can be transmitted using DC system.
- ✓ The DC transmission losses are less as compared to AC, thereby providing increased efficiency.
- ✓ AC system possess both skin and proximity effect. It restricts maximum utilisation of conductors for the transmission, which is completely absent in the DC system.
- ✓ Easy to implement the active power control in HVDC
- ✓ With both active and reactive current component present in the AC power, the useful power transmitted is always limited as shown in the Fig. 2.1. This issue

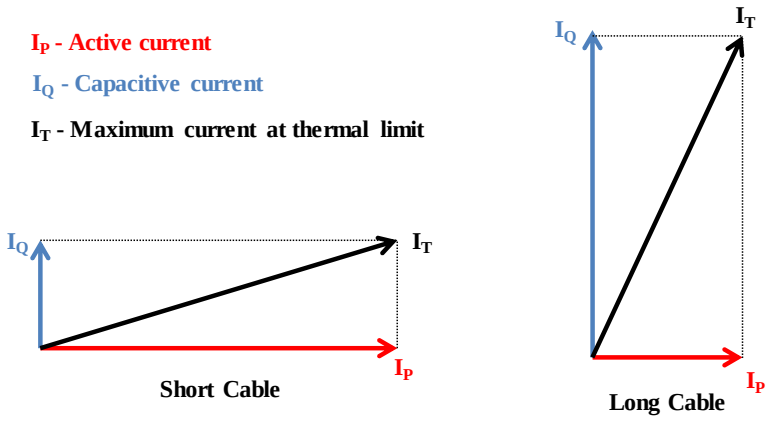

Figure 2.1: *HVAC Cable current limit [12]*

is further aggravated when the transmission of power is through AC cables. With increase in the cable length, capacitive nature of cable increases, resulting more charging current in the cable and restricting the active component of current [12]. In order to overcome this problem, reactive compensation is required, which in-turn increases the cost and space requirement. However, a DC transmission involves no reactive elements and does not require any reactive compensation.

In addition to the above benefits, HVDC scheme also facilitate the interconnection of two asynchronous AC grid operating with different frequencies using back-to-back HVDC configuration. With all the above advantages mentioned above, the cost of converter is

always a concern for HVDC system. Considering the cost of converters, other associated equipments and transmission losses, HVDC is economical for the transmission of electrical power when the distance is higher than the breakeven distance [13] of Fig. 2.2. The breakeven distance for overhead line is 500-800km, while for submarine cables, it is around 50-60km.

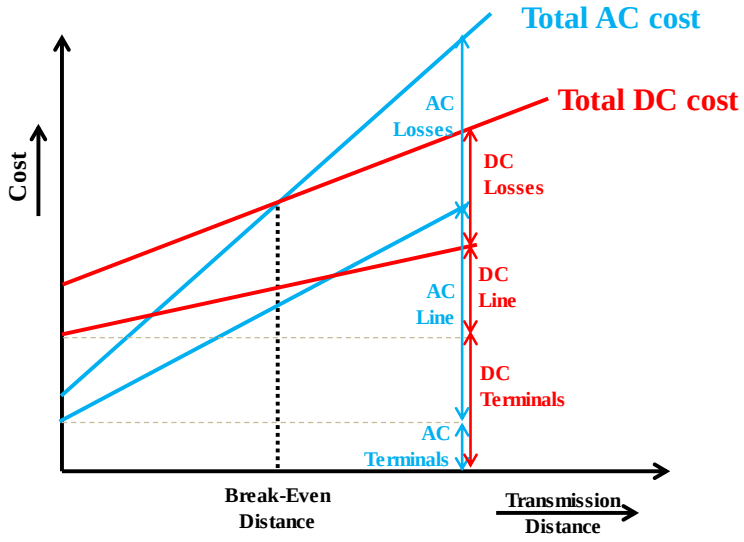

Figure 2.2: *Cost comparison of AC/DC*

To summarise with, HVDC systems is the preferred option for carrying bulk power over a very long distance, interconnection of asynchronous grids, power transmission through submarine cable etc.

2.3 Converter Technology

HVDC transmission in the early days used converter technology based on mercury arc valves. However, with the problem of ark-back fault, the rectifying property of the converter valve gets damaged and consequently results in many other associated problems [10]. HVDC technology currently being employed can be classified as

1. Line Commutated Converters(LCC)
2. Voltage Source Converters(VSC)

2.3.1 LCC based HVDC System

A 12 pulse LCC based HVDC scheme is shown in the Fig. 2.3. The system consists of AC filters and capacitor banks, converter transformer, two converter stations for rectification and inversion, DC filters, smoothing reactors(DC reactor) and DC line [14]. The converters use thyristor valves as the power electronic devices for the conversion and are

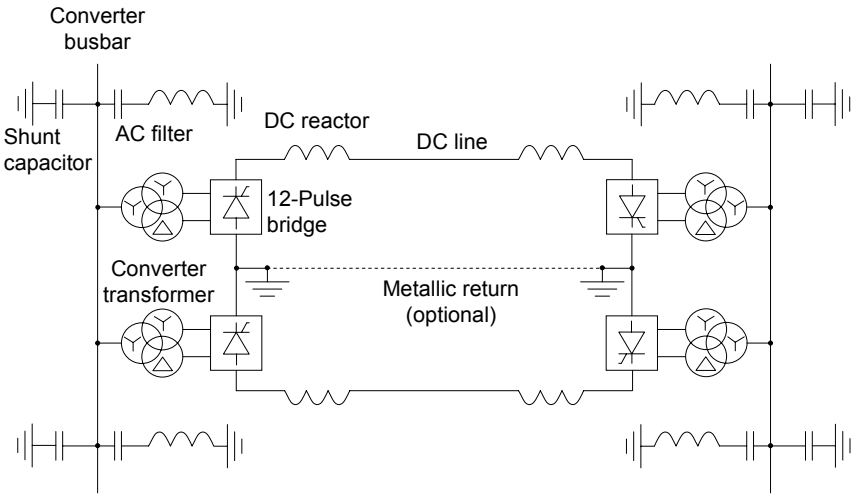

Figure 2.3: *LCC Based HVDC system [14]*

connected in series for the required DC voltage. Thyristors can be only turned ON by applying a gate signal, however needs commutation in the form of natural or line commutation to turn OFF the device. Converter transformer provides the necessary AC voltage for the thyristors and also facilitate the 12 pulse operation. AC filters are required to filter out the harmonics present in the AC and DC side. A major drawback of LCC scheme is that it always consumes reactive power in both the rectifier and inverter mode. Depending on the firing angles, the reactive power consumption of an LCC-HVDC converter station is nearly 50-60% of the active power [15].

LCC based HVDC schemes are still the main technology for bulk power transmission over 1000MW. Typical power loss per converter station is only 0.7% of the transmitted active, which is very low. Several projects worldwide are commissioned with LCC schemes and and are still being constructed. However, LCC suffers many disadvantages [16].

1. Reactive power requirement for the operation of converters. The reactive power compensation is provided by connecting large capacitor banks at AC side of the converters. This results in increased cost and large amounts of space.

2. Failure to commutate current from one valve to the next in sequence. A commutation failure occurs when the incoming valve fails to take over the current before the commutating voltage reverses the polarity, with sufficient extinction time. Although a single commutation failure will not cause any harm to the system, a repeated commutation failures may cause the converter to trip [17].

3. Thyristor based converters require a relatively strong AC voltage source for the commutation purpose. For the successful converter operation, a minimum three-phase symmetrical short circuit capacity equivalent to two times the converter rating is required from the AC network side.

2.3.2 VSC based HVDC System

The latest technology for the HVDC transmission is using Voltage source converters. This was first introduced by ABB in 1990's with the first VSC based HVDC system commissioned at Gotland island of Sweden with a rating of 50MW [18]. The general schematic of VSC based HVDC scheme is shown in the Fig. 2.4.

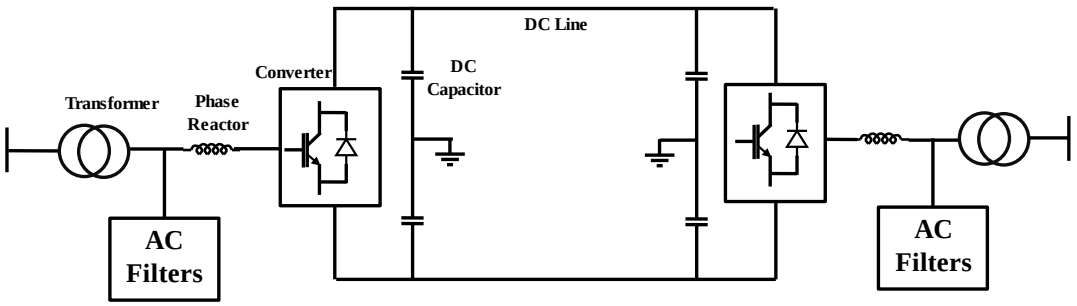

Figure 2.4: *VSC based HVDC system*

The system has 2 converters, one at the rectifying side and other at the inverter side. Each converter utilizes self commutating switches, e.g., GTO or IGBTs, as the power electronic switches for the power conversion. These devices can be turned ON and OFF by applying controlled gate pulses. A complete IGBT module consists of an IGBT, an anti-parallel diode, a gate unit, a voltage divider, and a water-cooled heat sink. Each gate unit includes gate-driving circuits, surveillance circuits, and optical interface [16]. The gate driving electronics control the gate voltage and current at turn-on and turn-off to achieve optimal turn-on and turn-off processes of the IGBTs. An ordinary transformer is connected for providing the voltage level suitable for the converter so as to get the required DC voltage. The phase reactor connected at each phase of the AC side provides low pass filtering for the switching harmonics, active and reactive power control and also limits the short circuit current. Since the gate pulses are provided using PWM technique with high switching frequency, AC filters are provided for eliminating the harmonics in the signal. The DC capacitor provides the stiff DC voltage and a low-inductance path for the turn-off switching currents in addition of serving as an energy storage and reducing the DC voltage harmonics ripples.

VSC based HVDC schemes offer many benefits over conventional LCC based, some of which are listed below.

- ✓ Control of both active and reactive power in one equipment. By decoupling active and reactive component of the current using vector control, VSC can independently control both active and reactive power. Reactive power can be controlled at each converter terminal regardless of the DC voltage level.
- ✓ Operation down to zero short circuit ratio. Converters can be operated anywhere in the AC network, as the operation of the converters does not require any short circuit power. This was one of the major drawback of thyristor based LCC system. It also provides the black start capability.

- ✓ No reactive power consumption for the operation of converters. Therefore huge capacitor banks are completely removed from the switchyard, thereby reducing the space requirement for the converter station.
- ✓ Instead of using converter transformers, ordinary transformer could be used for VSC station.

Some of the major HVDC projects with VSC based technology include 500kV 700MW Skagerakk-4 project between Denmark and Norway, ±320kV, 900MW DolWin2 project in the North sea etc. [19].

2.4 HVDC Configurations

The HVDC system can be configured in different ways [20]. The commonly used configurations are discussed in this section.

- ✓ **Monopolar HVDC system** - It is further divided into asymmetric and symmetric monopolar system. An asymmetric monopole configuration involves operation of DC system with single positive voltage, while the return path of current is through the earth. The system involves only one set of conductor as shown in the Fig. 2.5.

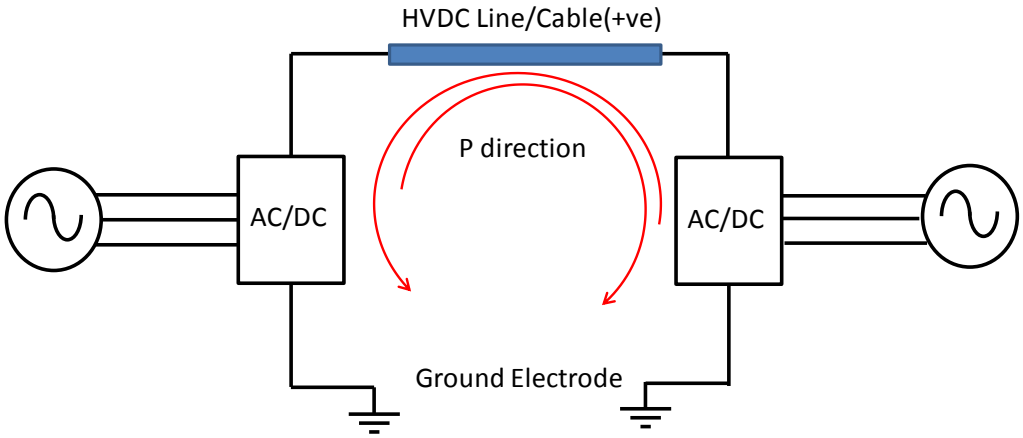

Figure 2.5: *Asymmetric Monopolar configuration*

As shown in the Fig. 2.5, there is a continuous flow of current through the earth during the operation. In some cases, where earth return path is not possible due to highly congested areas or fresh water cable crossing, a metallic earth return path could be used. However, losses increase in such arrangement due to resistance of metallic conductor.

Another configuration of monopolar system is symmetric monopolar type. In this system, each poles on both sides are connected to the high voltage cables, carrying half the rated power. This is illustrated in the Fig. 2.6. Each conductor in this configuration is subject to half the rated DC voltage and full rated current in opposite direction.

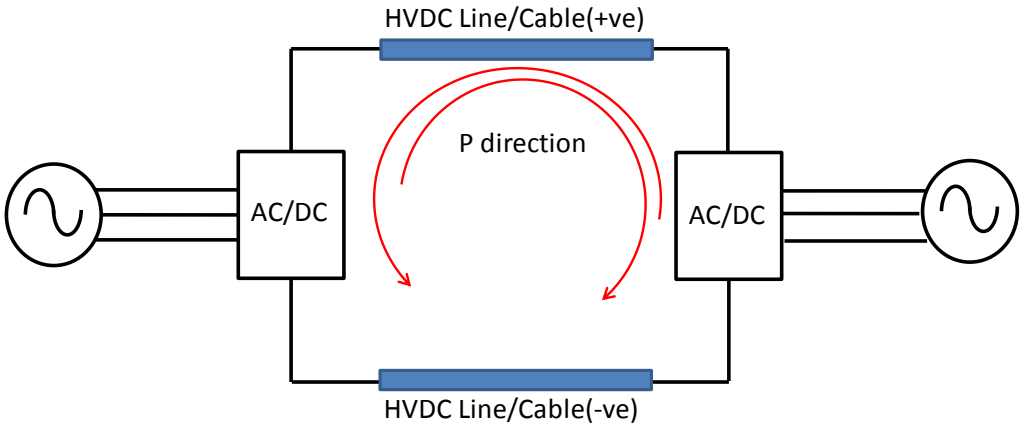

Figure 2.6: *Symmetric Monopolar configuration*

✓ **Bipolar HVDC system** - A higher power rating with greater reliability could be achieved using bipolar configuration. In a bipolar configuration, there are 2 poles, one as positive and the other as negative with respect to ground. Therefore, there are two sets of conductors each rated for full voltage. Current flowing through the earth electrode in bipolar configuration is negligible during normal operating condition. The schematic and the current direction of a bipolar configuration is shown in the Fig. 2.7. A metallic return path could be provided for operation of the converter at its half rating during a fault in one pole.

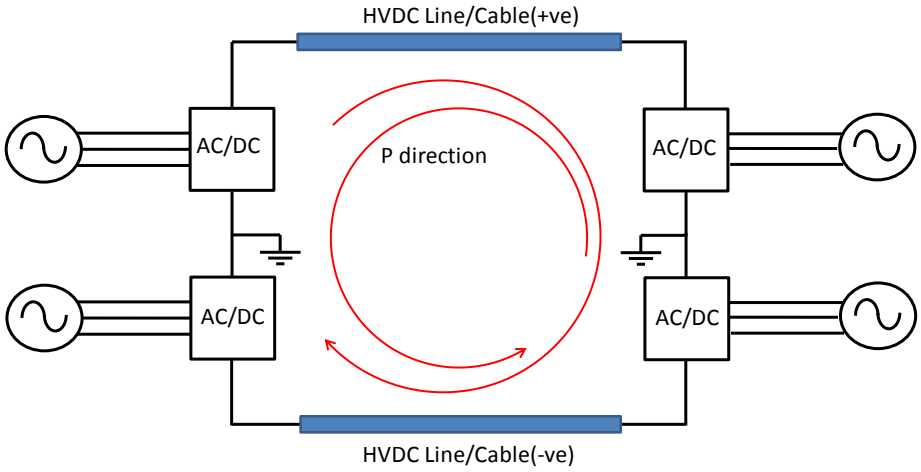

Figure 2.7: *HVDC Bipolar configuration*

✓ **Back-to-back HVDC system** - In Back-to-back HVDC system as shown in Fig. 2.8, there is no DC transmission line between the converters. Both rectifier and inverter are located at the same place. This configuration is used for the interconnection of two asynchronous AC networks.

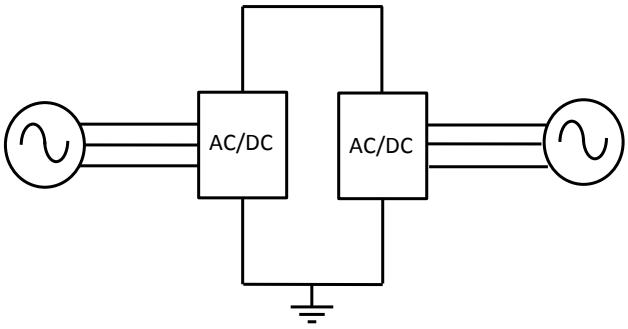

Figure 2.8: *Back-to-back HVDC configuration*

2.5 Multi-terminal HVDC System

Most LCC based HVDC systems currently existing are point-to-point with converter stations at both ends. The power transfer in such a configuration is achieved by manipulating the voltage magnitude of both the terminals and changing the voltage polarity. However, the need of flexible transmission capacity to balance the fluctuating power generation from renewable over wide geographical areas combined with corresponding potential benefits in a deregulated power market is expected to favour MTDC system with many converter terminals connected in a single grid. In such a system, the manipulation of voltage at each terminal become a tedious task and need complex control techniques and complicated switching and therefore LCC scheme does not favour multi-terminal system. However, with VSC technology, power reversal is now possible by changing the current direction with the voltage unaffected, thereby providing the ground for an MTDC grid.

A VSC MTDC system has many advantages over a two-terminal HVDC system, which includes increased transmission capacity, reduction in the cost and conversion losses, flexible control of the power flow and enhanced reliability. MTDC configuration can be broadly classified into two based on the converter arrangement.

1. **Series Configuration** - In series arrangement as shown in Fig. 2.9, one converter controls the current around the rated current, and is common for all converters, while other converters controls the power. LCC based system favours this configuration as they act as voltage source at DC side. However, this arrangement results in more losses, high insulation requirement and reduced reliability. A fault in one terminal of the system could results in complete MTDC to cut-off [15].

2. **Parallel Configuration** - In this configuration, one converter sets the voltage, while others operate in power mode. The arrangement can be done in radial or ring configuration as shown in Fig. 2.10. The parallel configuration is always a preferred way of connection due to its reliability, as failure in one terminal will not affect the total MTDC system, provided that other terminals could carry the total power.

With the above two configurations many types of MTDC systems based on various application were proposed in the literature [6], some of which are listed below.

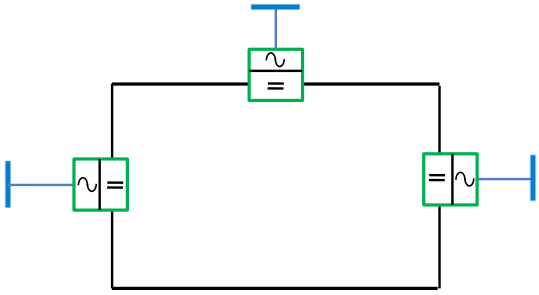

Figure 2.9: *Three terminal series MTDC system*

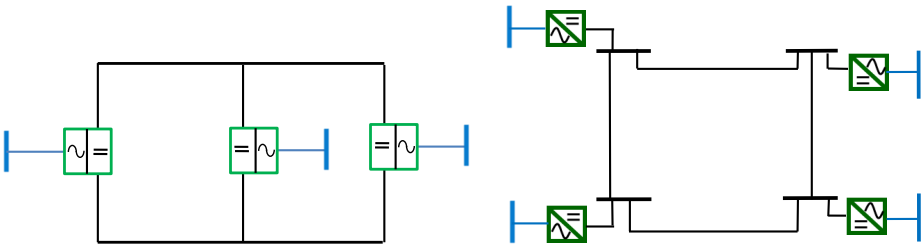

(a) (b)

Figure 2.10: *Parallel MTDC system) a)Radial configuration and b)Ring configuration*

✓ **Double input single output(DISO) HVDC system** for offshore wind farms as shown in Fig. 2.11 - A 3-terminal double input single output HVDC system for interconnecting two neighbouring wind farms to an AC grid.

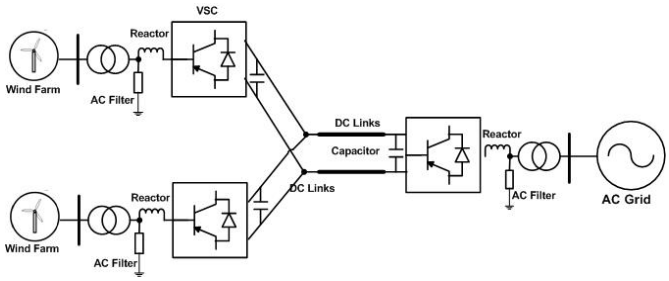

Figure 2.11: *Double input single output HVDC system [6]*

✓ **MTDC for oil and gas platforms** - A 3-terminal DC system of which a terminal for offshore wind farm is placed in between the oil platform terminal and onshore grid. Offshore wind farms can power up both oil platform and the onshore grid in this arrangement as shown in Fig. 2.12.

✓ **MTDC for urban distribution** - An HVDC network with multiple input-multiple output so that meshed ring shaped DC network is formed. The schematic is shown in Fig. 2.13.

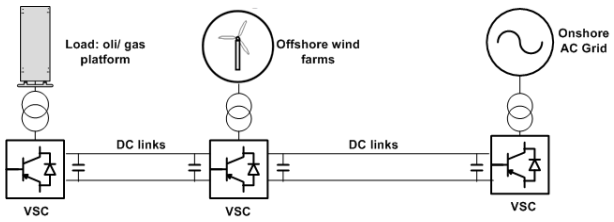

Figure 2.12: *3 Terminal DC system for oil and gas platforms [6]*

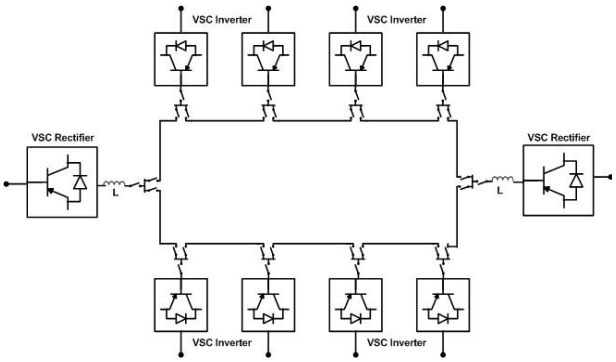

Figure 2.13: *Meshed ring shaped DC network [6]*

✓ **CIGRÉ B4 MTDC Test Grid** [8] - CIGRÉ has proposed an MTDC grid consisting of several offshore wind farm converter terminals, oil platform terminals and onshore grid terminals operating with both Bipole and Monopole configuration. This report in Chapter 5 will study in detail on this MTDC grid.

2.6 DC/DC Converters

A future HVDC grid is expected to emerge through a gradual development where point-to-point connections can later be connected into multi-terminal, meshed, configurations. A DC/DC conversion stage is required in such configuration due to following reasons.

✓ Two HVDC links operating at different voltage levels cannot be directly connected to each other. The exchange of power between these two networks need a DC/DC converter just like an AC transformer in an AC system

✓ Two HVDC links operating with the same voltage but with different configurations. i.e, bipole or monopole, need a DC/DC converter for their interconnection

✓ Power flow control through a particular section of the HVDC network

✓ Interconnection of existing LCC based HVDC scheme with latest VSC based HVDC system can be done through a DC/DC converter

The topology of DC/DC converter used in an HVDC grid varies for different applications. A high power DC interconnection could be classified according to the voltage ratio between two subsystems and is shown in Table 2.1 [21].

Table 2.1: *HVDC interconnections [21]*

Nomenclature	**Ratio**
Low Ratio	$\frac{V_{DC,HV side}}{V_{DC,LV side}} \leq 1.5$
Medium Ratio	$1.5 \leq \frac{V_{DC,HV side}}{V_{DC,LV side}} \leq 5$
High Ratio	$\frac{V_{DC,HV side}}{V_{DC,LV side}} \geq 5$

Wide range of DC/DC topologies including Buck converter, Boost converter, Buck boost converter, Cuk converter etc. are developed for low voltage applications. However, DC/DC converters for high voltage DC grid applications are not as mature as for low voltage applications. Based on the Table 2.1, a DC/DC converter used in an HVDC grid can be classified into two types.

1. DC/DC Converters without galvanic isolation
2. Galvanically isolated DC/DC converters

Non-(galvanically) isolated DC/DC converters, which are mainly employed for power flow control are addressed in detail in Chapter 3, while the modelling, designing and control of the later are discussed in chapter 4.

Chapter 3

DC/DC Converter without Galvanic Separation

This chapter presents the first class of DC/DC converters suitable for power flow control. A literature review on various converter topologies of this class is presented. Later, the design, modelling and control of 4Q Converter and Front-to-front DC/AC/DC converter are discussed separately

3.1 Introduction

Most HVDC schemes for cross-border transmission or offshore wind farm connections constructed first by point-to-point links might later be connected into a multi-terminal HVDC grid by adding new cables to increase the flexibility in the power transmission. For instance, a link for an offshore wind farm could be extended to connect to another country, or an existing transmission link can be interconnected to an offshore wind farm cluster. However, by such connections into a ring or meshed configuration, the steady-state power flow will depend on the resistance of the cables and on the control objectives of the different terminals, and it might happen that some cables get overloaded just because they are shorter and have lower resistance than other cables. In such configurations, it might be necessary to introduce DC/DC converters to control the power flow in the system.

When two DC systems operating at similar voltage with similar configuration (either monopole or bipole topology) require an interconnection for controlling the power flow through the line, low ratio DC/DC converter without galvanic separation can be utilised.

3.2 Different topologies

The DC/DC converter for the application of power flow control could be integrated into the HVDC networks by two ways.

1. Dedicated DC/DC converter
2. Front-to-front DC/AC/DC converter

Various topologies for above types are discussed in the literature and some of those topologies will be analysed in the coming section.

3.2.1 Dedicated DC/DC converters

2Q Converter

The interconnection of two DC subsystems, wherein one DC system is always operating with higher voltage than the other and the high voltage to low voltage ratio is less than 1.5 could be done through a 2Q converter [22] as shown in the Fig. 3.1. The circuit in the

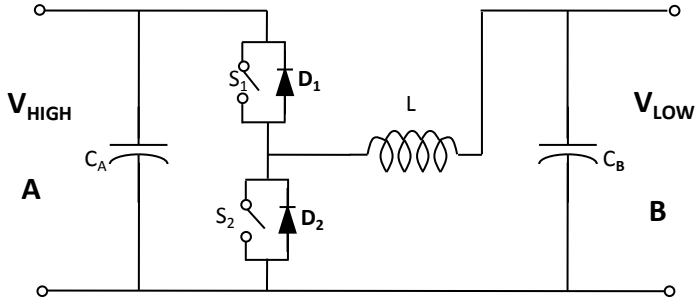

Figure 3.1: *Two Quadrant Converter*

Fig. 3.1 represents a bi-directional buck converter operating in first and second quadrant of the IV curve. Power flows from the high voltage side at A to low voltage side B, when S1 and D2 is active, while power reverses its direction when S2 and D1 is conducting.

However, such configuration cannot be utilised if the voltage on both sides of the converter is uncertain. This is mostly the case when a DC/DC converter is used for controlling the power flow in a line of an MTDC grid, wherein DC voltages at terminals of each converter change according to the set reference. This problem could be solved using a 4Q converter.

4Q Converter

The operation of the converter in four quadrants of the IV curve and non-necessity of galvanic separation permit to utilise the 4Q converter topology [23] as shown in Fig. 3.2 for a low voltage ratio DC/DC interconnection to control the power flow. The operation of the 4Q converter is explained in detail in Section 3.3.1.

3.2.2 Front-to-front DC/AC/DC Converter

One method of DC/DC conversion is converting DC into AC first and then back to DC. The converter consists of 2 AC/DC converters. The intermediate AC stage could be either

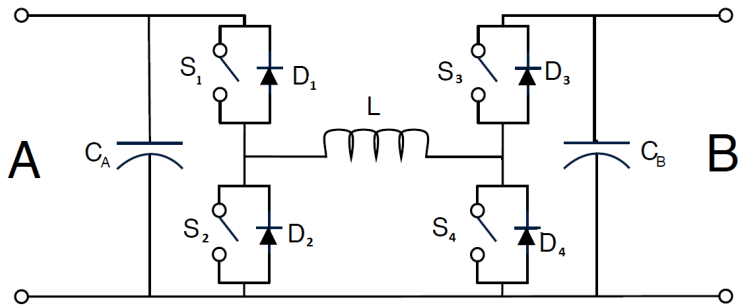

Figure 3.2: *Four Quadrant Converter*

1-phase or 3-phase. However, 3-phase system can be preferred due to following reasons [24].

- ✓ To match power through-put capability equal to the HVDC system
- ✓ 3-phase system has higher power density than a 1-phase
- ✓ RMS current flowing through power electronic switches in a 3-phase system is less and hence could reduce the rating of the device
- ✓ Voltage ripples in 3-phase system is less

Front-to-front DC/AC/DC converter can be implemented using Two level converter or Modular Multi-level converter.

Two Level DC/AC/DC Converter

The schematic of a two level configuration is shown in the Fig. 3.3, wherein each DC/AC converter consists of six valves of switching device(IGBT) and anti-parallel diode. Several

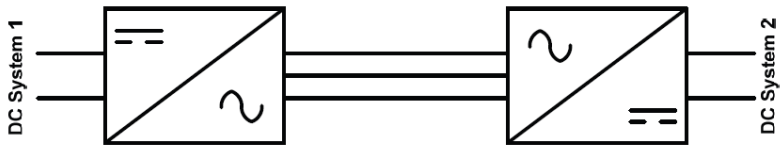

Figure 3.3: *Front-to-front DC/AC/DC Converter*

switching devices are connected in series to handle the very high voltage. However, interconnecting IGBT's in series is a challenging task, and usually they fail in open circuit. In-order to overcome this problem, ABB has proposed press packaging arrangement of IGBT. This arrangements of IGBT's makes it modular in terms of current and also facilitate IGBT for series connection [25].

Modular Multi-Level Converter

A typical modular multi-level converter configuration also called as Alternate arm converter is shown in the Fig. 3.4. The converter employs a hybrid combination of soft

switched H-bridge converters which are operating at fundamental frequency along with MMC cells. The series strings of IGBT's in each leg provides the necessary converter voltage rating. Due to the soft switching of the H-bridge converters, the switching power loss comes down which in turn increases the efficiency [26]. The two DC/AC converters operates in 3-phase to match up with sufficient power rating of the HVDC system. Compared with the two level DC/AC/DC converter, one major feature is that the DC capacitors are distributed into each module, and hence there is no common capacitor connected at the DC side. Each converter valve contains a series-connection of sub-modules, each one comprising a DC capacitor and a H-bridge. The major advantage of this design is reduction in the average switching frequency per device, which results in minimum harmonics and hence fewer filters. However, the design and control of MMC is very complex. It is important to make sure that the capacitor voltages in all the sub-modules are strictly controlled for avoiding the over-voltage problems [25].

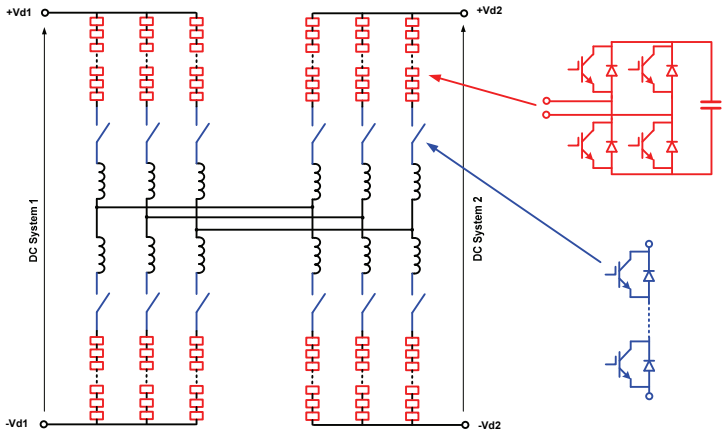

Figure 3.4: *Modular Multi-level DC/DC Converter [21]*

Various manufactures like ABB, Siemens, Alstom have developed the MMC topology and it is called with different names.

Out of the above converter topologies, 4Q converter and Front-to-front DC/AC/DC converter are analysed in greater detail and discussed in the following section.

3.3 Design, Modelling and Control of 4Q Converter

A 4Q converter is a good example for a dedicated DC/DC converter for low ratio connections and therefore, in this section, the detailed design, modelling and control of 4Q converter is analysed.

3.3.1 Operation of the converter

The 4Q converter as shown in Fig. 3.2 operates in all four quadrants of the IV curve based on the position of switches/IGBT and diodes. i.e, it is capable of transporting energy

in forward and reverse directions and of stepping voltage up and down. The topology resembles a buck and boost converter when operating the four switches in certain manner. The operation of switches and diodes in different modes is shown in Table 3.1 and Table 3.2, wherein A, 1 & 0 indicates status of the component, i.e, active, completely ON and completely OFF respectively.

Table 3.1: *Operations of switches in different DC-DC modes*

Voltage	Power direction	Mode	S1	S2	S3	S4
$V_A > V_B$	A → B	Buck	A	0	0	0
$V_B > V_A$	B → A	Buck	0	0	A	0
$V_A < V_B$	A → B	Boost	1	0	0	A
$V_B < V_A$	B → A	Boost	0	A	1	0

Table 3.2: *Operations of diodes in different DC-DC modes*

Voltage	Power direction	Mode	D1	D2	D3	D4
$V_A > V_B$	A → B	Buck	0	A	1	0
$V_B > V_A$	B → A	Buck	1	0	0	A
$V_A < V_B$	A → B	Boost	0	0	A	0
$V_B < V_A$	B → A	Boost	A	0	0	0

The current direction in each operational model is shown in the Fig. 3.5. Fig. 3.5 illustrates that the circuit behaves as either buck or boost according to the switch/diode position.

3.3.2 Sizing of Components

The main components in the DC/DC converter are diodes, switch/IGBTs, inductor and capacitors. The sizing of diodes and switch/IGBTs depends on many factors, including breakdown voltage, withstand capability, continuous current, power rating etc., while inductor and capacitor are sized considering the current and voltage ripples and are different for each converter topology due to the difference in the operation mode. 4Q converter behaves as a buck/boost in relation to the operational modes of switch/IGBTs and therefore sizing of components must be calculated taking into account both modes.

Inductor

The inductor is chosen such that ripple in the DC current is within the grid code acceptance limit. The calculation uses the standard formulas mentioned in [27], [28] and [29]. Inductor size in buck mode is given by (3.1):

$$L = [(V_{in} - V_{out}).\frac{V_{out}}{V_{in}}.\frac{1}{f_{sw}}.\frac{1}{2\Delta I_L}] \tag{3.1}$$

where, ΔI_L is the ripple inductor current, V_{in} and V_{out} are the input and output voltage respectively, while f_{sw} represents the switching frequency. Eq. (3.2) can be used to

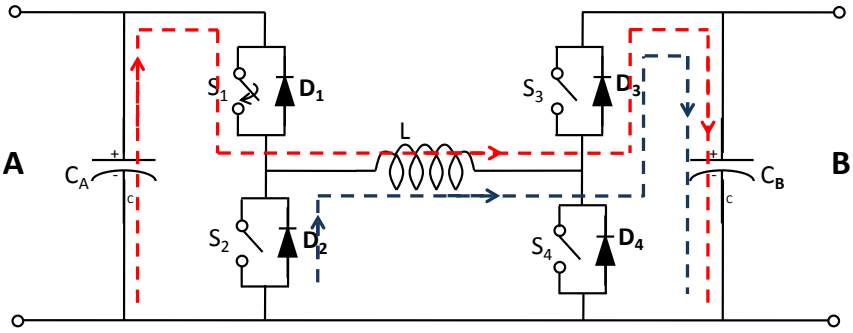

(a) Buck Mode from A to B

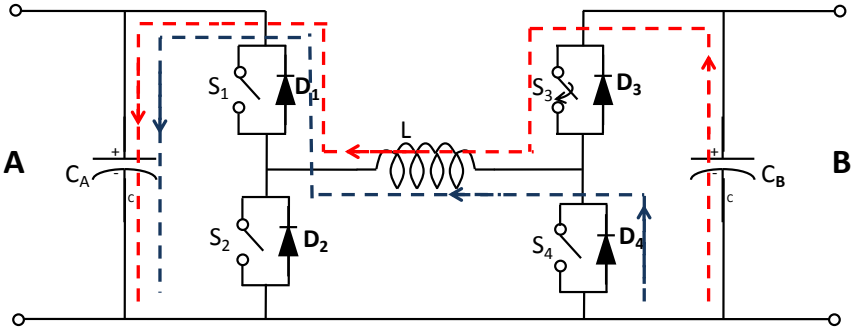

(b) Buck Mode from B to A

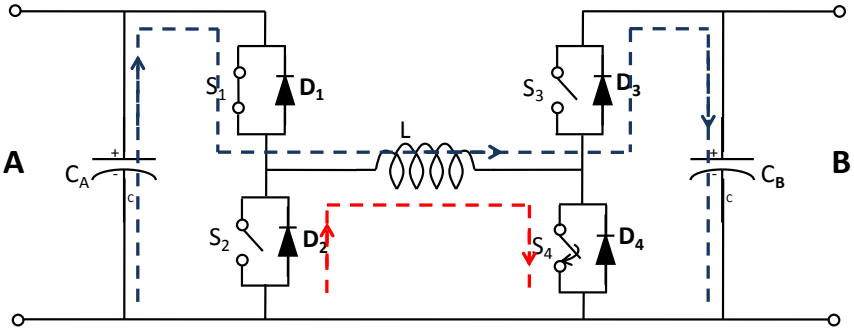

(c) Boost Mode from A to B

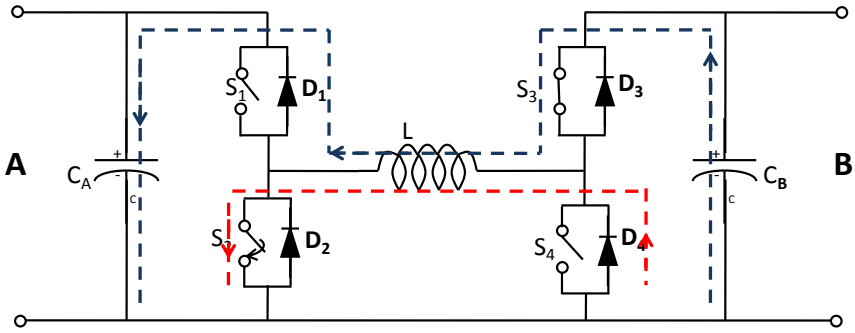

(d) Boost Mode from B to A

Figure 3.5: *Power direction and Operational Mode of 4Q Converter*

compute the inductance in boost mode.

$$L = [V_{in}.\frac{V_{out} - V_{in}}{V_{out}}.\frac{1}{f_{sw}}.\frac{1}{2\Delta I_L}] \tag{3.2}$$

Capacitor

The capacitors are required to maintain a regulated output voltage and the size of capacitor is a measure of the output voltage ripple. The computation is done using charge balance in the capacitor. In buck mode, the capacitance, C is given by (3.3):

$$C = \frac{1}{2}.\frac{1}{2f_{sw}}.\frac{V_{out}}{2L\Delta V_{out}}.\frac{(1-D)}{f_{sw}} \tag{3.3}$$

Capacitance in boost mode can be calculated using (3.4):

$$C = \frac{I_{out}D}{f_{sw}\Delta V_{out}} \tag{3.4}$$

ΔV_{out}, I_{out} and D represents the ripple in the voltage, output current and duty cycle, respectively. The results from buck and boost mode are then compared and maximum component value is considered for minimum current and voltage ripples.

3.3.3 Average Modelling of the converter

Various computer simulation programmes are available to simulate large power system networks with different power electronics components. However the detailed modelling with discontinuous switching schemes introduces significant increase in the computing time and hence restricts to simulate a very large system. This drawback is solved by developing dynamic average value models(AVM). AVM approximates the system by averaging the effect of fast switching within a switching interval. i.e., it replaces the switching cells, which are discontinuous, with some components which are continuous. By doing this, it still maintains the accuracy of dynamics of the system. The key step in AVM is to replace switch network with dependant voltage and current sources, yielding a time invariant circuit topology. Hence, the effect of switching harmonics is eliminated over the switching period. The DC/DC converter using AVM can be modelled as a current source behind a capacitor(C) and a voltage source behind an inductor(L) [29]- [30], as it is shown in the Fig. 3.6, where R and G represent the parasitics associated with the circuit elements and losses.

3.3.4 Controllers

The objective of the converter is to control the power flow, without much variation in the voltage. Therefore the control variables are voltage and current. The controller uses a cascaded control system with inner loop as current control. The inner loop restricts the current through the inductor to a specified range. The bandwidth (speed of response) of a cascade controller increases towards the inner loop with current loop being the fastest

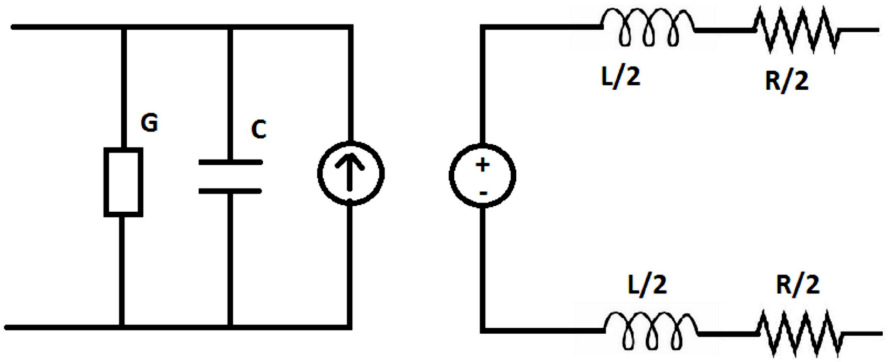

Figure 3.6: *Average Modelling of DC/DC Converter*

and outer loop being the slowest [31]. The fast dynamics of the inner loop in the cascade control structure allow the attenuation of disturbances in faster rate and therefore reduce the possible effect, before the outer loop variable is affected [32]. The outer loops can be implemented in three possible ways, i.e., using current, voltage or power as the controlled variable. Since power is the parameter of interest, voltage and current are needed for the reference power to be calculated using (3.5).

$$P = VI \tag{3.5}$$

Non linear control strategies with variable frequency methods like hysteresis control, sliding mode control etc. could be utilised as the control strategy to provide a fast transient response for the system, which is non linear due to the switching devices [33]. However, linear control technique using PI controllers and PWM with fixed frequency allows more flexible control and is easy to implement while still providing good transient response.

Inner Loop Controller

The reference to the inner PI controller is the output from outer loop, with a limiting block (saturation) to restrict current to a pre-defined range. This current is calculated for the rated power of converter using Kirchhoff's voltage law keeping switch in ON state. This value also depends on the transmission line resistance. The transfer function for the PI regulator can be represented as (3.6):

$$G_1(s) = \frac{V_{conv}(s)}{I_{L,ref}(s) - I_L(s)} = Kp.\frac{1 + T_i s}{T_i s} \tag{3.6}$$

where $T_i = K_p/K_i$, K_p and K_i being the gains of proportional and integral controller. The PWM converter can be considered as a first order system with a time delay, T_a. The corresponding transfer function can be written as (3.7):

$$G_2(s) = \frac{1}{1 + T_a s} \tag{3.7}$$

The control to output transfer function for the system differs according to the mode of operation. For the buck mode [34], it is given by (3.8):

$$G_{sys,buck}(s) = \frac{V_0}{D(1 + \frac{sL}{R}s + s^2(LC))} \tag{3.8}$$

The small signal transfer function when the system is operated in boost mode [35] is given by (3.9):

$$G_{sys,boost}(s) = \frac{(1-D)V_0 - (LI_L)s}{LCs^2 + \frac{L}{R}s + (1-D)^2} \tag{3.9}$$

The complete block diagram representation for inner loop is shown in Fig. 3.7.

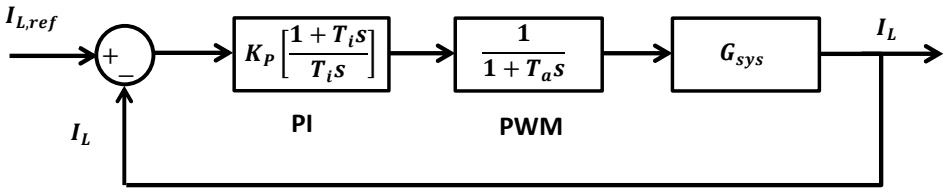

Figure 3.7: *Inner loop controller*

Outer Loop Controller

The outer loop controller could be either Power, Voltage or Current. Fig. 3.8 shows three alternative ways of implementing the controller in Simulink. V_{ref} and I_{ref} can be calcu-

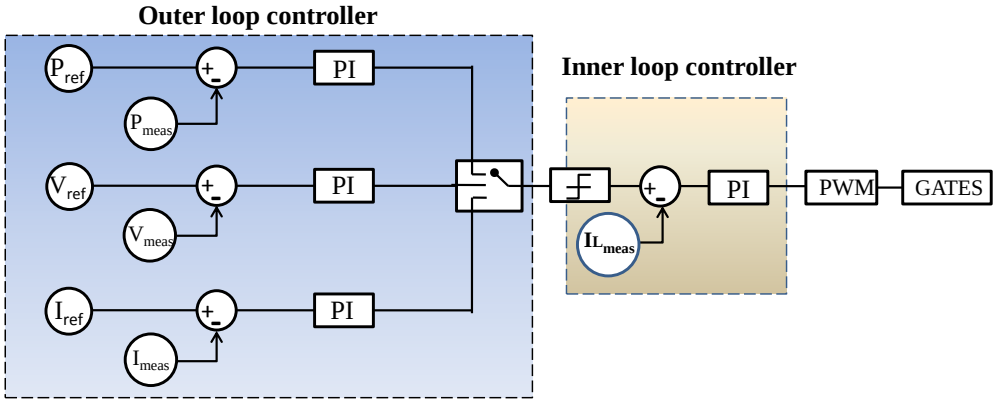

Figure 3.8: *Cascaded controller strategies for 4Q Converter*

lated using the DC power equation of (3.5) for the given power reference. The controller with voltage at the outer loop can be implemented only when system is operating in a particular mode. The current in this case goes to zero resulting an infinite voltage reference when the power direction changes from A to B and vice versa. All the parameters are calculated in per unit for the easiness of implementation. The controllers are designed for 2% overshoot and 0.3s settling time.

3.3.5 Simulation Model of the DC/DC converter

A 2000MW, 380 to 420kV converter with Power controller in the outer loop was simulated in MATLAB Simulink, using SimPowerSystems toolbox and is shown in Fig. 3.9.

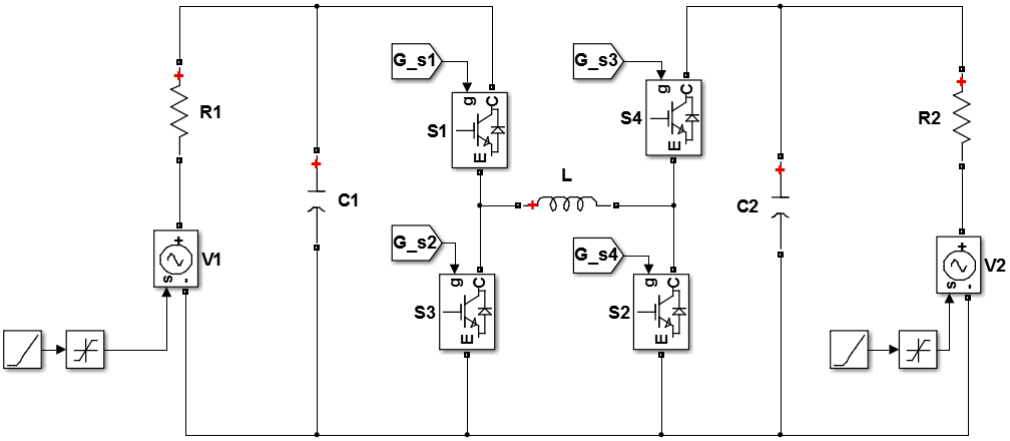

Figure 3.9: *Simulink Model:4Q Converter*

Table 3.3 shows the DC/DC converter parameters used for the simulation, calculated as described in section 3.3.2. The variables of interest like input and output voltage and current, inductor current etc. are measured. The switching of IGBTs depends on the power and voltage values and the corresponding logic for the operating mode is developed using logic gates.

Table 3.3: *DC/DC converter design parameters*

Parameters	L	$C1$	$C2$	f_{sw}
Values	$34mH$	$10\mu F$	$10\mu F$	$1kHz$

3.3.6 Results

Simulation is carried out to verify the controller performance when the DC/DC converter is operating in all the four quadrants. Initial power reference for the outer loop is set at 1000MW in boost mode and then changed to -1000MW to verify the bi-directionality. The above conditions are then simulated for buck mode from t=2.5s. The power flowing through converter for both buck and boost mode are shown in Fig. 3.10 and 3.11. The

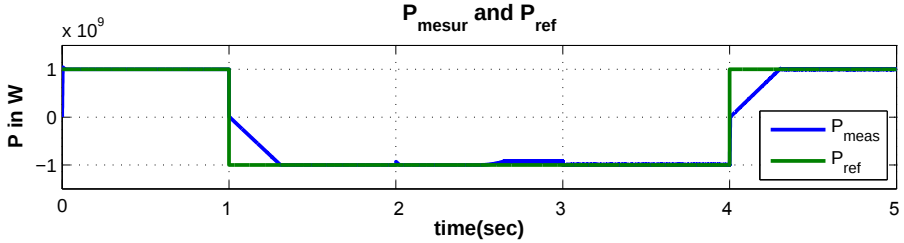

Figure 3.10: *Output response with Power(outer) and Current(inner) control loop*

results suggest good performance of controllers by tracking the reference in all four modes with an acceptable degree of error. The current flowing through the inductor of 4Q converters is shown in Fig. 3.12. The operation of switches in accordance with the

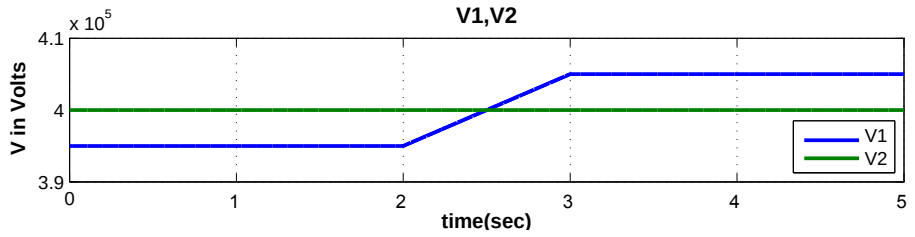

Figure 3.11: *Voltage Variation for simulating buck and boost mode*

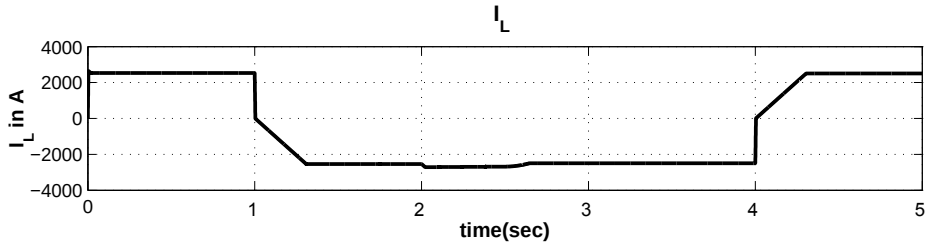

Figure 3.12: *Current through the Inductor of 4Q converter*

operational mode is shown in the Fig. 3.13. The simulation is then performed with current controller in both outer and inner loops. The results almost match those obtained with previous controller.

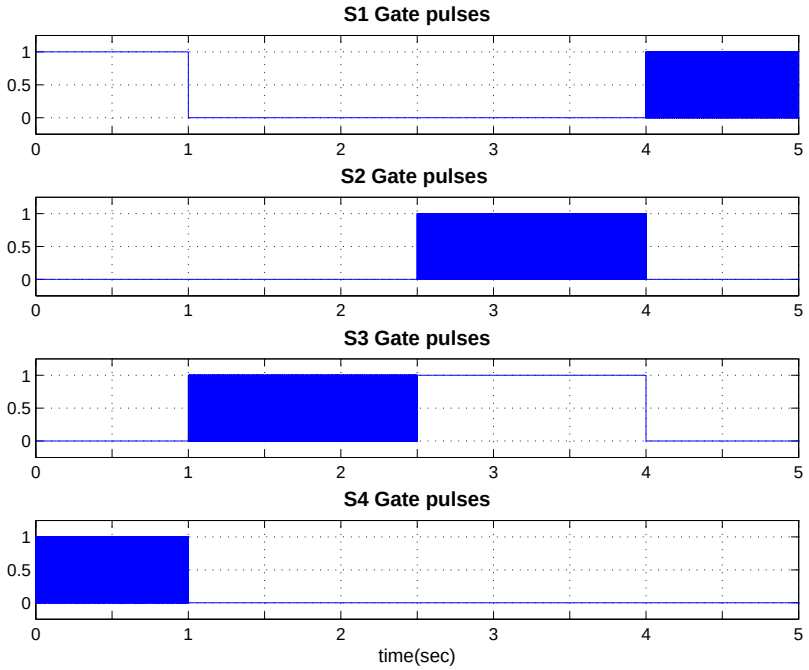

Figure 3.13: *Gate Signals*

3.4 Design, Modelling and control of Front-to-front DC/AC/DC converter

The Front-to-front DC/AC/DC converter analysed and implemented in the following section uses 2-level topology as an example case. However, the natural evolution of the study would be using Modular Multi-level converter topology as discussed in section 3.2.2.

3.4.1 Design of DC/AC/DC converter

A DC/AC/DC converter converts DC to AC and then back to DC to control the DC power flow. The converter consists of 2 AC/DC converters. The schematic of DC/AC/DC converter is shown in the Fig. 3.14. The model consists of 2 DC systems and intermediate AC system. Each converter leg consists of power electronic switches and anti-parallel diodes. The switching model imposes huge harmonics to the system and therefore, filters are inevitable in the model.

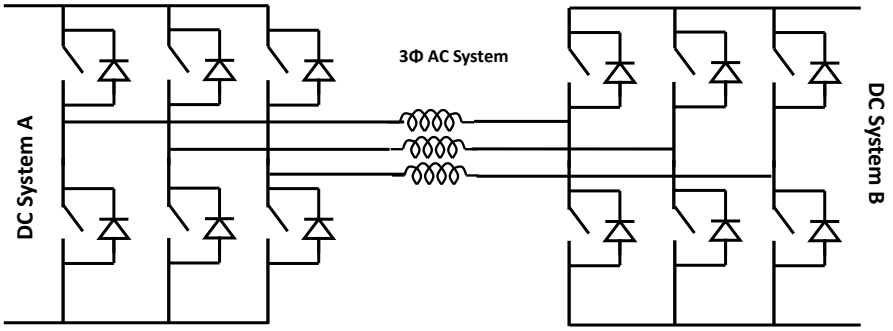

Figure 3.14: *Switching model of DC/AC/DC converter*

Average model

The converter under analysis is intended to be implemented in a larger MTDC system. However, the discontinuous switching schemes of power electronic devices could result in substantial increasing in computing time and hence restrict the size of system, which can be simulated. In order to overcome this, dynamic average modelling is implemented. The two AC/DC converters are modelled as current source on the DC side behind a capacitor and a voltage source on the AC side behind an inductor. The model thus developed in shown in the Fig. 3.15. The model in the Fig. 3.15 is now continuous and can be hence used with larger time steps increasing the speed of simulation.

3.4.2 Controllers

The main purpose of the converter is to control the DC power flow. Since the model consists of 2 converters, one converter is set to voltage controlled, while other is set to power controlled.

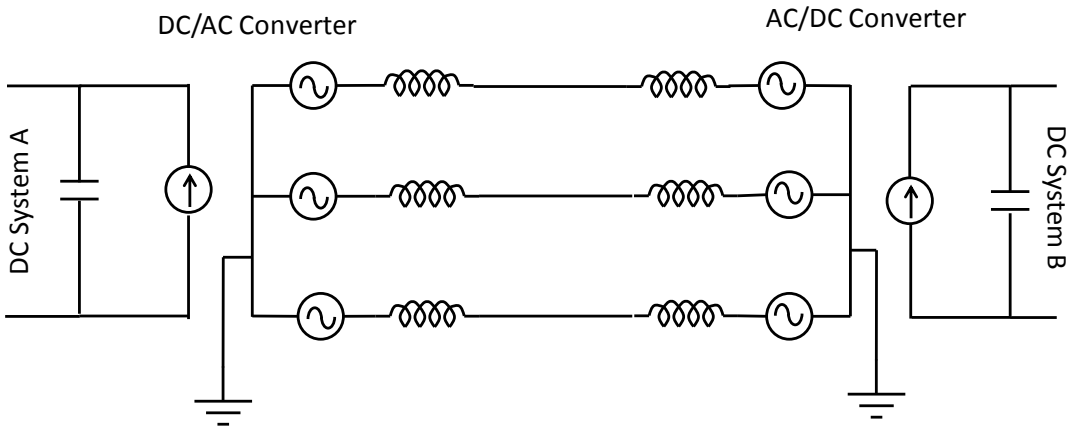

Figure 3.15: *Average model of DC/AC/DC converter*

Voltage Controller

A voltage controller controls the amplitude of the output voltage. Fixed frequency pulse width modulation technique is used for obtaining the required output. PWM compares control signal with carrier signal of fixed amplitude and frequency [28]. In PWM technique, amplitude of the output signal is expressed in-terms of amplitude modulation index, m_a. m_a expresses the capability of the DC-link voltage utilization in generating the PWM voltages at the input of the AC/DC converter during the control process. m_a is given by the (3.10).

$$m_a = \frac{A_{control}}{A_{carrier}} \tag{3.10}$$

where, $A_{carrier}$ and $A_{control}$ are the amplitude of carrier and control signal respectively. Another important variable in PWM is the frequency modulation index m_f. m_f defines the switching frequency of the power electronic devices. It is defined as (3.11).

$$m_f = \frac{f_{carrier}}{f_{control}} \tag{3.11}$$

where, $f_{carrier}$ and $f_{control}$ are the frequency of carrier and control signal respectively. In a single phase sinusoidal PWM, the amplitude of fundamental frequency component is given by (3.12).

$$(V_{A0})_1 = m_a V_{DC}/2 \tag{3.12}$$

(3.12) shows that amplitude of fundamental frequency component of the output voltage varies linearly with m_a for the value of $m_a \leq 1$. Therefore the range of m_a between 0 to 1 is also referred to as linear region. The waveforms of voltage controller and the generated gate pulses for 3-phase AC/DC converter used in our model is shown in the Fig. 3.16. The control signal is a fixed 50Hz 3-phase sinusoidal signal with phase angle difference of 120° between and an amplitude of 0.95 pu, while the carrier signal is a triangular wave with frequency 2kHz and amplitude of 1 pu. The comparator compares both signals and correspondingly generates the gate pulses for the converter. The signal to the average model of the converter will be 3-phase sinusoidal signal with phase angle difference of 120° between and an amplitude of 0.95 pu, as shown in the Fig. 3.17, since the system has eliminated the effect of switching.

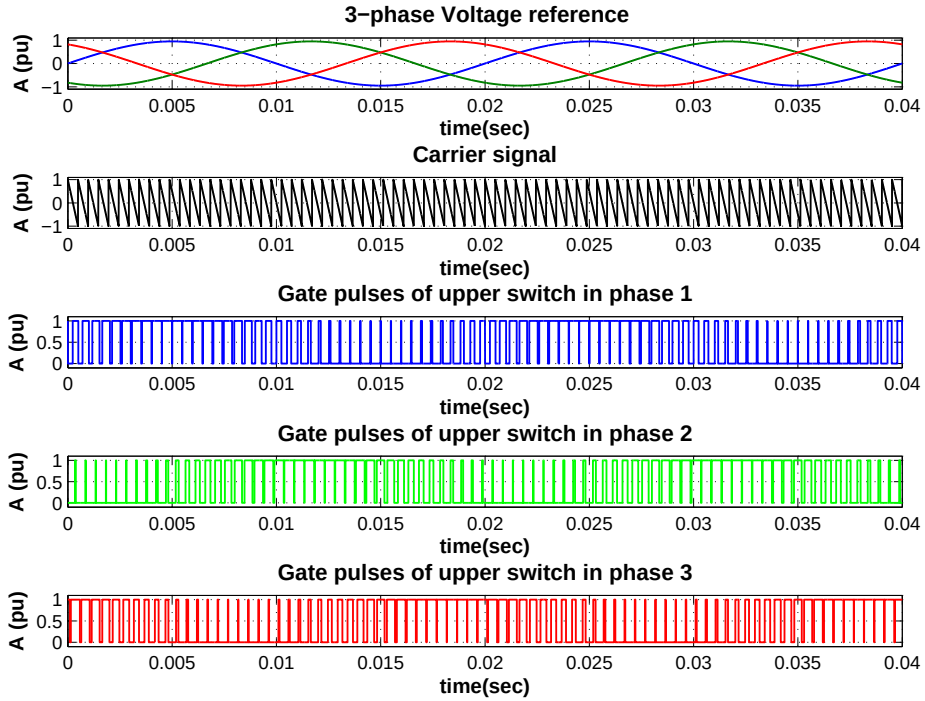

Figure 3.16: *Waveforms of PWM Modulation with m_a=0.95*

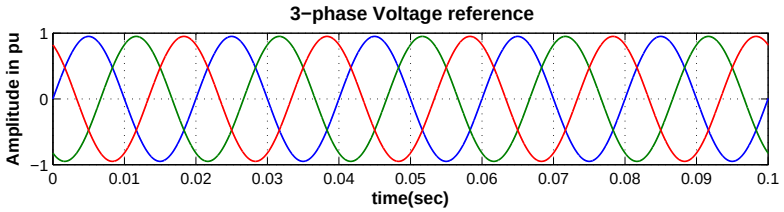

Figure 3.17: *Voltage reference signal for average model*

Power Controller

The 2^{nd} AC/DC controls the power using vector based control [36] - [37]. Vector based control is carried out by transforming 3-phase abc quantities which are in the stationary reference into into rotating dq reference frame. The dq quantities are rotating with synchronous speed. This transformation is carried out as follows.

- ✓ Stationary 3-phase abc quantities into stationary 2-phase quantities(abc to $\alpha\beta$)
- ✓ Stationary 2-phase quantities into rotating(synchronous) 2-phase quantities ($\alpha\beta$ to dq)

The transformation is shown in the Fig. 3.18. The transformation help in controlling the real and the reactive power through the converter independently. For a VSC converter as shown in Fig. 3.14, the ac side voltage can be represented as (3.13).

$$V_{abc} = RI_{abc} + L\frac{d}{dt}I_{abc} + V_{abc,conv} \tag{3.13}$$

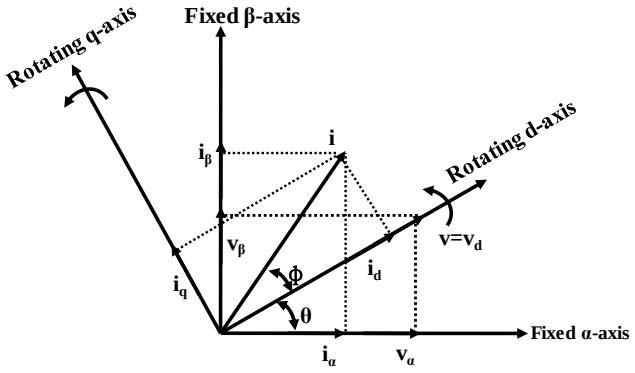

Figure 3.18: *Axes transformation in vector control*

Transforming (3.13) from abc to dq reference frame and equating the power of DC and AC side by neglecting the losses, we get

$$P = \frac{3}{2} v_d i_d \tag{3.14}$$

$$Q = -\frac{3}{2} v_q i_q \tag{3.15}$$

(3.14) and (3.15) implies that the real power is a function of current and voltage in the d-axis, while reactive power depends on q-axis current and voltage. Therefore, the transformation of abc quantities from time variant coordinate system to rotating dq quantities of time invariant coordinate system allows to independently control the real and the reactive power through the VSC converter.

The schematic of vector based control as implemented for the AC/DC VSC converter is shown in the Fig. 3.19. The control of active and reactive power is realised through

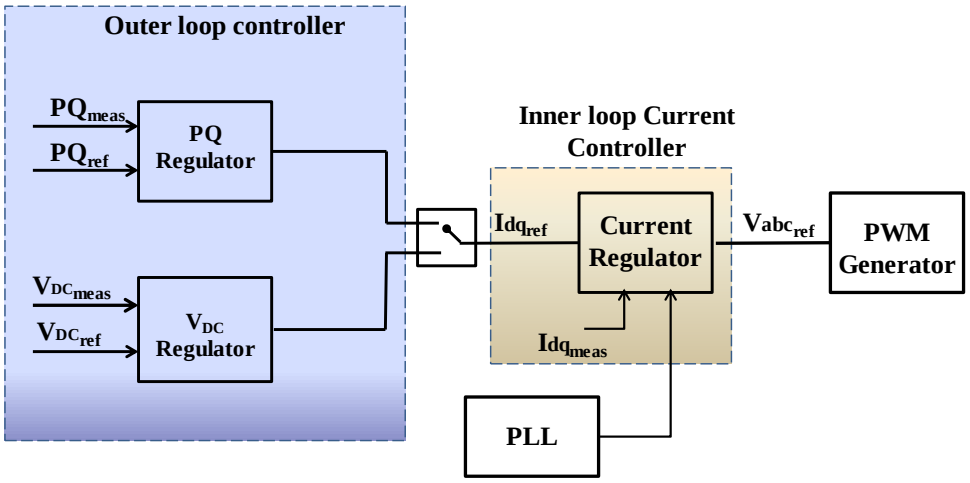

Figure 3.19: *Vector based control of AC/DC converter*

cascaded controller, with two PI control loops in cascade, one in outer control loop and other in inner current control as shown in the Fig. 3.19. The ac current references are

supplied by outer controllers. The outer controllers include the dc voltage controller, the active power controller and the reactive power controller, depending upon the application. The outer loop regulates PQ and V_{DC} reference by calculating the active and reactive current reference for the inner loop, while the inner current controller calculates the required AC voltage reference for the PWM [38]. The reference value for active current(d current) can be provided by DC voltage regulator or the active power regulator, while the reference value for reactive current is provided by reactive power controller. The output of the two PI controller gives the voltage reference for the PWM generator, which in turn produce the necessary gate signals by comparing it with a triangular carrier signal with fixed amplitude and frequency.

Inner loop controller

The schematic of inner loop controller is shown in the Fig 3.20.

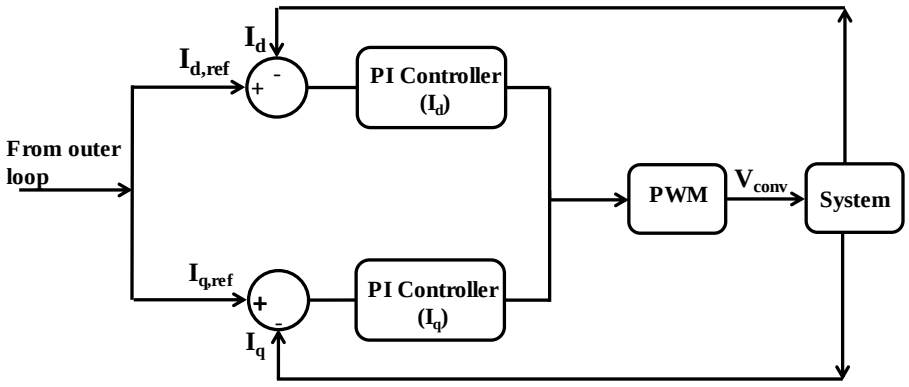

Figure 3.20: *Inner current controller loop*

The gain of the PI controller are tuned using modulus optimum (MO) criteria [39] - [40]. The MO criteria is applied to a system having one dominant time constant. The gains of the PI controller and hence the transfer function is obtained as follows.

1. Cancelling the largest time constant of the open loop transfer function of the complete system
2. Maintaining the closed loop gain to unity for very higher frequencies

The open loop transfer function of the inner loop for the system shown in the Fig. 3.20 is given by

$$G_{IL} = K_P \frac{1+T_i s}{T_i s} \frac{1}{1+T_a s} \frac{1}{R} \frac{1}{1+\tau s} \tag{3.16}$$

Applying the first point of modulus optimum criteria, we get Ti=τ. The closed loop transfer function of the system after cancelling pole and zero of the transfer function using the 1^{st} point given by

$$G_{CL} = \frac{\frac{K_P}{\tau R T_a}}{s^2 + \frac{1}{T_a} s + \frac{K_P}{\tau R T_a}} \tag{3.17}$$

Evaluating for the 2^{nd} point of modulus optimum criteria, $K_P = \frac{\tau.R}{2.T_a}$ is obtained.

Outer loop controller

As mentioned earlier, outer loop controller could be P, Q or V_{DC} depending on the application. The block diagram of outer loop controller is shown in the Fig. 3.21. The

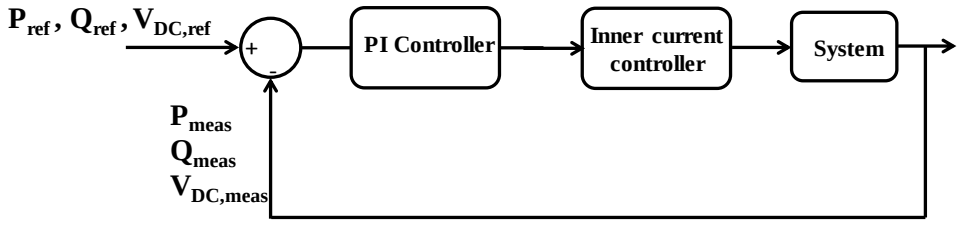

Figure 3.21: *Outer loop controller*

output of the controller, which is active or reactive current, is fed as the input reference for the inner loop. The gain of the PI controller are tuned using symmetric optimum criteria [40] - [41]. The criteria is usually applied to a cascaded controlled system for tuning outer loop. When one or more poles of the system is close to origin, pole-zero cancellation cannot give a satisfactory result. In this case, tuning criteria is obtained using the Nyquist criteria of stability and finding the frequency for which maximum phase margin occurs. The Nyquist criteria for stability is given by (3.18).

$$\begin{aligned} |G_{OL}(j\omega)| &= 1 \\ \angle G_{OL}(j\omega) &= -180^o + \phi_M \end{aligned} \tag{3.18}$$

where ϕ_M is the phase margin. A higher phase margin indicates more stable system. The overshoot and the settling is minimised by selecting optimum damping coefficient.

3.4.3 Simulation Model of the DC/AC/DC converter

A 2000MW, 400kV converter was simulated in MATLAB Simulink, using SimPowerSystems toolbox. The Simulink model is shown in the Fig. 3.22. The controller gains are

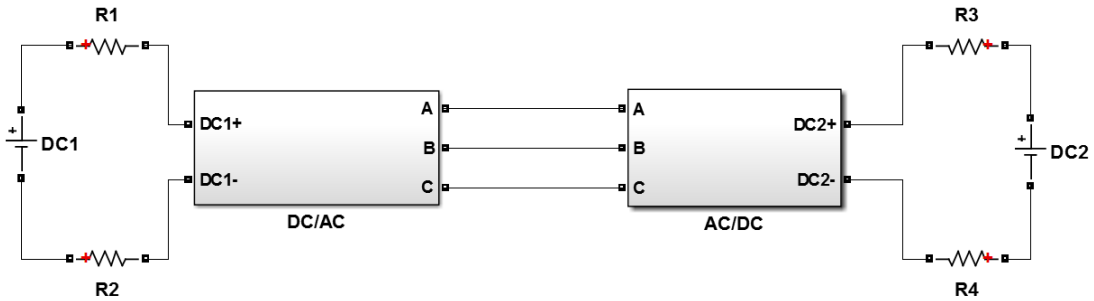

Figure 3.22: *Simulink Model of DC/AC/DC Converter*

calculated using the symmetric optimum and modulus optimum criteria and are tabulated

in the Table 3.4. Case scenarios with different power flow setting are simulated for both average and switching model.

Table 3.4: *PI Controller Parameters*

	$\mathbf{K_P}$	$\mathbf{T_I}$
Inner controller	4	0.04
Outer controller	10	0.001

Results with Average Model

In order to verify the bi-directionality, a case is considered where power flow setting changes from -600MW to 300MW at t=2.5s. The DC waveforms are plotted in Fig. 3.23. As evident from the Fig. 3.23, DC voltage remains constant, while DC current

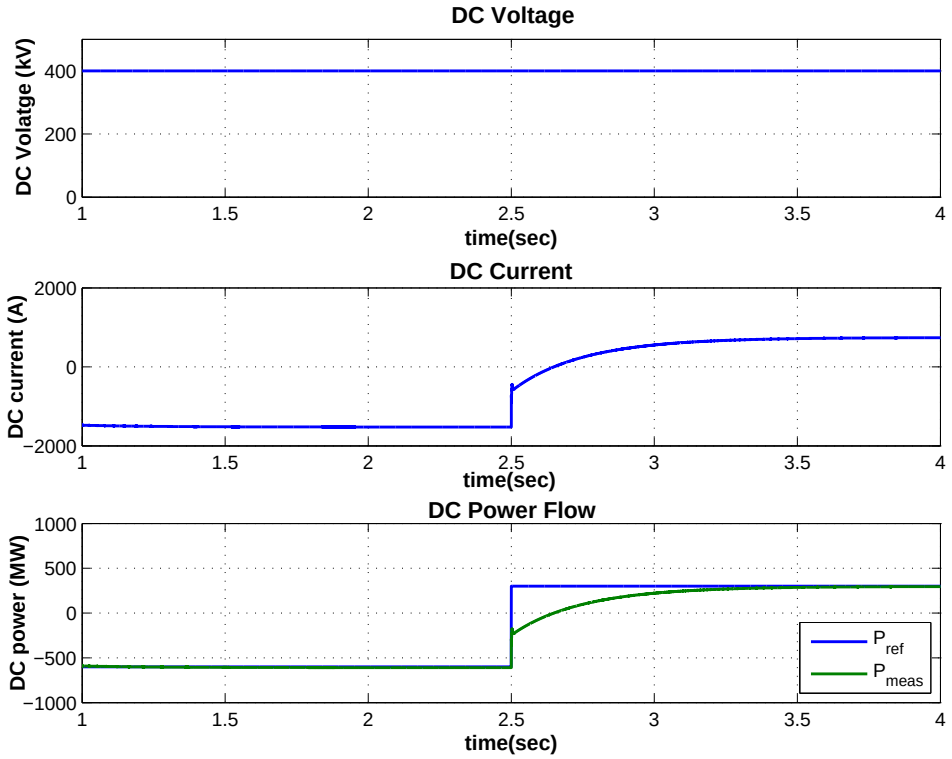

Figure 3.23: *DC Waveforms using Average Model*

changes according to the setting. The controller tracks the reference power with very small overshoot and settling time. As explained earlier, the reference for the inner loop, $I_{dq,ref}$ is the output of outer loop. Since our objective is to control the active power, only I_d will be affected. The active current is hence plotted and is shown in the Fig. 3.24. As expected, the measured current is in-line with the reference value. The voltage reference to the IGBT switches are also plotted in the Fig. 3.25. The intermediate AC system is designed for 50Hz fundamental frequency. The voltage controller sets the amplitude of voltage for the AC signal, while power setting determines the current. The AC voltage

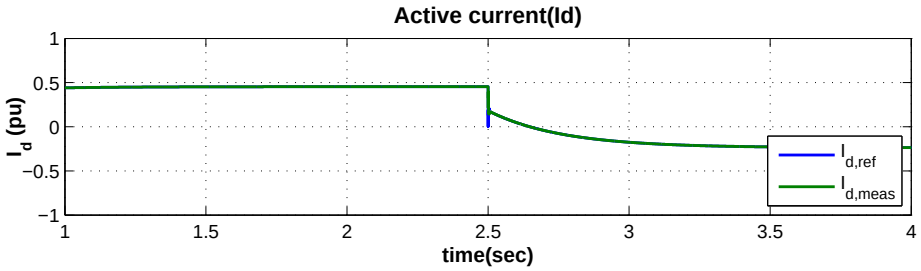

Figure 3.24: *Active current for the inner loop*

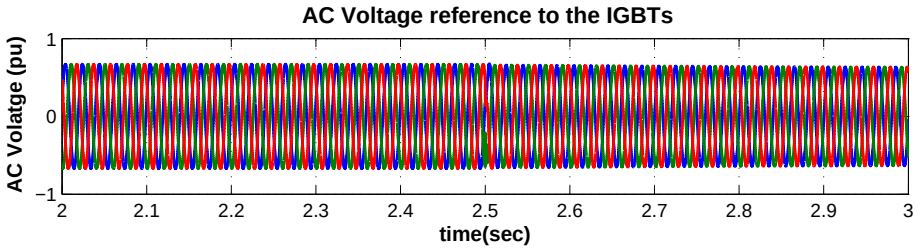

Figure 3.25: *Voltage reference to the IGBT switches*

and current are measured and are shown in the Fig. 3.26. Simulation using average model

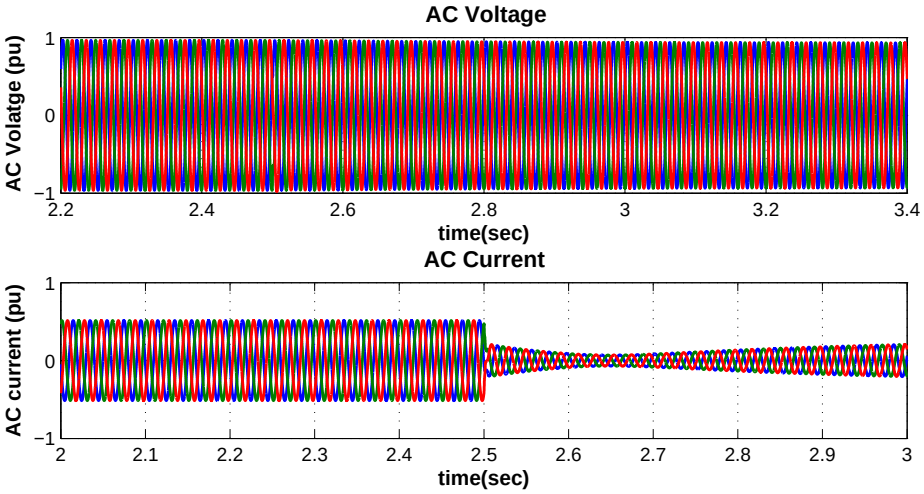

Figure 3.26: *AC Waveforms using Average Model*

is very fast and hence less time consuming.

Results with Switching Model

The earlier case is then simulated using developed switching model. Due to the effect of discontinuous switching schemes, harmonics are now introduced into the system. The DC waveforms thus obtained are shown in the Fig. 3.27. Due to the harmonics generated due to switching of power electronic devices, the waveforms are distorted. The voltage and current wave forms of AC system is also plotted in the Fig. 3.28. The simulation is

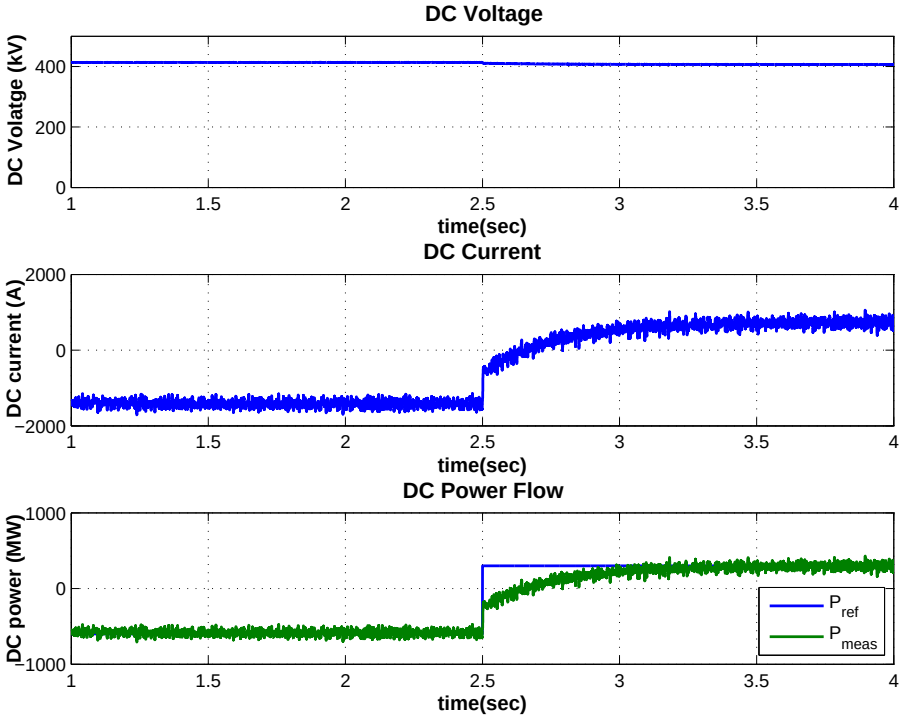

Figure 3.27: *DC Waveforms using Switching Model*

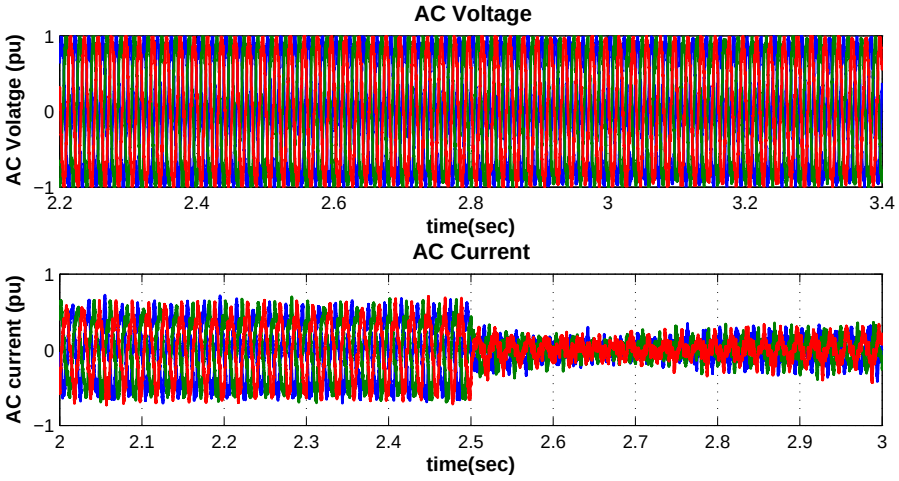

Figure 3.28: *AC Waveforms using Switching Model*

time consuming due to the switching schemes and introduces harmonics. However, proper designing of filters could results in reducing the harmonics in the system.

Chapter 4

DC/DC Converter with Galvanic Separation

This chapter presents the second class of DC/DC converters for interconnecting independent HVDC systems into multi-terminal HVDC grid. A literature review on various converter topologies of this class are presented before particular attention is dedicated to transformer coupled DC/AC/DC converters. The chapter further presents converters suitable for interconnecting DC systems with different voltages and different configurations

4.1 Introduction

The exponential growth in offshore energy installations and other renewables coupled with deregulated energy markets, has resulted in more attention towards VSC based HVDC system that can eventually evolve in the interconnection of existing point-to-point HVDC connections. However, due to the lack of standard HVDC voltage for the power transmission, most existing HVDC schemes are operating at different voltages and it is not a straightforward task to interconnect these systems. AC systems also operate in different voltages. However, a transformer with its capability to transform voltage/current to any ratio with high efficiency makes it very simple. Therefore similar kind of devices are also required in DC systems to perform the operation of AC transformer. Another challenge in DC system is the operation of systems in various configurations. A submarine HVDC cable transmission system with moderate power requirement utilises monopole configuration, while offshore wind farms with the need of high power corridor and increased reliability has made use of bipolar configuration. The above two different HVDC configurations cannot be interconnected as such and need some interconnecting devices. A DC/DC converter in addition to the power flow control as described in the previous chapter could be utilised for performing the above function. This chapter in detail analyses various galvanically isolated converter topologies used for the interconnection of high voltage ratio systems.

4.1.1 Galvanic separation

Galvanic separation is defined as "prevention of electric conduction between two electric circuits intended to exchange power and/or signals" [21]. A DC/DC converter with galvanic separation therefore blocks the direct current path between two interconnected subsystems. Consider a DC/DC converter interconnecting two DC systems with bipolar configuration. In the event of pole-to-ground fault in one pole would result in pole-to-ground voltage of the other pole to become double [21]. In the absence of galvanic isolation, this voltage doubling will be transferred to the other side of DC/DC converter. Therefore, DC/DC converter in this case provides a path to propagate the fault generated in one side to other. In a low voltage ratio connection, the power electronic switches of the converter are rated for withstanding this higher voltage as the voltage transfer is not excessive. However, this becomes a serious issue for a high voltage ratio connection. When a galvanic isolation in the form of transformer is introduced between the two subsystems, the direct connection between the systems is blocked and hence the transfer of voltage stress is avoided. Instead, it is then exchanged to the transformer.

In a transformer with separate windings between primary and secondary side, there is no direct electrical connection between the primary and secondary windings. Instead, they are magnetically coupled to each other through the magnetic core of high permeability and therefore could be an effective solution for galvanic isolation.

4.2 Different topologies

The DC/DC converters with galvanic separation could be broadly classified as

1. Transformer coupled DC/AC/DC converter
2. Converter with soft switching schemes

Various topologies for above types are discussed in the literature and some of these topologies will be analysed in the coming section.

4.2.1 Transformer coupled DC/AC/DC Converter

Transformer coupled DC/AC/DC converter converts first a DC into an intermediate AC stage. The AC stage is composed of a transformer and therefore step up/step down the signal according to the requirement. The transformed signal is converted back to DC. A general schematic of the converter is shown in the Fig. 4.1. The voltage at each converters are developed by the interconnection of several switching devices in series.

The DC/AC/DC converter could be either Two level converter or Modular multi-level converter (MMC). The schematic of transformer coupled converter with MMC is shown in Fig. 4.2. As compared to two level converter, modular topology provides low switching rates, redundancy and increased reliability. Either of the full H-bridge or half H-bridge could be used as a module for the converter.

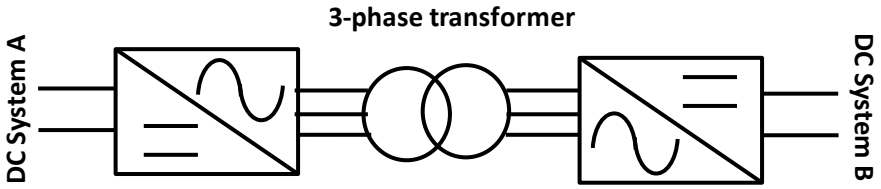

Figure 4.1: *DC/DC converter with transformer coupling*

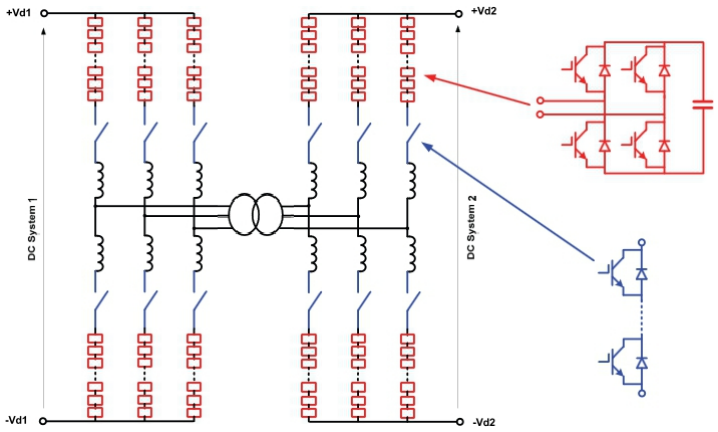

Figure 4.2: *Modular Multi-level DC/DC Converter with transformer coupling [21]*

4.2.2 Resonant DC/DC Converter

The DC/DC conversion in a Bi-directional Resonant DC/DC converter is achieved by utilising bi-directional thyristor valves, inductor and capacitors [42]. The circuit is shown in the Fig. 4.3. The converter could be used with VSC technology as the bi-directional power flow is achieved by changing the current polarity. The LC resonant circuit provides zero crossing of the current, which implies natural commutation and hence thyristors could be employed as the power electronic switching device. The operation of the converter in discontinuous conduction mode(DCM) along with the LC circuit provides soft switching and hence reduces the switching losses.

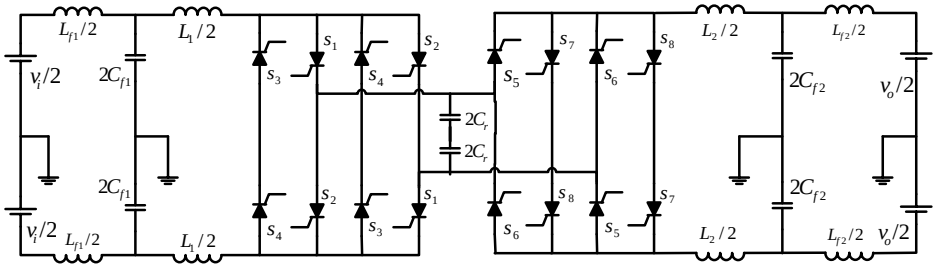

Figure 4.3: *Bidirectional Resonant DC/DC converter [42]*

4.2.3 Resonant(ZVS) Bi-directional DC/DC Converter

Zero voltage switching(ZVS) bi-directional DC/DC converter creates a resonant circuit using inductor and capacitors for performing the switching of power electronic switches at zero voltage so as to reduce the switching losses [43]. The circuit diagram of ZVS DC/DC converter is shown in the Fig. 4.4. The circuit consists of S1 to S6 switches at the low

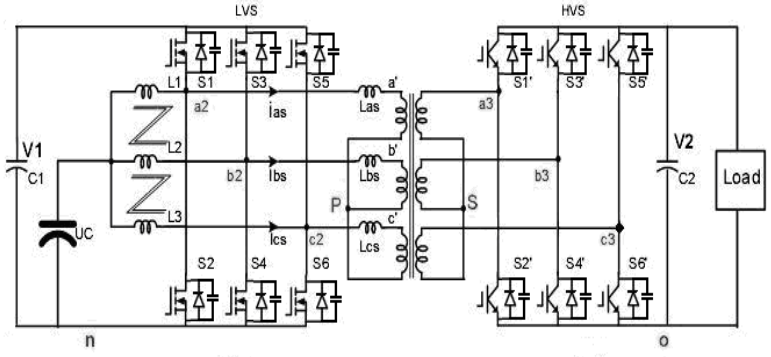

Figure 4.4: *ZVS Bidirectional DC/DC Converter [43]*

voltage side and S1′ to S6′ at high voltage side. The phase inductance L1 to L3 along with the switches forms a boost circuit. The voltages of the interconnecting systems determines the transformation ratio of transformer. By making a phase shift angle between LVS and ZVS, power can be transferred between two sides, with the direction of the power transfer determined by the sign of the angle and the quantity, determined by the angle magnitude.

Out of the above converter topologies, Transformer coupled DC/AC/DC converter is analysed in greater detail and discussed in the following section.

4.3 Design and Modelling of Transformer coupled DC/AC/DC Converter

The switching model of a transformer coupled DC/AC/DC converter is shown in the Fig. 4.5. The model consists of 2 AC/DC converters interconnecting 2 DC systems of different voltage. The converters are coupled using a transformer. Each converter leg consists of power electronic switches and anti-parallel diodes. Due to the switching of power electronics, filters are required to reduce the harmonics in the system. A transformer coupled DC/AC/DC converter could be utilised for the following purpose.

- ✓ Interconnecting DC subsystems with different voltages
- ✓ Interconnecting DC subsystems with different configurations
- ✓ To control the power flow between two subsystems

As mentioned in the previous chapter, a 3-phase AC system is preferred as the intermediate stage over 1-phase system to match the through-put capability of HVDC system.

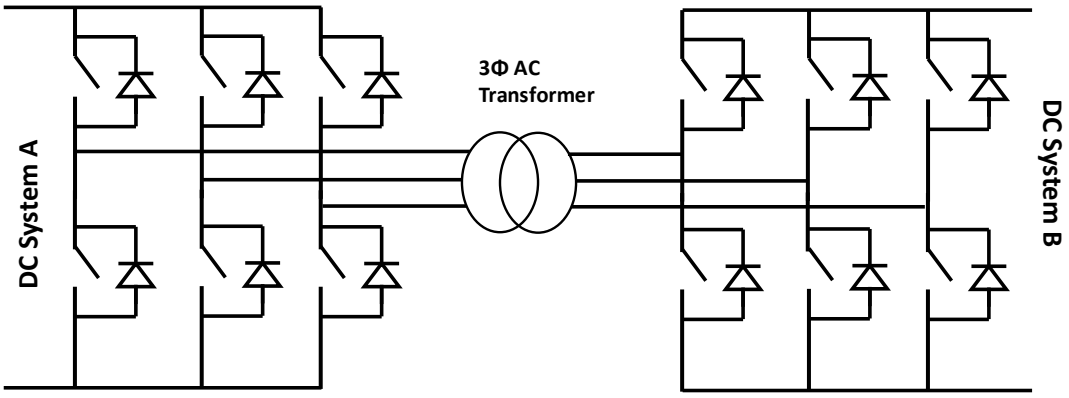

Figure 4.5: *Switching model of transformer coupled DC/AC/DC converter*

Interconnecting systems with similar configuration and different voltage

When two DC systems with different voltages operating both in similar configuration(i.e, either bipole or monopole) need to be interconnected, a high conversion ratio DC/AC/DC converter as shown in Fig. 4.5 can be used. The high conversion ratio is achieved through the coupling transformer, which also provides the galvanic separation. The converter provides the additional flexibility of controlling the power flow between the two interconnected subsystems. The average model is also studied for implementing in a large MTDC system. The average model developed is shown in the Fig. 4.6. Each converter is a modelled as current source on the DC side behind a capacitor and a voltage source on the DC source behind an inductor. Since the transformer involves no switching devices, the model of the transformer remains the same.

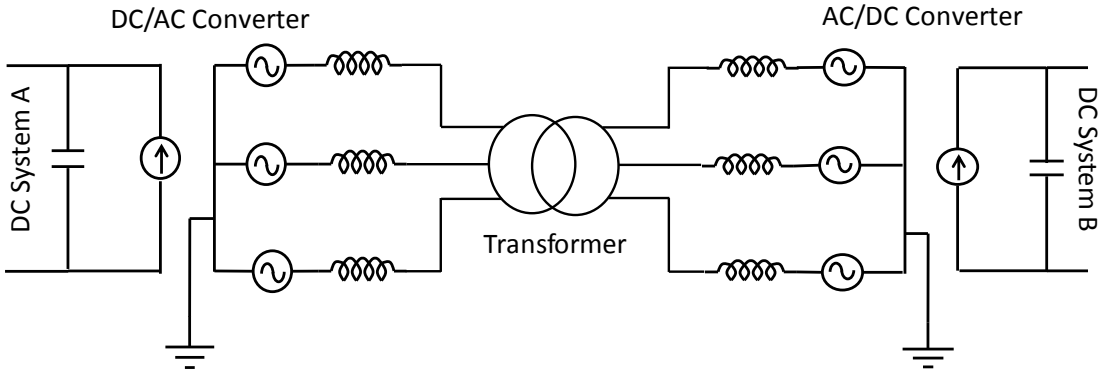

Figure 4.6: *Average model of transformer coupled DC/AC/DC converter*

Interconnecting systems with different configuration

The model described in the previous section is intended for interconnection of two systems of similar configuration. The converters in a DC system can be connected in different ways. ie, asymmetric monopole, symmetric monopole or bipole. The interconnection

between bipolar configuration with metallic return and an asymmetric monopole system could be done as shown in the Fig. 4.7 provided that the voltage matches [44]. However,

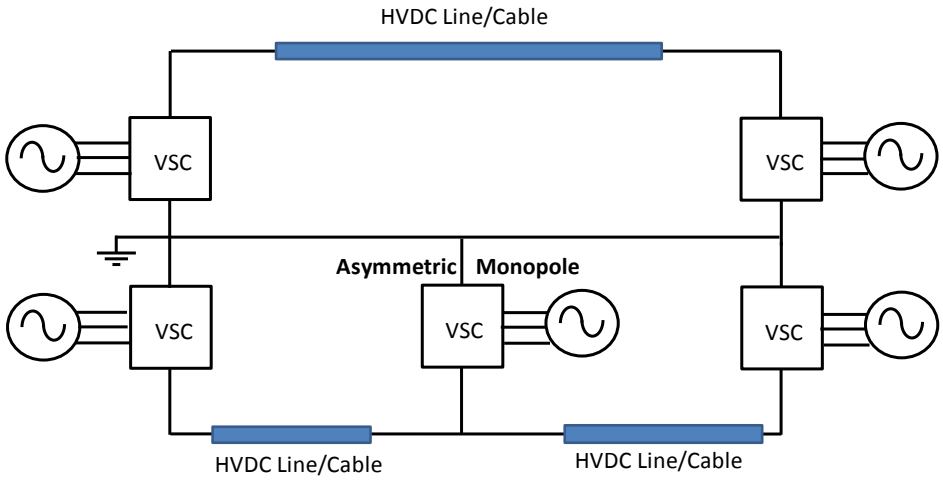

Figure 4.7: *Bipole system interconnected with asymmetric monopole system*

interconnection of any other system is challenging and difficult.

A DC/DC converter can be utilised to interconnect two DC subsystems of different configurations operating with different voltages. The interconnection of a bipolar configuration with monopole system operating in different voltages can be done in two ways.

- ✓ Using two separate 2-winding 3-phase transformers
- ✓ Using a single 3-winding 3-phase transformer

A schematic of DC/AC/DC converter with 2-winding transformer is shown in the Fig. 4.8. It has four AC/DC converters and two 2-winding transformers. Each converter and

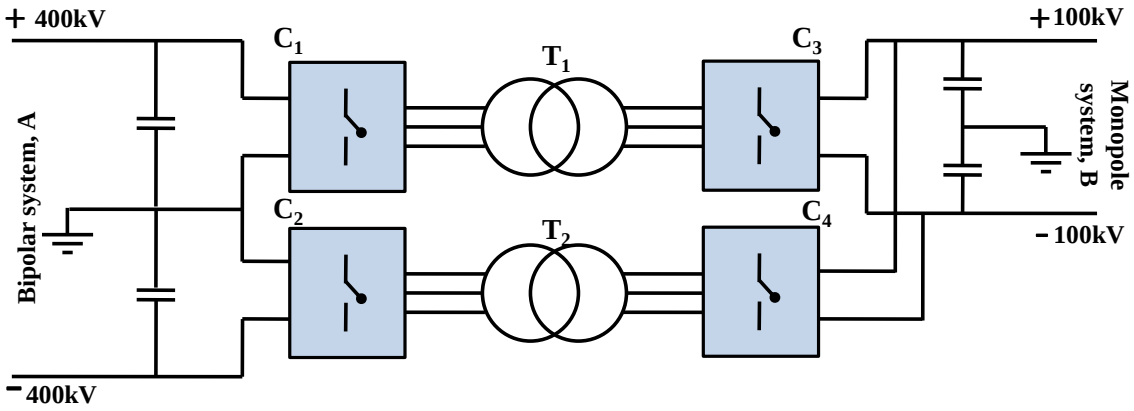

Figure 4.8: *DC/AC/DC Converter with 2-winding transformer*

transformer are rated for half the power rating of the total system. Table 4.1 shows the

Table 4.1: *Component ratings of the converter with 2-winding transformer*

Component	Name	Voltage rating (kV)	Power rating
Converter	C1	400	$P_{rated/2}$
Converter	C2	400	$P_{rated/2}$
Converter	C3	200	$P_{rated/2}$
Converter	C4	200	$P_{rated/2}$
Transformer	T1	400/200	$P_{rated/2}$
Transformer	T2	400/200	$P_{rated/2}$

rating of each converter and transformer for the interconnection of a bipolar system at A operating at ±400kV with symmetric monopole system operating at ±100kV at B.

All the components in the system are rated for half the rated power. The converters C1 and C2 are rated for half DC voltage at A, while C3 and C4 are rated for full DC voltage at B. A major drawback of this model is the larger number of components, which could result in increased space requirement and cost. The same interconnection could be also carried using one 3-winding transformer as shown in the Fig. 4.9. Fig. 4.9

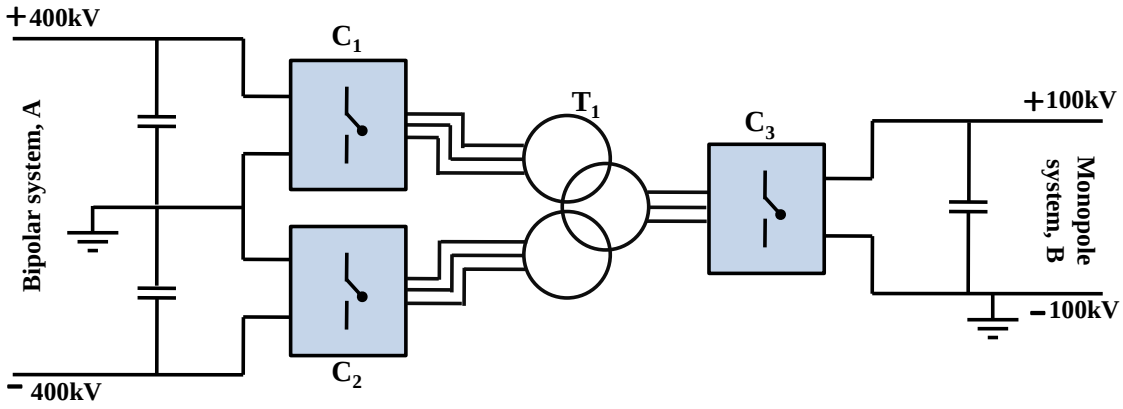

Figure 4.9: *DC/AC/DC Converter with 3-winding transformer*

shows that the number of AC/DC converters has come down to 3, while two 2-winding transformers are replaced by one 3-winding transformer. The rating of each component in this configuration is shown in Table 4.2. In this case, the converter at the B side and

Table 4.2: *Component ratings of the converter with 3-winding transformer*

Component	Name	Voltage rating (kV)	Power rating
Converter	C1	400	$P_{rated/2}$
Converter	C2	400	$P_{rated/2}$
Converter	C3	200	P_{rated}
Transformer	T1	400/200(both connections)	P_{rated}

the transformer are rated for full power, while the other converters are rated for half the rated power. This scheme is economical and also reduces the size of total system. Since the Simulink implementation and control philosophy for the both the types are almost the same, we have considered DC/AC/DC converter with 3-winding transformer in our

design. The average model of DC/AC/DC converter with 3-winding transformer is shown in the Fig. 4.10.

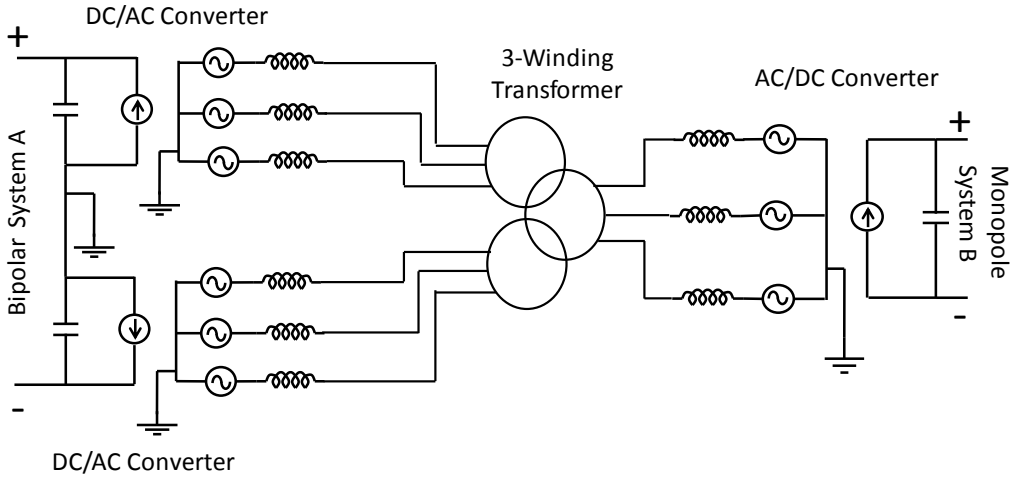

Figure 4.10: *Average model of DC/AC/DC Converter with 3-winding transformer*

4.3.1 Transformer design in DC/AC/DC Converter

Transformers in DC/AC/DC converters are required for

- ✓ Providing galvanic separation between two sides
- ✓ Stepping up/stepping down of voltage/current

A transformer is designed for an optimum size, efficiency and cost for the rated electrical parameters like power, voltage, frequency etc. However, as the intermediate AC system is only intended for the conversion, a convenient operating frequency could be selected providing an additional degree of freedom. The size of transformer is related to its operating frequency by (4.1) [45].

$$EMF = 4.44fBNA \tag{4.1}$$

where f, B, N & A represents the operating frequency, flux density, number of turns and cross sectional area of the core respectively. Eq. (4.1) states that size is inversely proportional to the operating frequency. Therefore, a higher frequency operation could substantially reduce the volume of transformer. In addition, it also helps in reducing the size of the components in the DC/AC converters, say capacitors. However the maximum switching frequency is restricted by the core design. The magnetic core is a material with high permeability that provides the path for flux to flow from primary to secondary side of a transformer. A 50HZ high power transformer utilises cold rolled grain oriented(CRGO) iron cores due to its very low core losses. Core losses are classified as hysteresis loss and eddy current loss. Hysteresis and eddy current losses are related to the operating

frequency by (4.2).

$$\begin{aligned} P_{Loss,Hyst} &\propto fB^{1.6} \\ P_{Loss,Eddy} &\propto f^2B^2 \\ P_{Total\ core\ loss} &= P_{Loss,Hyst} + P_{Loss,Eddy} \end{aligned} \tag{4.2}$$

Various core materials and different grades of ferrite, amorphous, nano crystalline materials, Vitroperm, etc. [46]-[47] are proposed in the literature for high frequency applications. However, the immaturity in the development of special materials for the core for higher power applications has restricted the maximum frequency of transformer design. The transformer in the model can be operated with any kind of alternating signals like sinusoidal, trapezoidal or square wave. However, the converter also has to be integrated and controlled accordingly. The wave shape is chosen for an optimum component rating and converter losses. A typical 3-phase transformer is shown in the Fig. 4.11 [48].

Figure 4.11: *3-phase transformer(ABB make) [48]*

4.4 Controller design

For dissimilar voltage interconnection, Vector based control strategy as explained in Chapter 3 is used to control the power flow in one converter, while the other is set using voltage controller as shown in the Fig. 4.12. The system and the controller is implemented in per unit and controller parameters are calculated using modulus optimum and symmetric optimum. The voltage controller is set with a modulation index of m_a=0.95 and a control signal of 3-phase sinusoidal signal. As explained earlier, the AC intermediate stage could be implemented with higher frequency and any alternating waveforms. However for implementation in Simulink, we have considered 50Hz sinusoidal AC system.

For the DC/AC/DC converter with 3-winding transformer used for interconnecting two different configurations, converters at bipolar side use active power control using vector

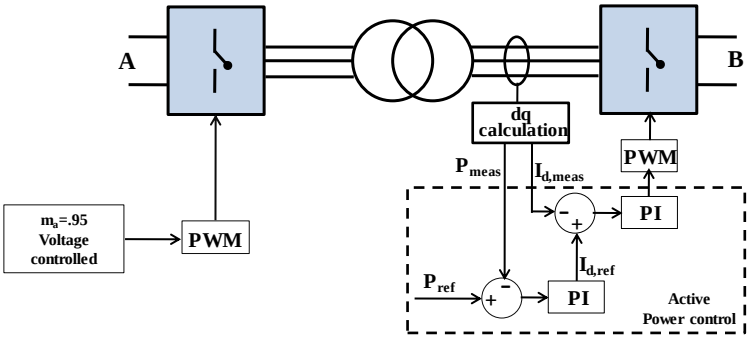

Figure 4.12: *Control strategy for Transformer coupled DC/AC/DC Converter*

control method for power regulation, while the converter at monopolar side is set with voltage controlled as shown in the Fig. 4.13. This arrangement allows the independent control of the power flow in each pole of bipolar configuration.

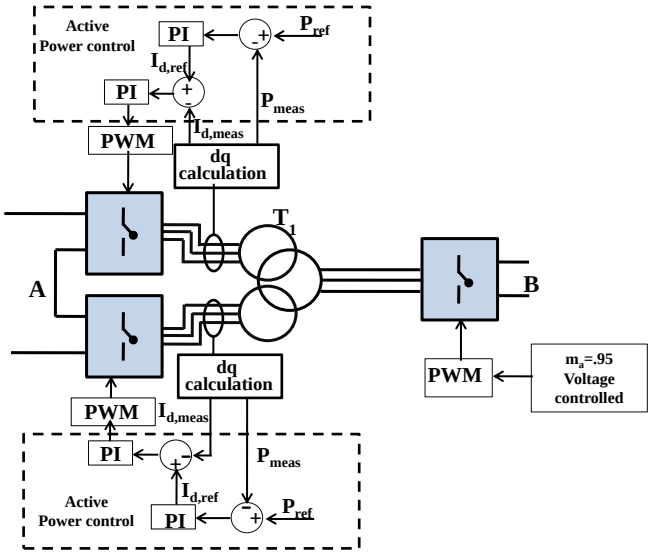

Figure 4.13: *Control strategy for DC/AC/DC Converter with 3-winding transformer*

4.5 Simulation Results

The simulation models using both average and switching models are implemented for the two types of DC/AC/DC converter discussed above.

4.5.1 Results of DC/AC/DC converter for interconnecting systems with dissimilar voltages

A 2000MW, 400/200kV converter was implemented in MATLAB Simulink, using SimPowerSystems toolbox. The converter interconnects two DC systems of 400kV and 200kV

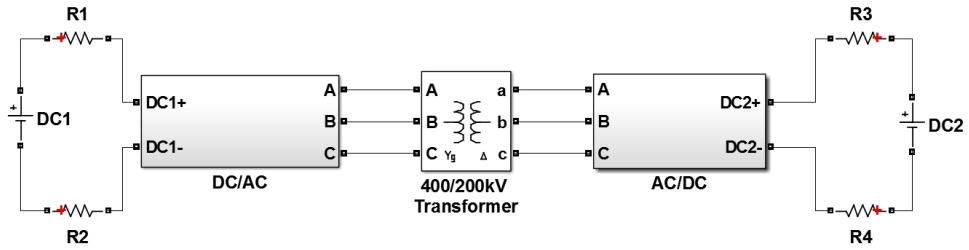

Figure 4.14: *Simulink model of Transformer coupled DC/AC/DC converter*

DC voltage. The Simulink model is shown in the Fig. 4.14. As explained earlier, in addition of providing an interconnection, transformer coupled DC/AC/DC converter also provides the flexibility of power control. Therefore, various case scenarios were considered to verify the power flow control in both directions. The results of a case, wherein change of power reference from -800MW to 400MW at t=2.5s using average model are plotted in Figs. 4.15 and 4.16. The DC power in both the Figs. 4.15 and 4.16 are almost the

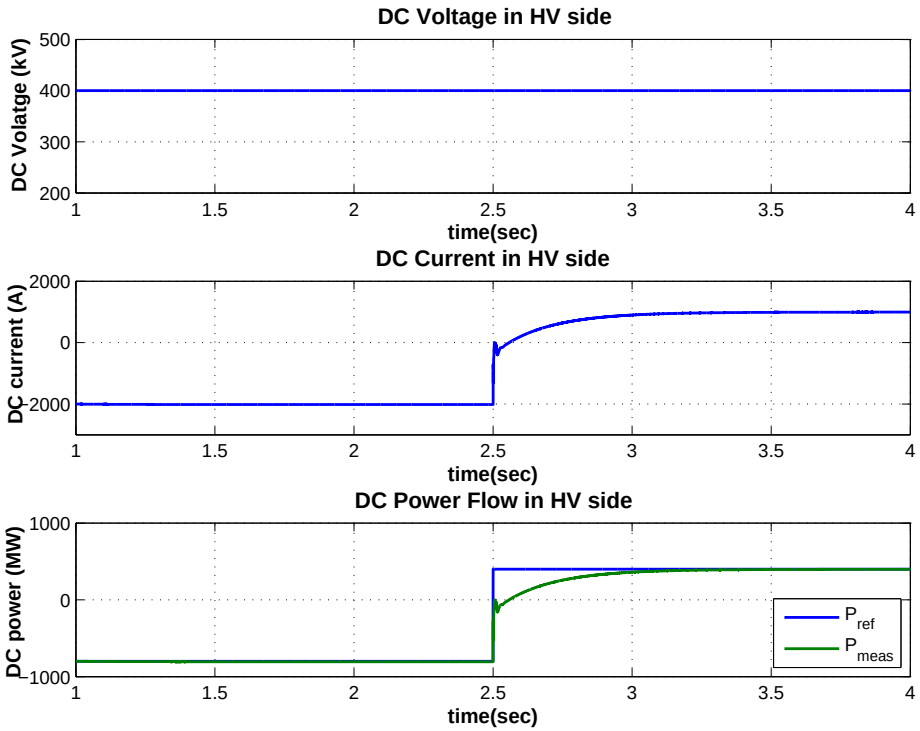

Figure 4.15: *HV side DC Waveforms using Average Model*

same, while the magnitude of voltage and current depends on the interconnected DC system. It is evident from the figures that DC voltage remains constant, while DC current changes according to the setting. The controller tracks the reference power with very small overshoot and settling time. As explained earlier, the reference for the inner loop, $I_{dq,ref}$ is the output of outer loop. Since our objective is to control the active power, only I_d will be affected. The active current is hence plotted and is shown in the Fig. 4.17. The intermediate AC system is connected with a transformer. The AC voltage and

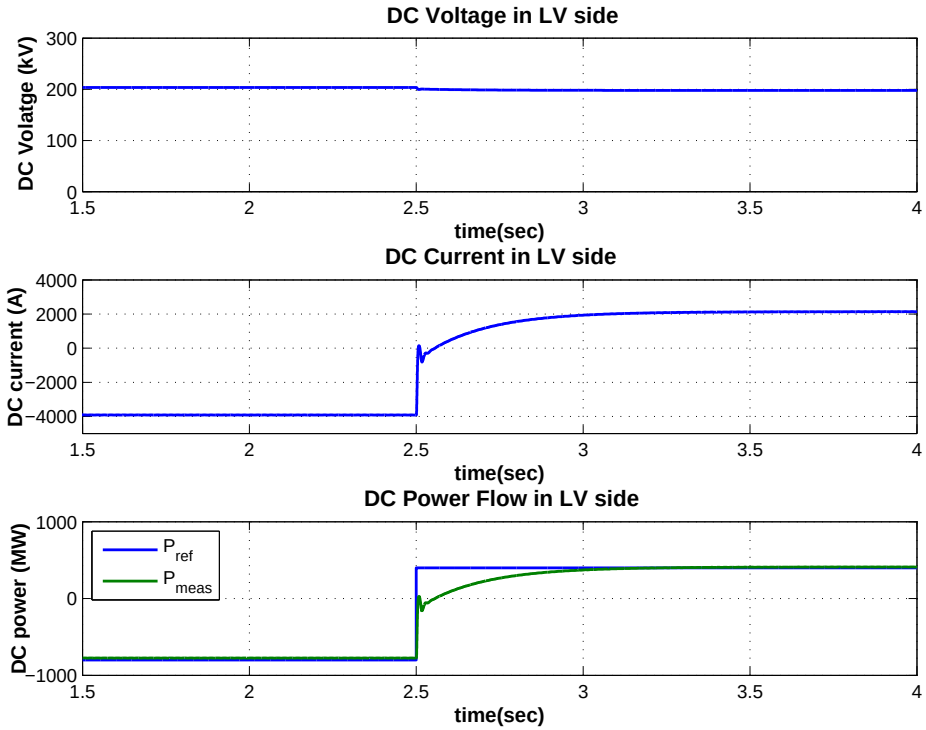

Figure 4.16: *LV side DC Waveforms using Average Model*

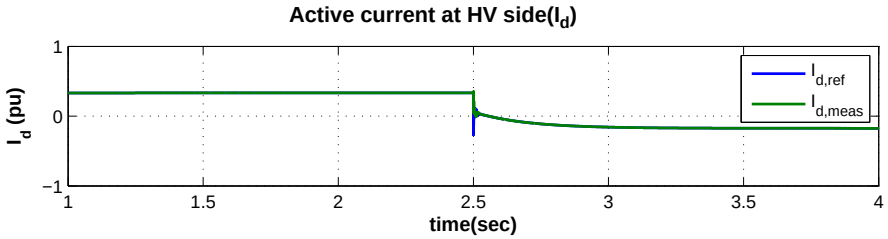

Figure 4.17: *Active current for the inner loop*

current at both the HV side and LV side are measured and are shown in the Figs. 4.18 and 4.19 respectively. It is evident from the plot that the magnitude of voltage is set by modulation index m_a, which is kept constant, while the current value changes according to the power reference.

The simulation is then carried out with switching model also and the results are plotted in the Fig. 4.20. The controller tracks the reference with high switching harmonics. The harmonics could be reduced by proper designing of filters. The AC voltage and current at both the HV side and LV side are also plotted in the Figs. 4.21 and 4.22

4.5.2 Results of DC/AC/DC converter for interconnecting systems with dissimilar configurations

A 2000MW converter with 3-winding transformer was implemented in MATLAB Simulink, using SimPowerSystems toolbox. The converter interconnects two DC system of which,

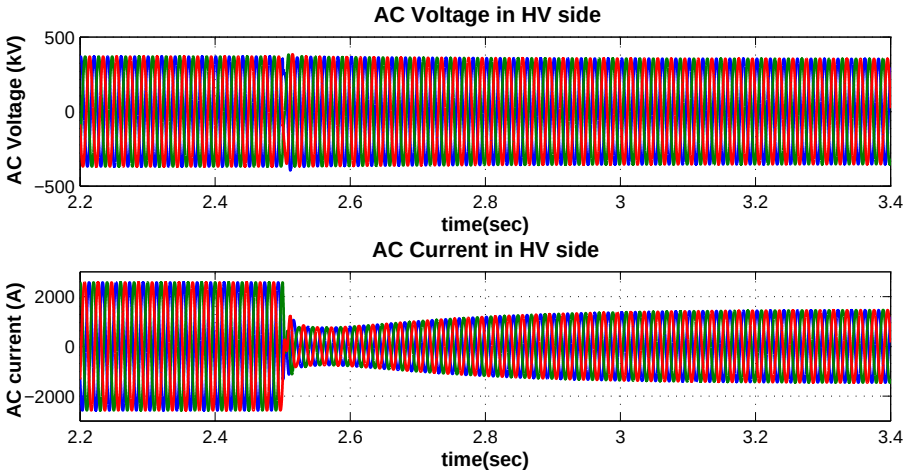

Figure 4.18: *AC Waveforms at HV side using Average Model*

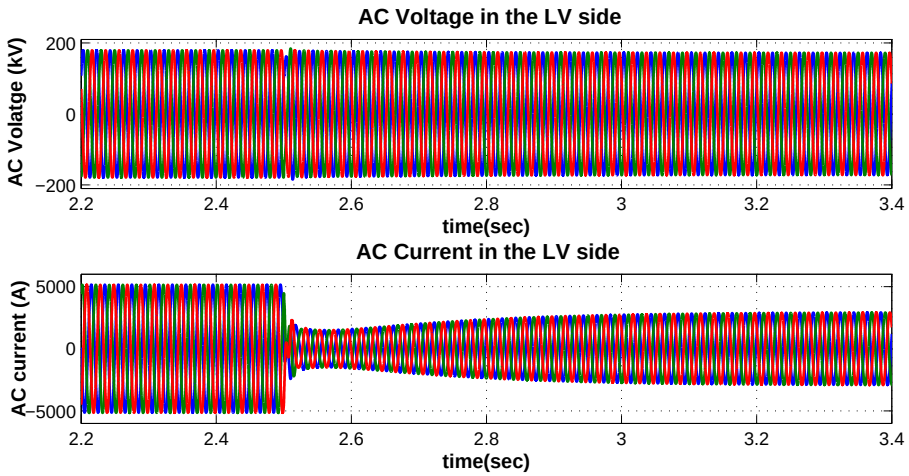

Figure 4.19: *AC Waveforms at LV side using Average Model*

one DC system is ±400kV bipolar configured, while other system is ±100kV symmetric monopolar. 3-phase transformer is rated for 2000MVA, with both the connection between bipolar to monopolar side voltage rated for 400/200kV. Simulation is carried out to verify the functionality and power control. The DC output response for the case, wherein change of power reference from -500MW to 300MW at t=2.5s are plotted in the Figs. 4.23 and 4.24. As explained earlier and from the Fig. 4.23, it is understood that each pole of the bipolar configuration carries half of the total power, while the monopole carries the full rated power. The controller tracks the reference without much overshoot. The AC waveforms at both sides of 3-winding transformer are also shown in the Fig. 4.25 and 4.26.

Fault in one pole of Bipolar side

The controller design with independent active power control in the bipolar side and voltage controller in monopolar side, allows a local control of power flow through each pole of the bipolar side, as discussed in section 4.4. This can demonstrated considering a fault

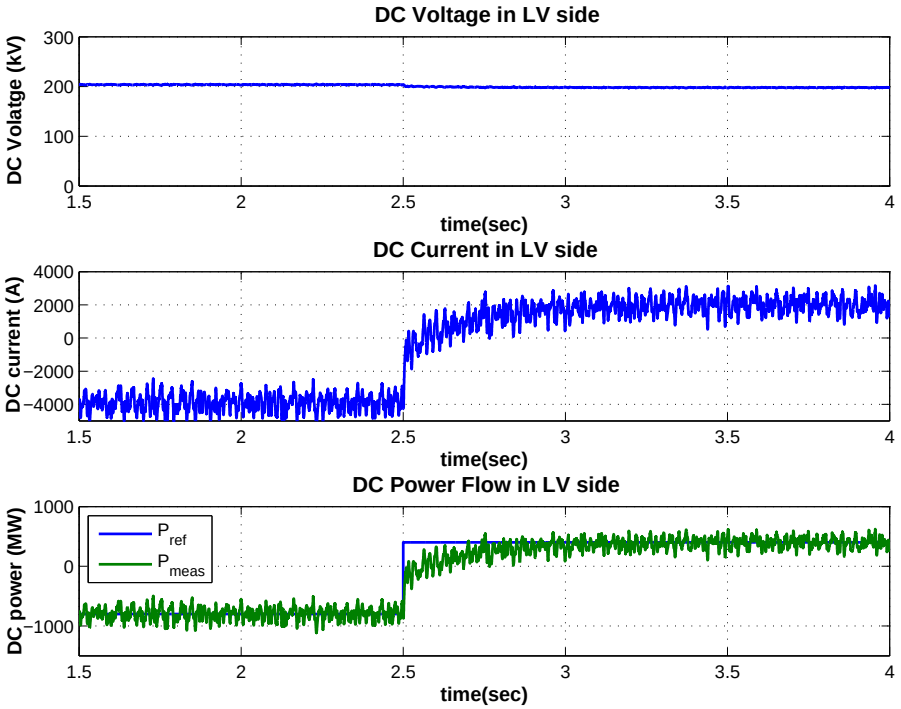

Figure 4.20: *LV side DC Waveforms using Switching Model*

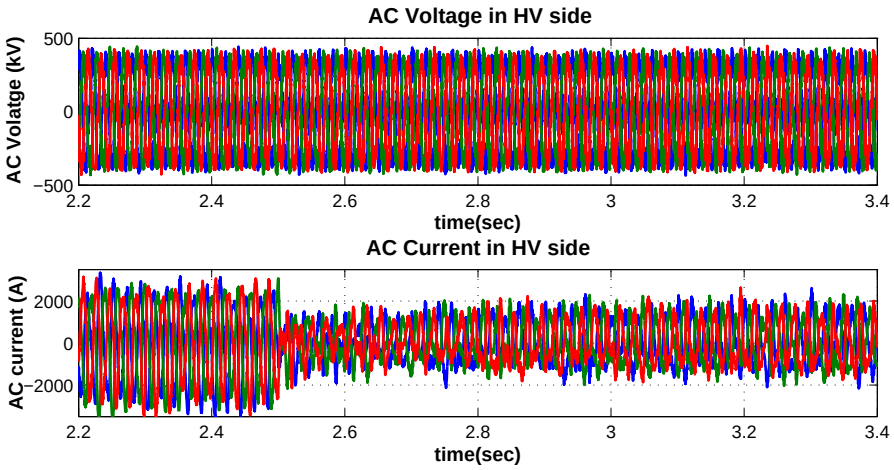

Figure 4.21: *AC Waveforms at HV side using Switching Model*

scenario. Consider a case, where both converters at the bipolar side is carrying 200MW until one pole is tripped due to a fault at t=2s. The simulation results are shown in Figs. 4.27, 4.28 and 4.29

The converter still could transmit the total power of 400MW (200MW+200MW), by setting the power reference of healthy pole to total power. As shown in the Fig. 4.28, the power flowing through healthy pole is 400MW from t=2.5s, until the other pole is taken into service after clearing the fault at t=4s.

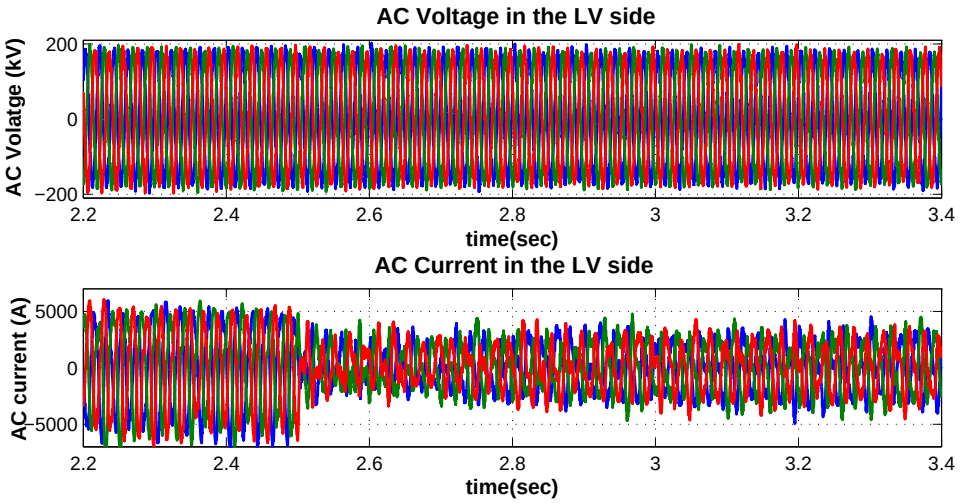

Figure 4.22: *AC Waveforms at LV side using Switching Model*

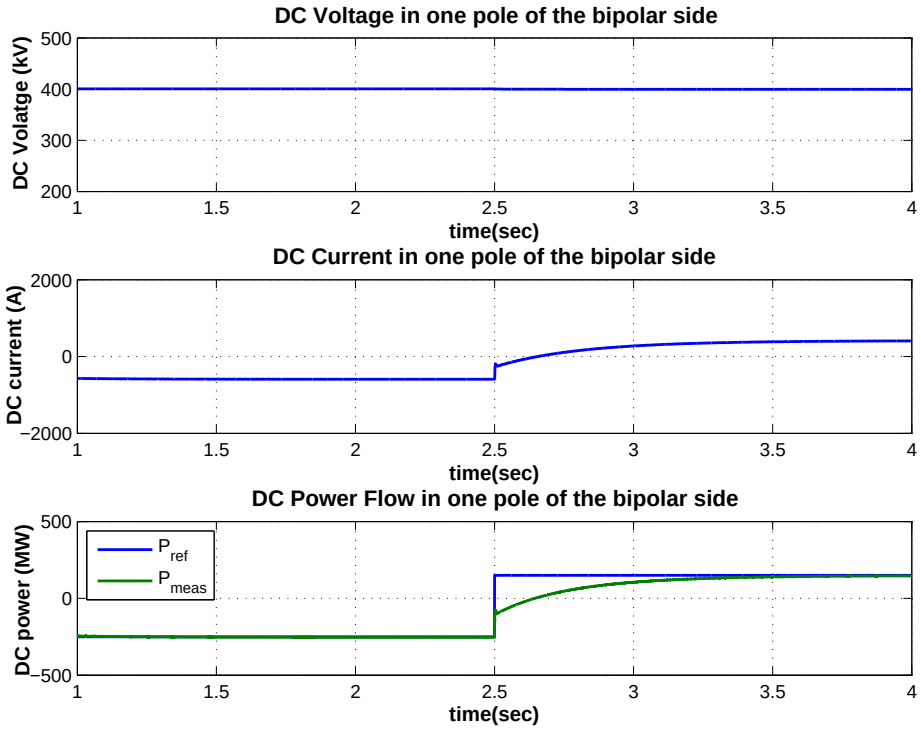

Figure 4.23: *Bipolar side DC Waveforms using 3-winding transformer (one pole)*

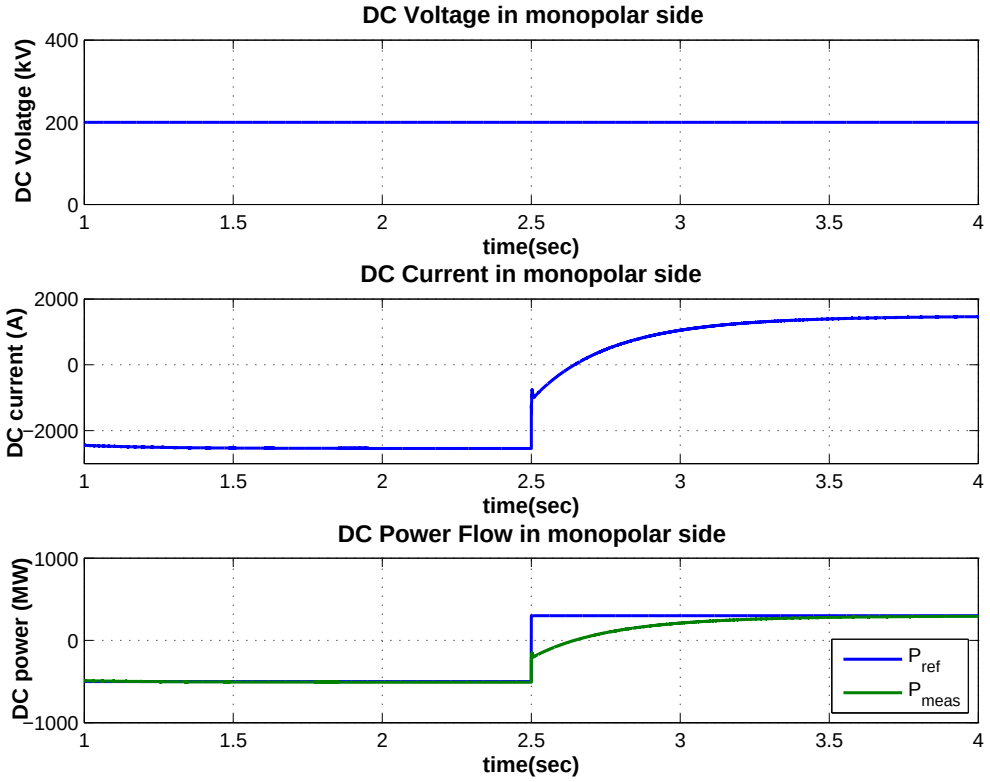

Figure 4.24: *Monopolar side DC Waveforms using 3-winding transformer*

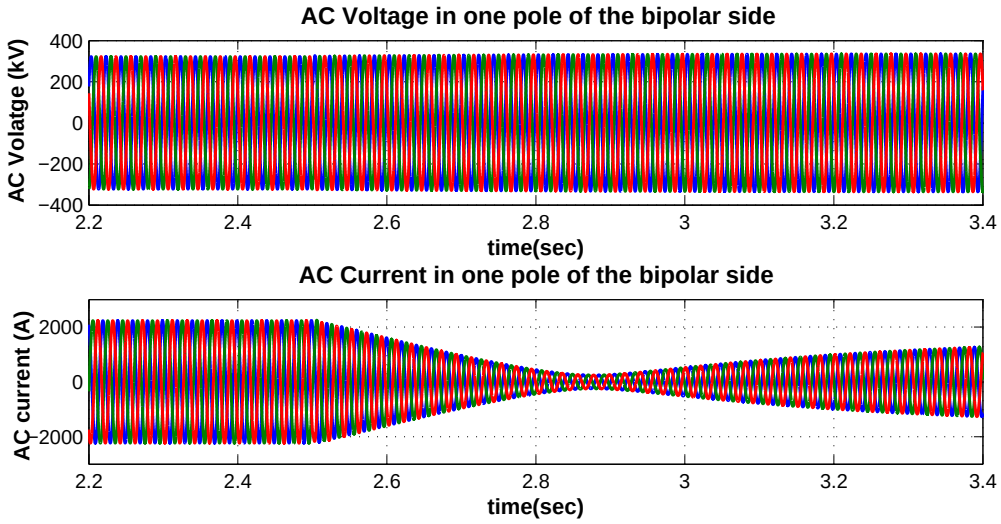

Figure 4.25: *AC Waveforms at Bipolar side of 3-winding transformer (one pole)*

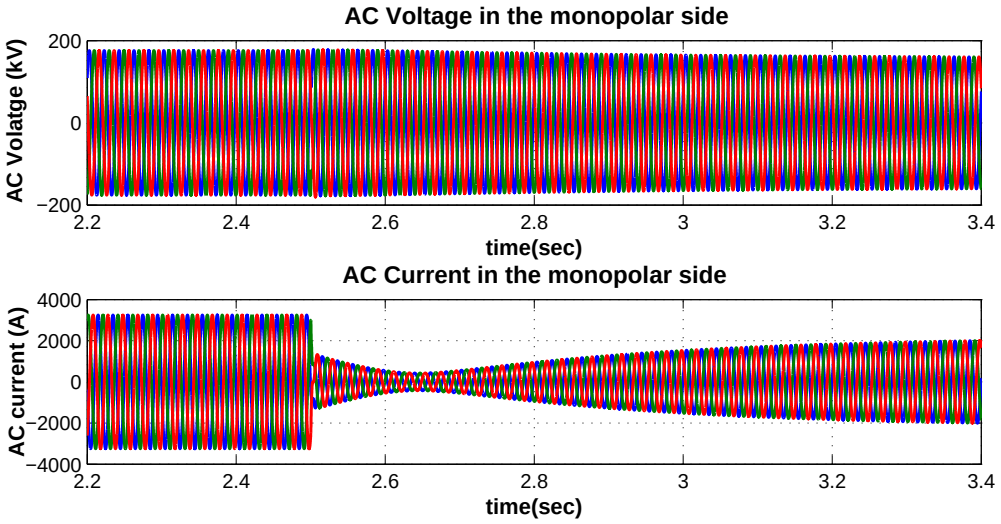

Figure 4.26: *AC Waveforms at Monopolar side of 3-winding transformer*

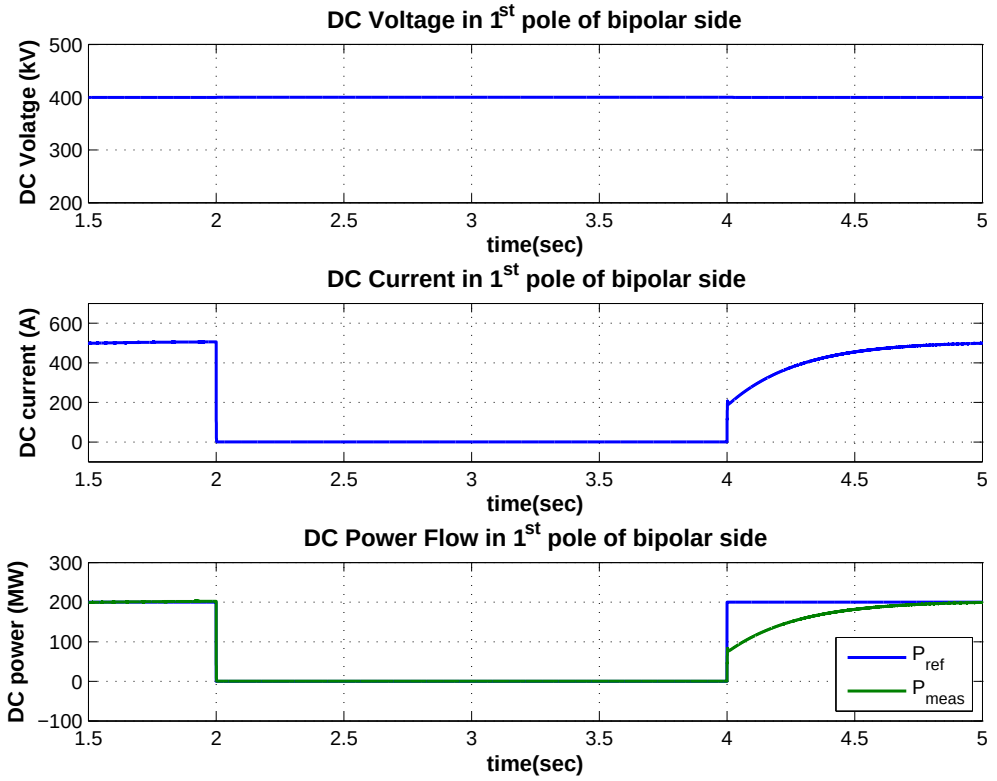

Figure 4.27: *DC Waveforms of the faulty pole at the bipolar side*

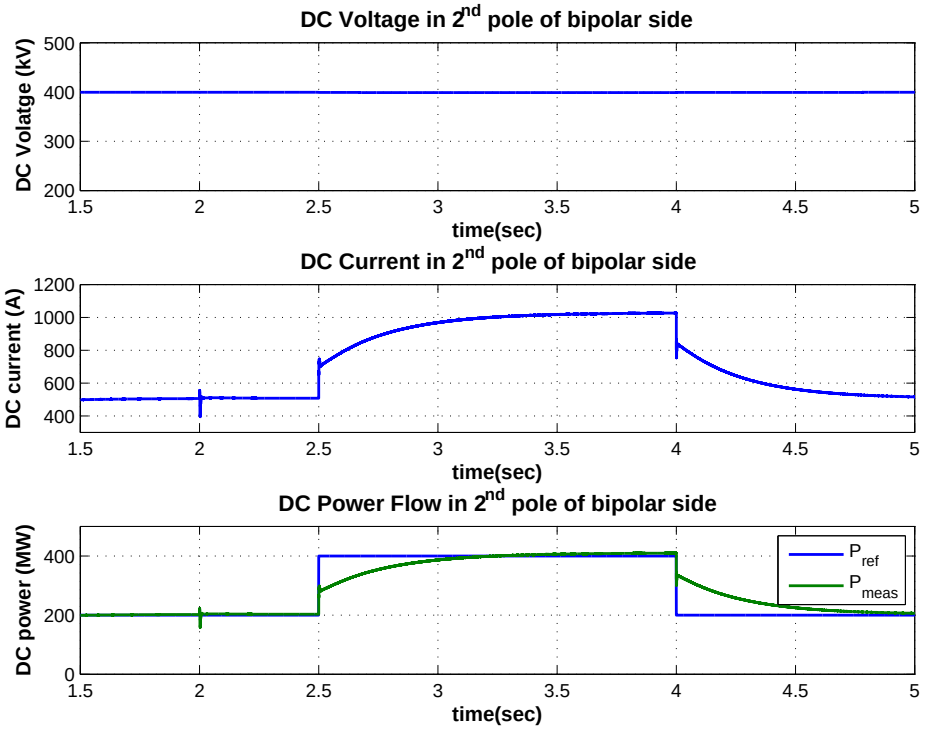

Figure 4.28: *DC Waveforms of the healthy pole at the bipolar side*

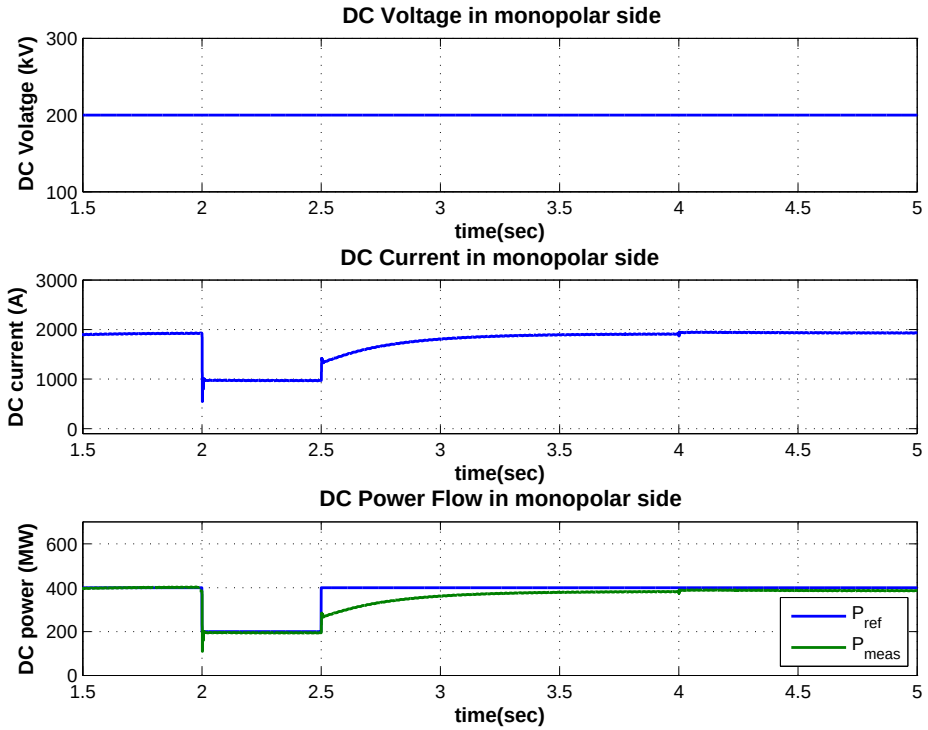

Figure 4.29: *DC Waveforms at the monopolar side*

Chapter 5

CIGRÉ B4 HVDC Grid System

This chapter gives an overview on CIGRÉ multi-terminal HVDC system. All the converters discussed in the previous chapters are then incorporated into the system to demonstrate the functionality and performance of each converters

5.1 Introduction

B4 working group of CIGRÉ has developed a VSC based multi-terminal HVDC grid test system composing of 11 AC/DC converters, to have a common benchmark for conducting DC grid analysis. With this common platform, research carried out by the engineering community now can be discussed and compared on a common basis. The corresponding system is shown in Fig. 5.1.

The system in the Fig. 5.1 consists of both AC and DC networks. The main system can be sub divided as follows.

- ✓ 2 onshore AC systems, i.e., System A and B
- ✓ 4 offshore AC systems, i.e., System C, D, E and F
- ✓ 2 DC nodes with no connection to AC
- ✓ 3 VSC DC systems

The 3 VSC DC systems are named as DCS1, DCS2 and DCS3. DSC1 is a 2-terminal symmetric monopole HVDC link (±200kV), which connects offshore wind farm at C1 to onshore node A1, while DSC2 is a 4-terminal symmetric monopole with ±200kV. Oil platform at E1 and offshore wind farm at F1 are connected to the onshore grid at B3 through this network. The DCS3 system, a 5-terminal bipole HVDC grid of ±400kV interconnects 2 offshore farms at C2 and D1 to the onshore grid through both HVDC cables and DC overhead lines. The system also has two DC/DC converter stations, one

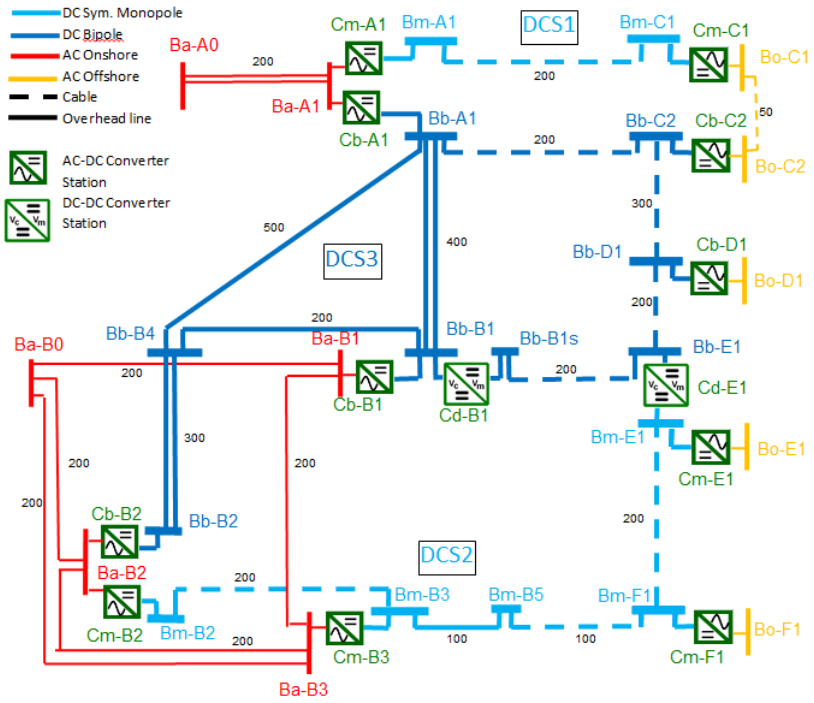

Figure 5.1: *CIGRÉ B4 DC Grid Test System [8]*

at DCS3 (B1) and the other in between DCS2 and DCS3 (E1). The rating of the AC/DC converter is shown in the Table 5.1. The ratings of the 2 DC/DC converter station is listed in the Table 5.2. The DC/DC converter Cd-B1 controls the power flow through

Table 5.1: *AC/DC Converter data of CIGRE B4 DC system [8]*

DC system	Converter ID	Voltage rating(kV)	Power rating(MVA)
DCS1	Cm-A1	±200	800
	Cm-C1		800
DCS2	Cm-B2	±200	800
	Cm-B3		1200
	Cm-E1		200
	Cm-F1		800
DCS3	Cb-A1	±400	2x1200
	Cb-B1		2x1200
	Cb-B2		2x1200
	Cb-C2		2x400
	Cb-D1		2x800

Table 5.2: *DC/DC Converter data of CIGRE B4 DC system [8]*

Converter ID	Voltage rating(kV)	Power rating(MVA)
Cd-B1	±400	2000
Cd-E1	±200 to ±400	1000

the line B1-E1, while Cd-E1 interconnects DCS2 and DCS3 which are operating with monopole and bipole configuration respectively.

5.2 Implementation of DC/DC converter into the system

The DC/DC models developed in the previous chapters are now incorporated into the CIGRÉ B4 system to verify the functionality and performance. The converter at Cd-B1 is integrated as a first step into the system for the analysis. Later the other converter at Cd-E1 is also included for an extended analysis of the system. The AC/DC converter in the system are modelled using averaging method(AVM) as explained in chapter 4.

5.2.1 DC/DC Converter in DCS3 system

The model considered for the simulation of ±400kV bipole DCS3 system is shown in the Fig. 5.2. The system has 4 AC/DC converters, i.e, Cb-A1, Cb-B1, Cb-C2 and Cb-D1.

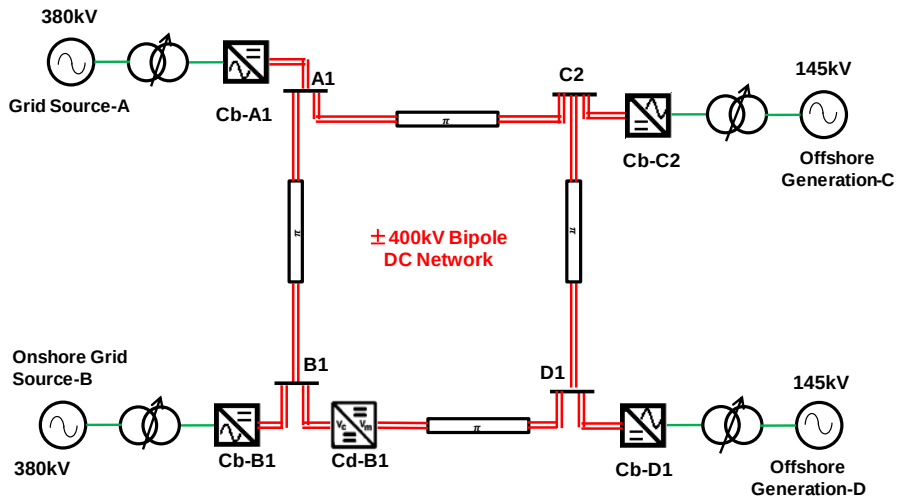

Figure 5.2: *DCS3 subsystem*

A DC/DC converter Cd-B1 is connected between Cable B1-D1 to control the power flow through the cable. All the converters are connected in ring configuration using bipole DC cables. The DC cables are modelled using pi-configuration. The details of the cable are shown in Table 5.3. As Cd-B1 DC/DC converter only needs to operate for a low voltage

Table 5.3: *DC Cable Parameters [8]*

Cable ID	**Length** (km)	**R** (Ω)	**L** (mH)	**C** (μF)
A1-B1	400	3.80	844.8	76.24
A1-C2	200	1.90	422.4	38.12
C2-D1	300	2.85	633.6	57.18
B1-D1	400	3.80	844.8	76.24

ratio interconnection, either of the two DC/DC converter without galvanic separation i.e, 4Q Converter or Front-to-front DC/AC/DC converter, developed in the previous chapters could be utilised.

The 4 AC/DC converters Cb-A1, Cb-B1, Cb-C2 and Cb-D1 in the model imposes control strategies with either PQ or V_{DC} regulator in the outer loop and current regulator in the inner loop using PI controller. The outer loop regulates PQ and V_{DC} reference by calculating the active and reactive current reference for the inner loop, while the inner current controller calculates the required AC voltage reference for the PWM/Power electronic devices. A phase-locked loop (PLL) is utilised for the synchronization of control voltage to the AC grid voltage [49].

The simulation is carried out with various case scenarios without the DC/DC converter. An analysed case scenario is summarised in the Table 5.4. The DC output power of

Table 5.4: *AC/DC Converter settings*

Converter	Operating set-point
Cb-A1	$V_{DC,A1} = 404.8kV$
Cb-B1	$P_{DC,B1} = 1000MW$ to $600MW$ at t=4s
Cb-C2	$P_{DC,C2} = -600MW$
Cb-D1	$P_{DC,D1} = -800MW$

AC/DC converters for the above case scenario is plotted in the Fig. 5.3. The result

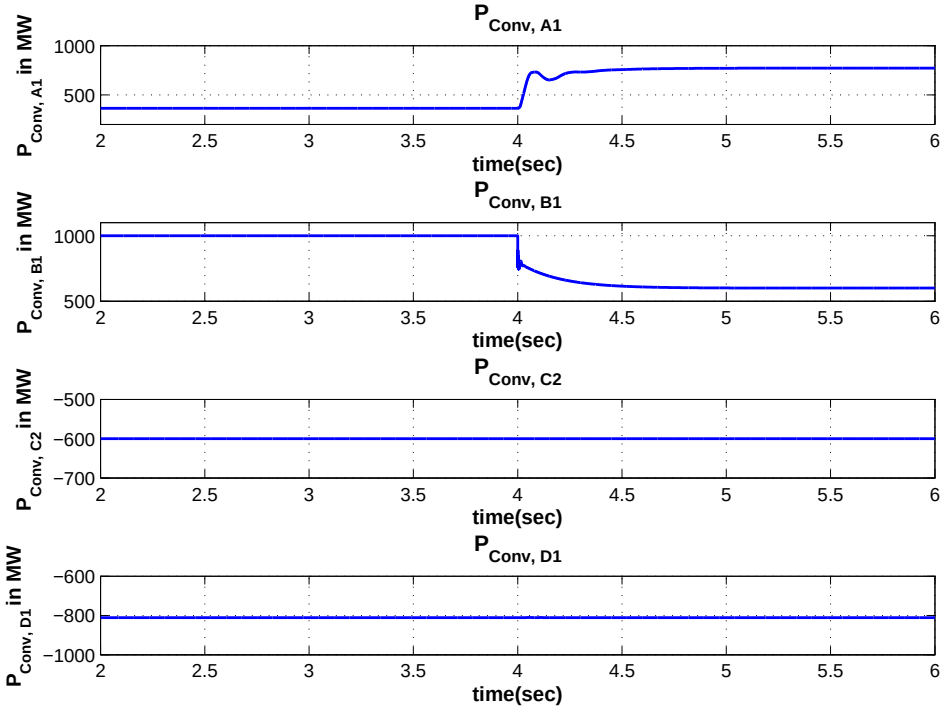

Figure 5.3: *DC Power output from AC/DC Converters*

suggests that AC/DC converter delivers power according to the set point. The power

delivered by Cb-A1 changes from 366MW to 775MW when the setpoint of Cb-B1 was changed. This is to keep the voltage at Cb-A1 at constant value of 404.8kV. Power flowing through the DC lines is plotted in the Fig. 5.4. It can be noted from the Figs. 5.4 that the

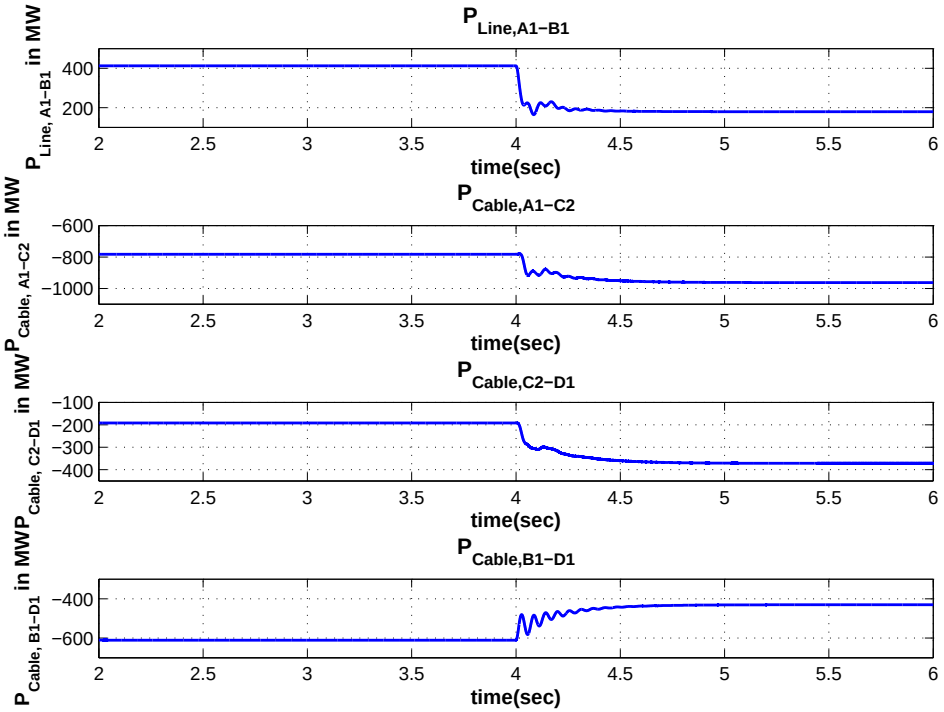

Figure 5.4: *Power flowing through DC cables without DC/DC Converter*

the AC/DC converters only control the power delivered to its DC side of the converter. The proportion of power flowing through lines connected to it depends on the resistance of the line and hence there is no control of line power flow. The power flowing through the cable changes when the converter setting is varied. The load flow results for the case is summarised in the Fig. 5.5 and 5.6. The DC voltage at each terminals of the AC/DC converters are plotted in the Fig. 5.7. The allowable range of operation of the DC voltage is 0.95pu to 1.05pu. Fig. 5.7 shows that the voltage at each terminals for both the cases are within the operational limit.

As a second case, Cd-B1 DC/DC converter implemented using 4Q converter is enabled and simulations are carried out. AC/DC converter Cb-B1 is set to 1000MW, while other converters are defined as per the Table 5.4. The power reference at Cd-B1 is varied from 300MW to -200MW at t=4s to verify the bi-directional operation. The power flowing through each cable is plotted in Fig. 5.8. Fig. 5.8 illustrates the performance of the converter by tracking the set reference. It is evident that the power flow through the cable B1-D1 is now controlled using the converter according to the set value. The power control in line DB affects the power flow through other lines as expected since the case scenario of four AC/DC converters determines the total power in the DC network, which is still the same as without DC/DC converter. The DC power measured at the DC side of AC/DC converters are shown the Fig. 5.9. It can be observed that the DC power of each AC/DC converter remains the same irrespective of changing the power at

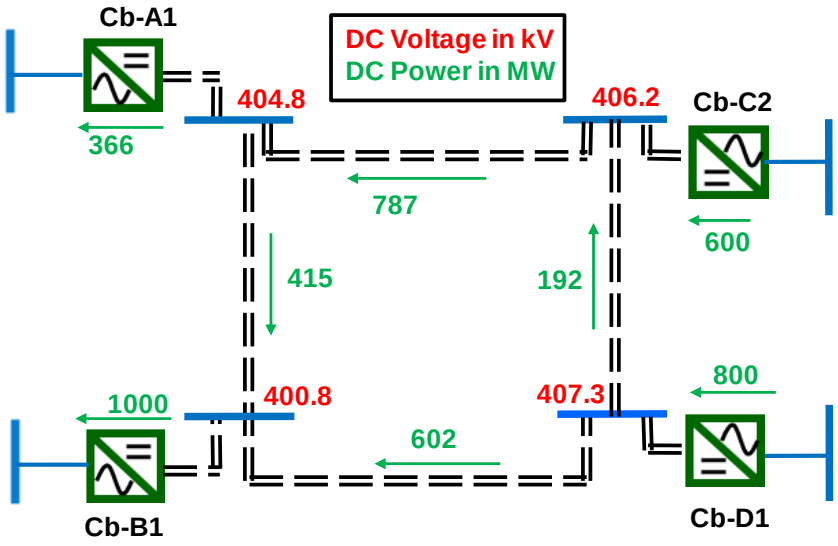

Figure 5.5: *Load flow result without DC/DC converter with* $P_{DC,B1}$*=1000MW*

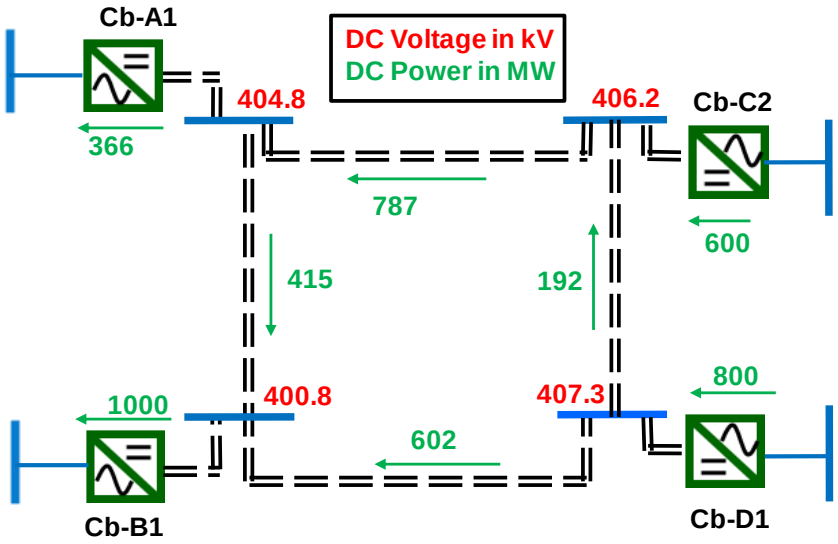

Figure 5.6: *Load flow result without DC/DC converter with* $P_{DC,B1}$*=600MW*

DC/DC converter, although with some ripples during the power change. The converter DC voltages are also analysed to verify compliance with their operational limit. Results are plotted in Fig. 5.10. The current flowing through the inductor of 4Q DC/DC converter is shown in Fig. 5.11, where the current is regulated using the inner loop of the controller and always limits the current within the allowed range. The load flow results for two cases with DC/DC converter are shown in Figs. 5.12 and 5.13. Load flow results show the performance of both AC/DC and DC/DC converter. 602MW of power was flowing from D1 to B1 in the absence of DC/DC converter. However, introducing DC/DC converter in to the system allows the flexibility of power flow control both in magnitude and direction through the line B1-D1, as it is evident from the Fig. 5.13, where 200MW of power is flowing in the opposite direction for the same AC/DC converter setting.

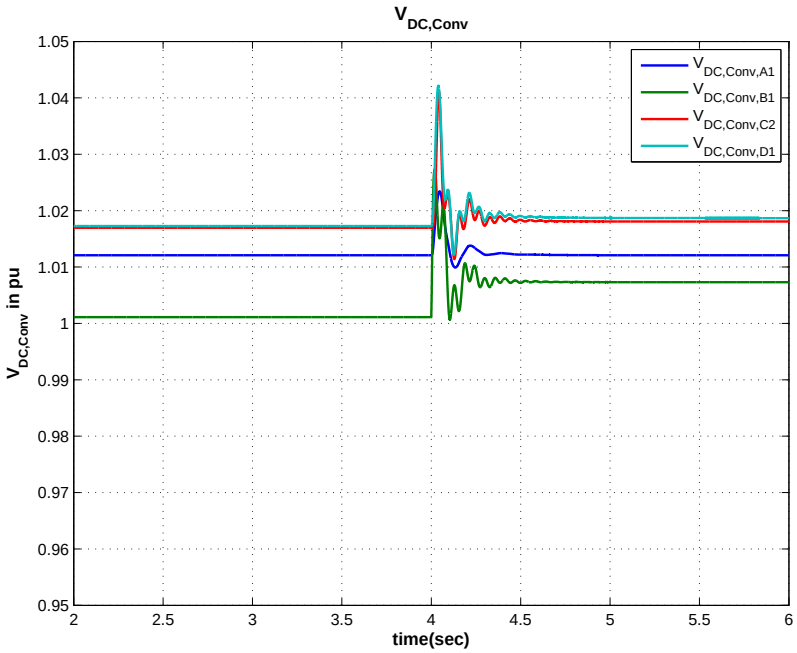

Figure 5.7: *DC Voltage at AC/DC converter in pu*

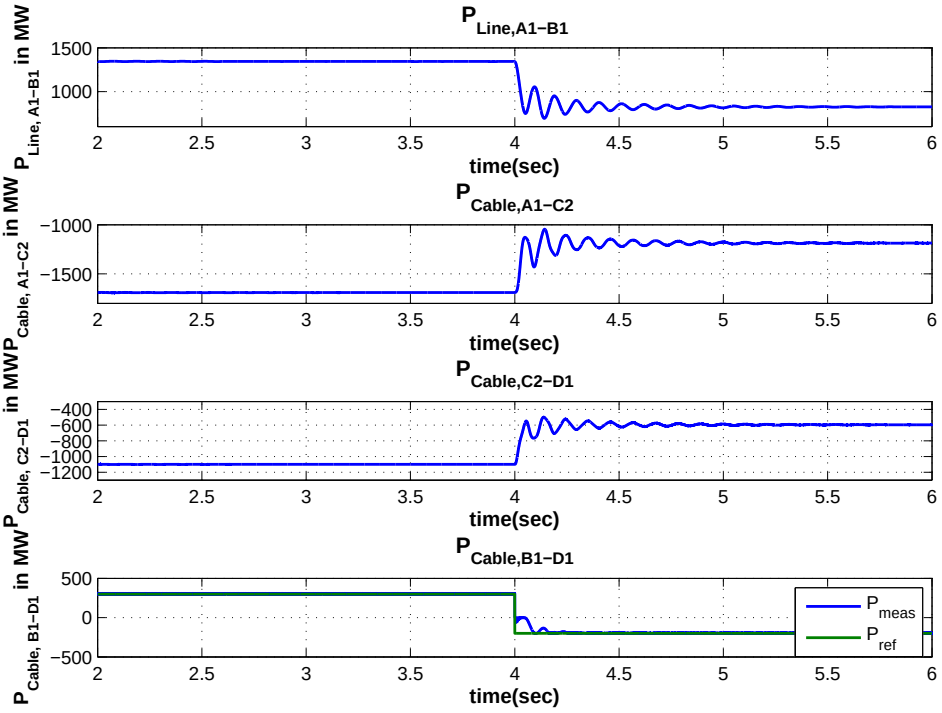

Figure 5.8: *DC Power flow through the Cables*

5.2.2 DC/DC Converter for interconnecting DCS2 and DCS3 system

CIGRÉ B4 HVDC grid has another DC/DC Converter Cd-E1 at E1 to interconnect DCS2 and DCS3 system. DCS2 is symmetric monopole HVDC system operating with ±200kV,

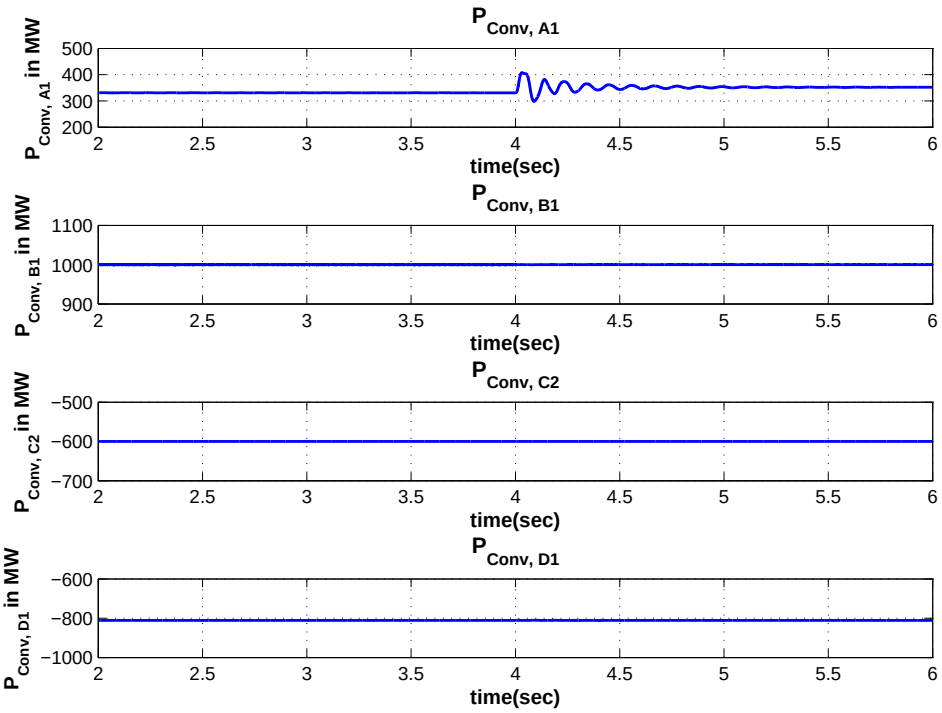

Figure 5.9: *DC Power output from AC/DC Converters*

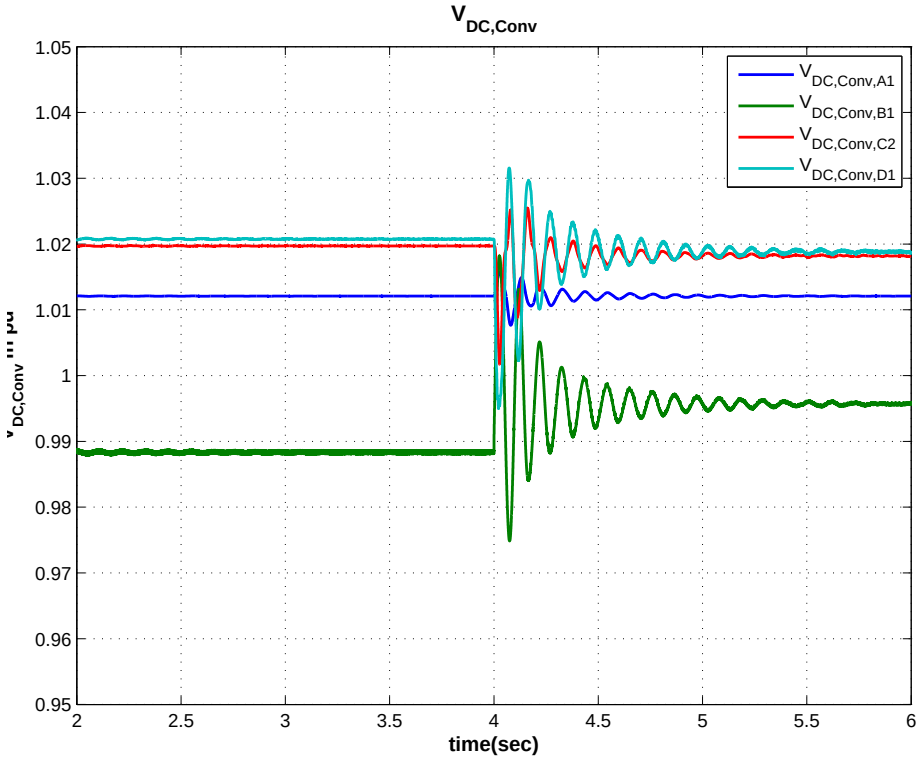

Figure 5.10: *DC Voltage at AC/DC converter in pu*

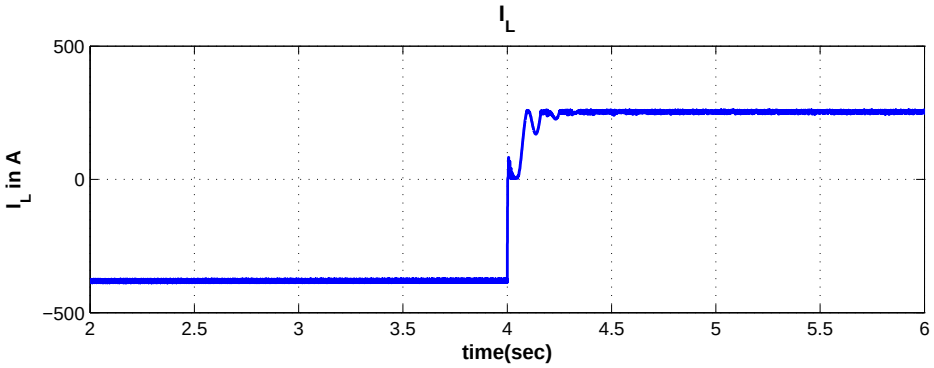

Figure 5.11: *Current through the inductor of 4Q converter*

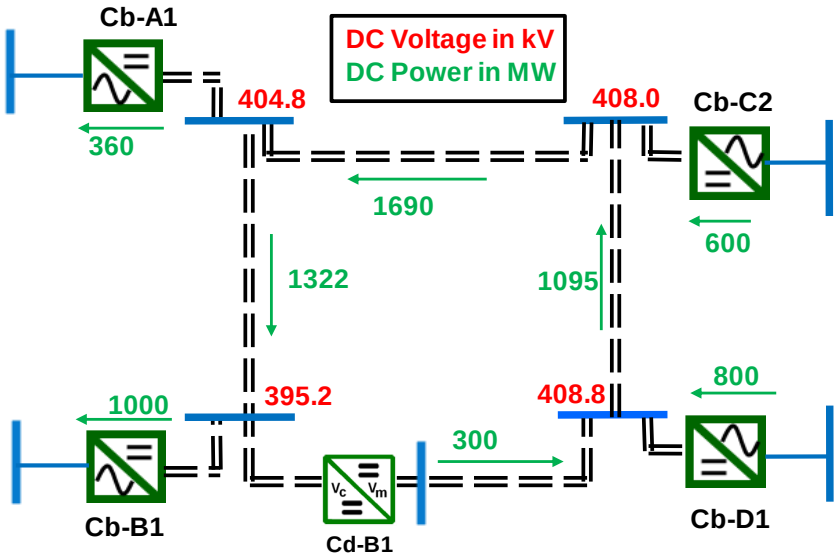

Figure 5.12: *Load flow result with $P_{DC,Cd-B1}$=300MW*

while DCS3 is bipole HVDC system operating with ±400kV. As both the systems are operating with different voltages and different configurations, they cannot be connected as such as explained in Chapter 4 and needs galvanic separated DC/DC converter for interconnection. The 3 - winding transformer coupled DC/AC/DC converter developed for this application is included in the system to verify its operation in this meshed MTDC grid.

The model considered for simulation is plotted in Fig. 5.14. The system consists of 4 bipole AC/DC converters Cb-A1, Cb-B1, Cb-C2 and Cb-D1 and 2 monopole AC/DC converters Cm-F1 and Cm-B3. DC/DC converter Cd-B1 is connected in the cable B1-D1 to control the power flow, while Cd-E1 interconnects both networks. The cables are modelled using pi configuration. The cable parameters are shown in the Table 5.5. The two networks DCS2 and DCS3 are also interconnected from the AC side of AC/DC converters Cb-B1 and Cm-B3 through a 380kV AC transmission line. The parameters of the AC line are shown in the Table 5.6. The model is simulated for various case scenarios with both the DC/DC converters. An analysed case scenario with AC/DC converter

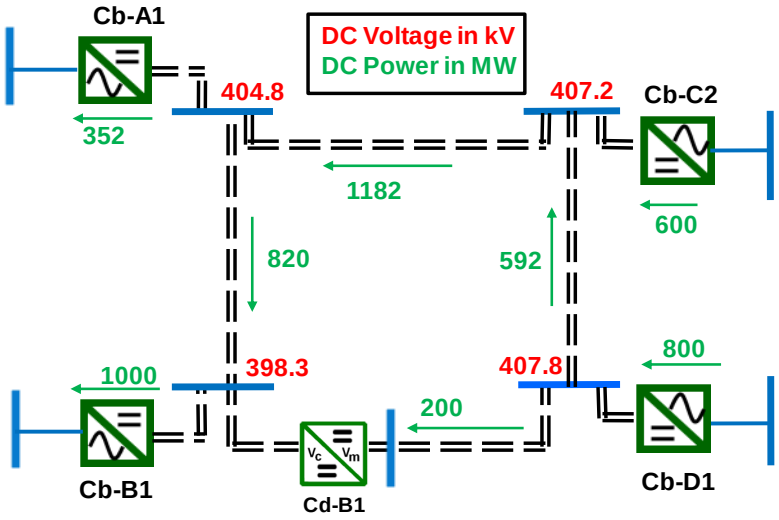

Figure 5.13: *Load flow result with $P_{DC,Cd-B1}$=-200MW*

Table 5.5: *DC Cable Parameters [8]*

Cable ID	**Length** (km)	**R** (Ω)	**L** (mH)	**C** (μF)
A1-B1	400	3.80	844.8	76.24
A1-C2	200	1.90	422.4	38.12
C2-D1	300	2.85	633.6	57.18
D1-E	200	1.90	422.4	38.12
B1-E	200	1.90	422.4	38.12
E1-F1	200	1.90	422.0	42.08
B3-F1	200	1.90	422.0	42.08

Table 5.6: *AC Transmission line Parameters [8]*

Overhead Line	**Length** (km)	**R** (Ω)	**L** (mH)	**C** (μF)
B3-B1	200	4.0	170.6	2.7

setting and DC/DC converter settings is summarised in the Table 5.7. The AC/DC

Table 5.7: *Converter settings*

Converter	**Operating setpoint**
Cb-A1	$V_{DC,A1} = 404.8kV$
Cb-B1	$P_{DC,B1} = 1000MW$
Cb-C2	$P_{DC,C2} = -600MW$
Cb-D1	$P_{DC,D1} = -800MW$
Cm-F1	$V_{DC,F1} = 204.6kV$
Cm-B3	$P_{DC,B3} = 400MW$
Cd-B1	$P_{set} = 300MW$ to $P_{set} = -200MW$ at t=6s
Cd-E1	$P_{set} = -300MW$ to $P_{set} = 400MW$ at t=4s

converter DC output is shown in the Figs. 5.15 and 5.16. The Figs. 5.15 and 5.16 show

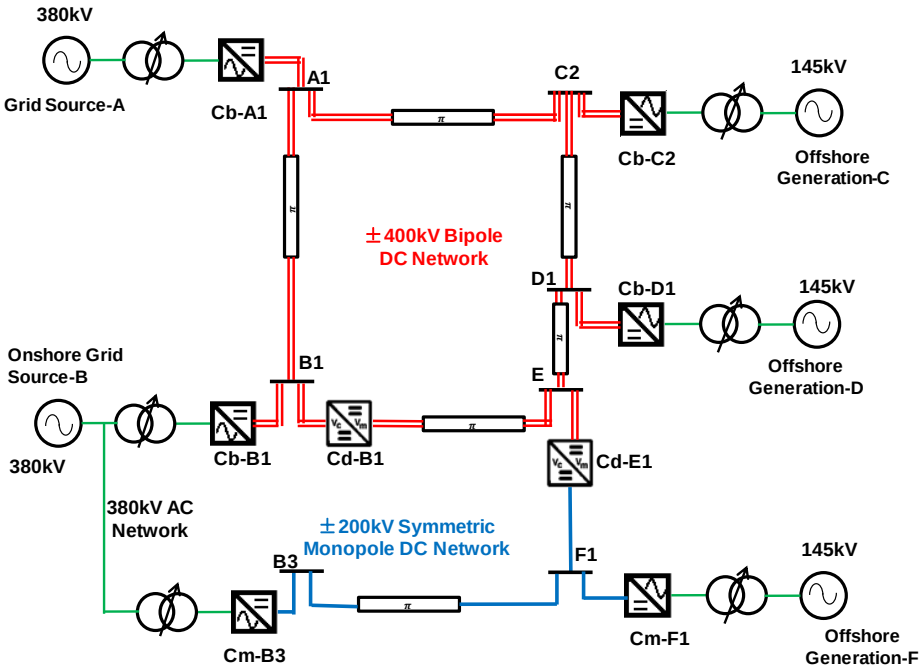

Figure 5.14: *DCS2 and DCS3 subsystem*

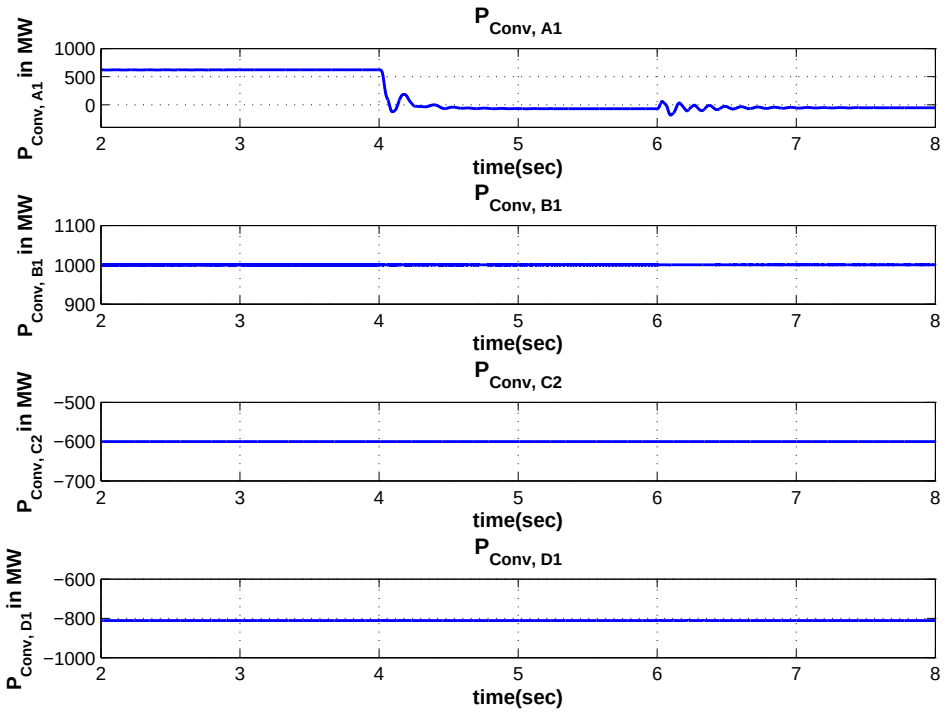

Figure 5.15: *DC Power output from AC/DC Bipole Converters*

good performance of the converter by following the set point defined in the Table 5.7. The power delivered by the converter Cb-A1 and Cm-F1 changes when the set point of DC/DC converter is changed at t=4s and t=6s to keep the terminal voltage constant.

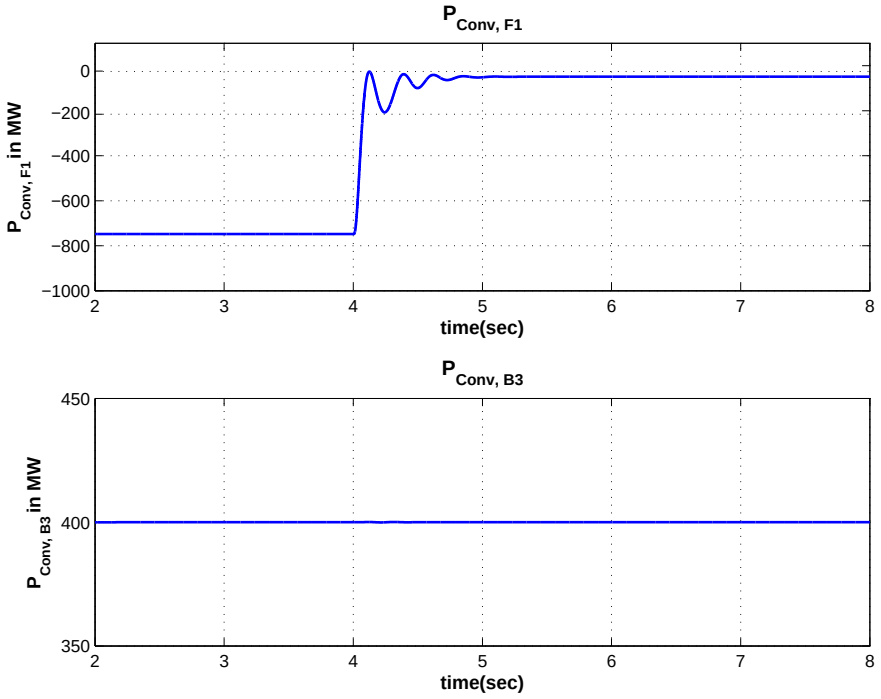

Figure 5.16: *DC Power output from AC/DC Monopole Converters*

However, all other converters power output remains constant as they are defined with active power control. The power flowing through the DC lines are shown in Figs. 5.17 and 5.18. In addition of providing the interconnection between two different networks, DC/DC converter Cd-E1 also provides the flexibility of power control. The power set point of Cd-E1 is varied from -300MW to 400MW at t=4s. This setting defines the power flow through the cable E1-F1. Power flowing through other cables changes when the set point is changed to match the total power flow in the system as defined by Figs. 5.15 and 5.16. The DC/DC converter, Cd-B1 is also implemented using 4Q converter and is set to 300MW until t=6s, after which it is changed to -200MW in order to examine the influence of one DC/DC converter behaviour over other. Figs. 5.17 and 5.18 show the performance of both the converters by tracking the reference.

Each DC/DC converter parameters are independently analysed. The waveforms of the intermediate AC stage of Cd-E1 is plotted in Figs. 5.19 and 5.20. As expected, the current magnitude changes according to the power setting, while voltage remains constant. The minor change in the voltage magnitude is due to the change in DC voltage of the terminal E and F1. The current through the inductor of Cd-B1 converter is also plotted in Fig. 5.21. The current is unaffected with the change in the setting of Cd-E1 and only changes for Cd-B1 power setting. The DC voltage of all 6 AC/DC converter is measured to verify its operational limit and are shown in Fig. 5.22. Fig. 5.22 shows that voltage at the DC terminals of all converters are within the range of 0.95 to 1.05pu. The load flow for the 3 cases are summarised in the Figs. 5.23, 5.24 and 5.25. Load flow results show the performance of DC/AC converters and DC/DC converters. V_{DC} at Cb-A1 and Cm-F1 is maintained at 404.8kV and 202.4kV respectively, while Cb-B1, Cb-C2, Cb-D1 and Cm-B3 is delivering constant DC output power irrespective of the change in set point at both Cd-B1 and Cd-E1.

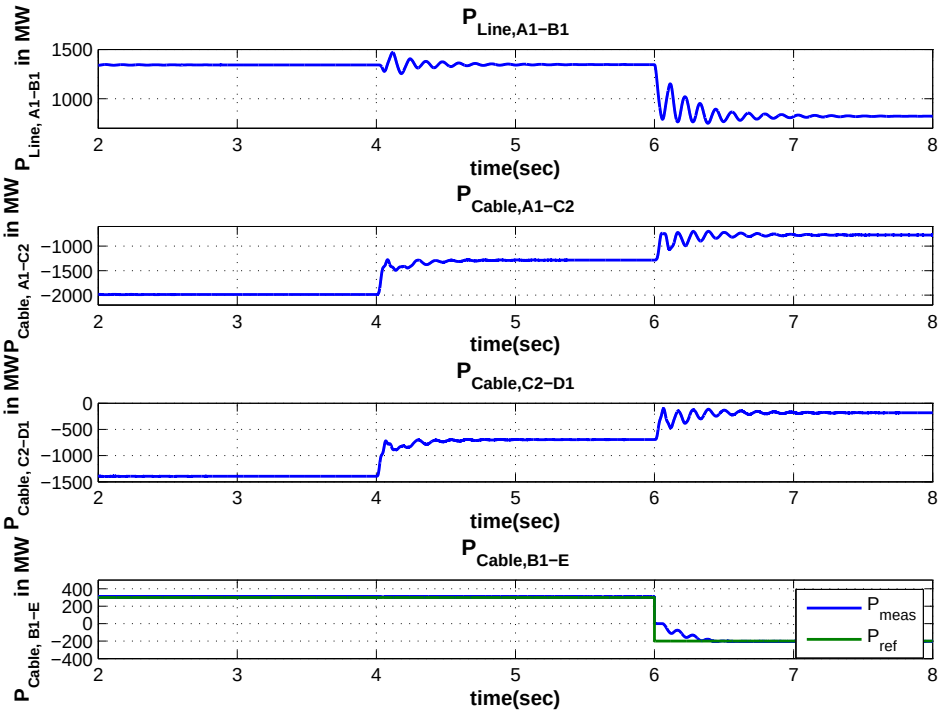

Figure 5.17: *DC Power flow in Bipole network*

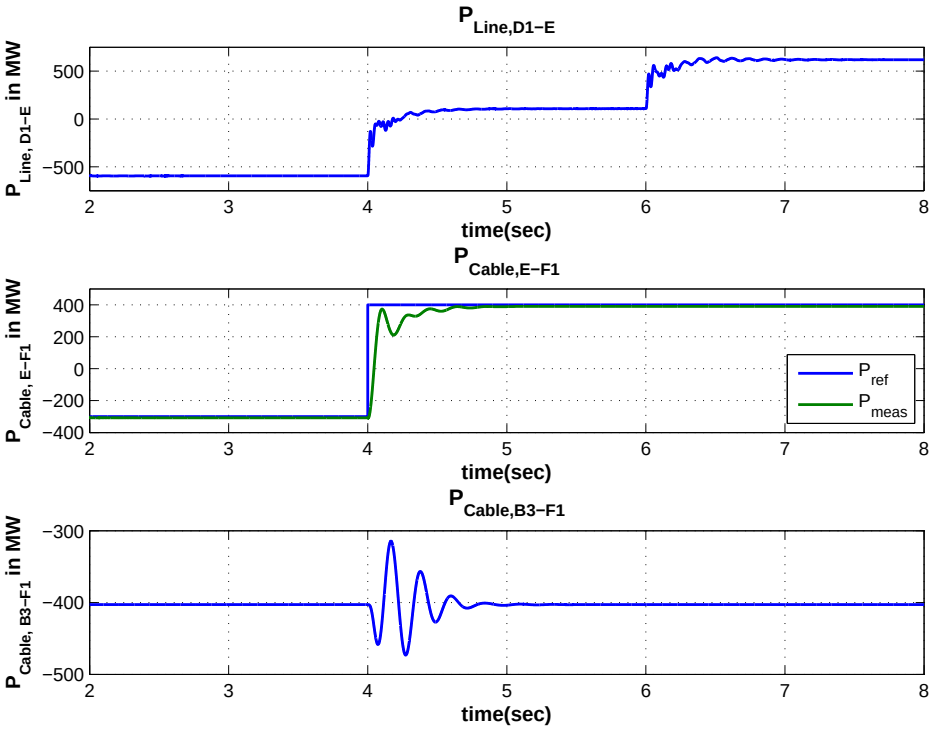

Figure 5.18: *DC Power flow in Monopole network*

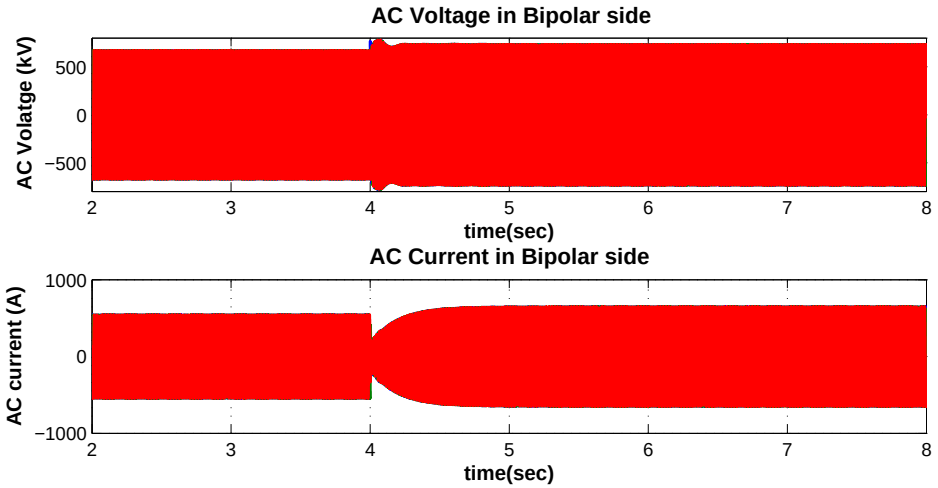

Figure 5.19: *AC Waveforms in the Bipole side*

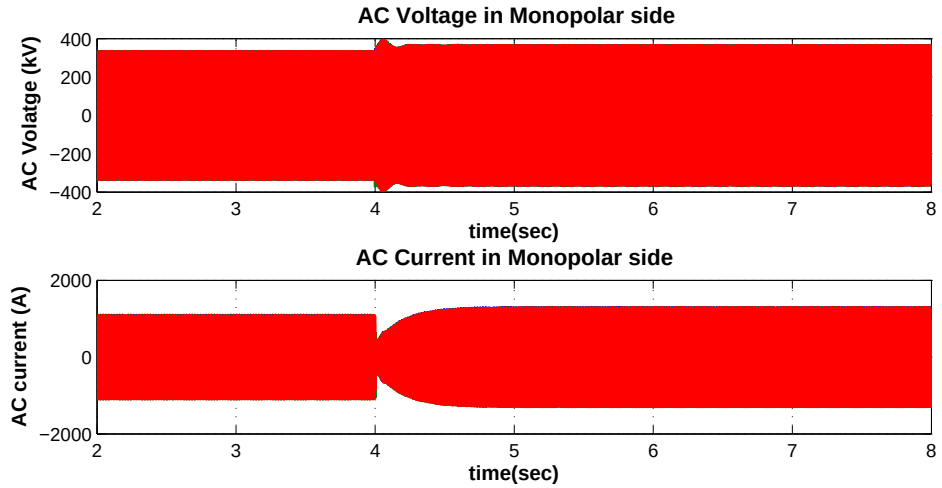

Figure 5.20: *AC Waveforms in the Monopole side*

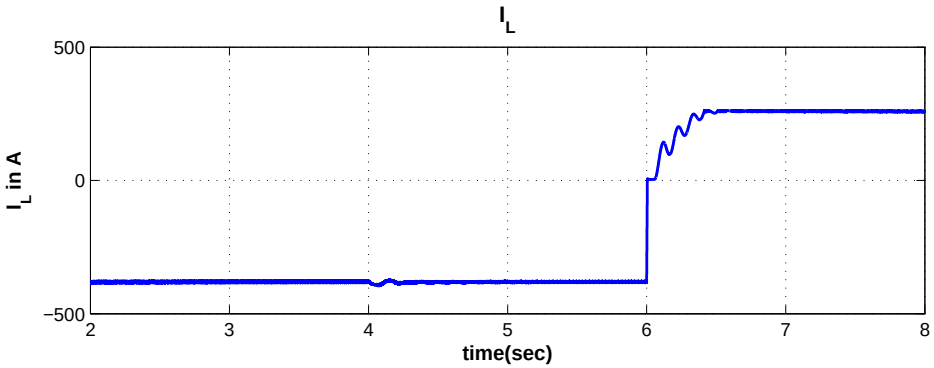

Figure 5.21: *Current through the inductor of Cd-B1*

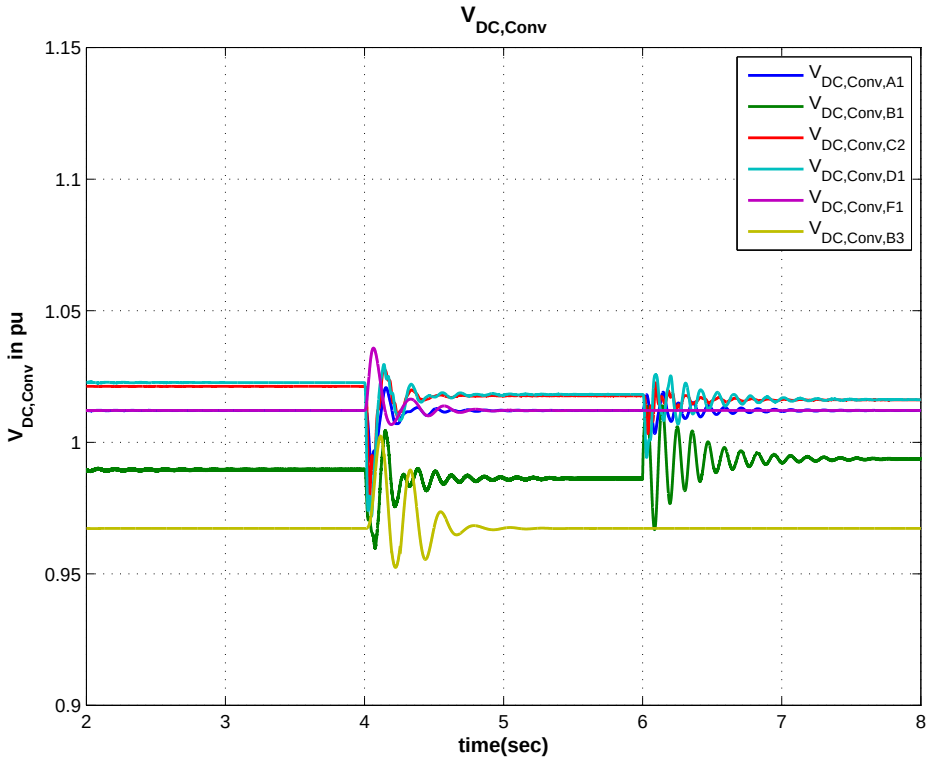

Figure 5.22: *DC Voltage of 6 AC/DC converters in pu*

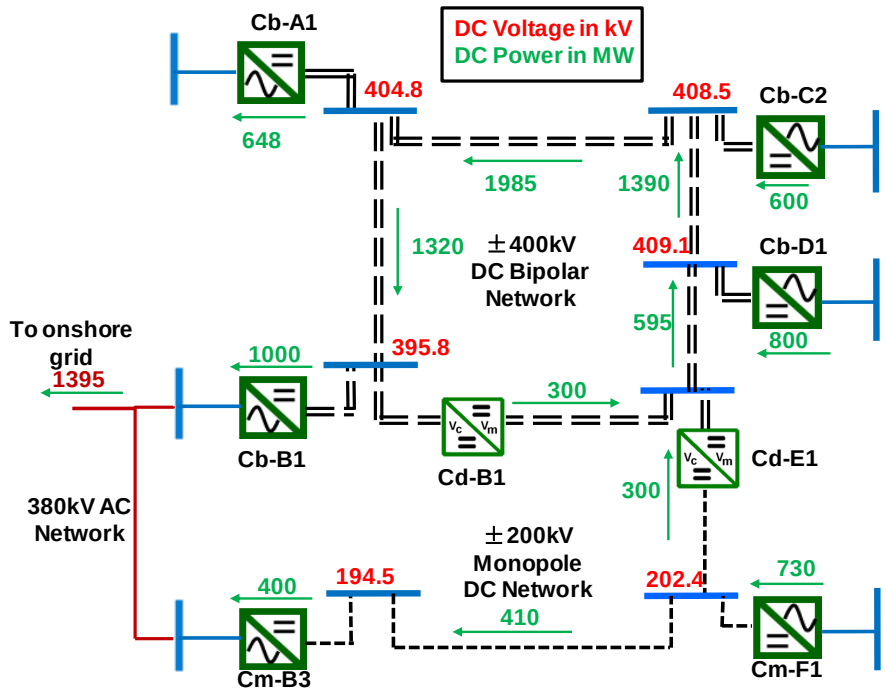

Figure 5.23: *Load flow result with $P_{DC,Cd-B1}$=300MW and $P_{DC,Cd-E1}$=300MW*

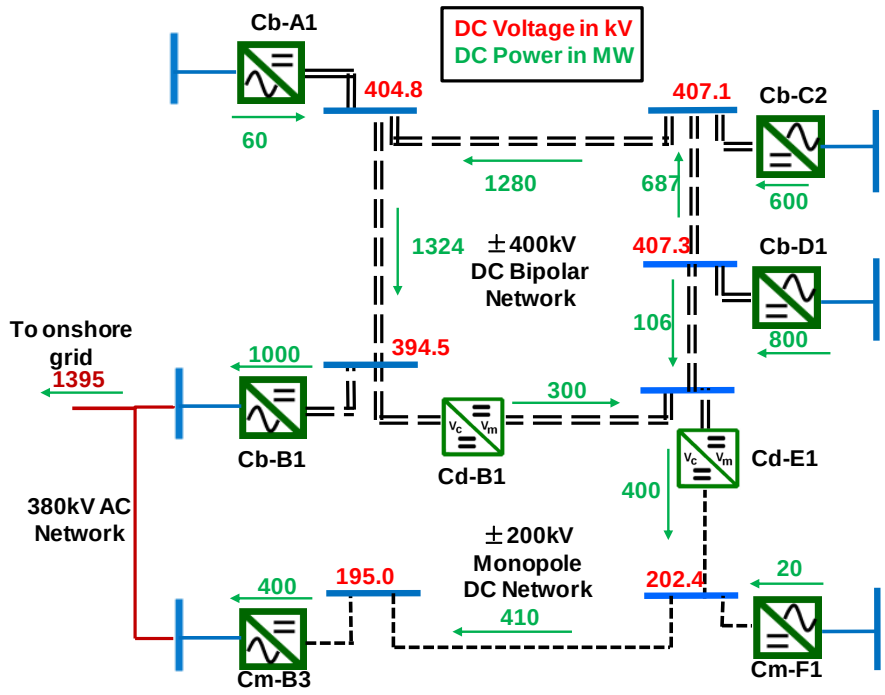

Figure 5.24: Load flow result with $P_{DC,Cd-B1}$=300MW and $P_{DC,Cd-E1}$=-400MW

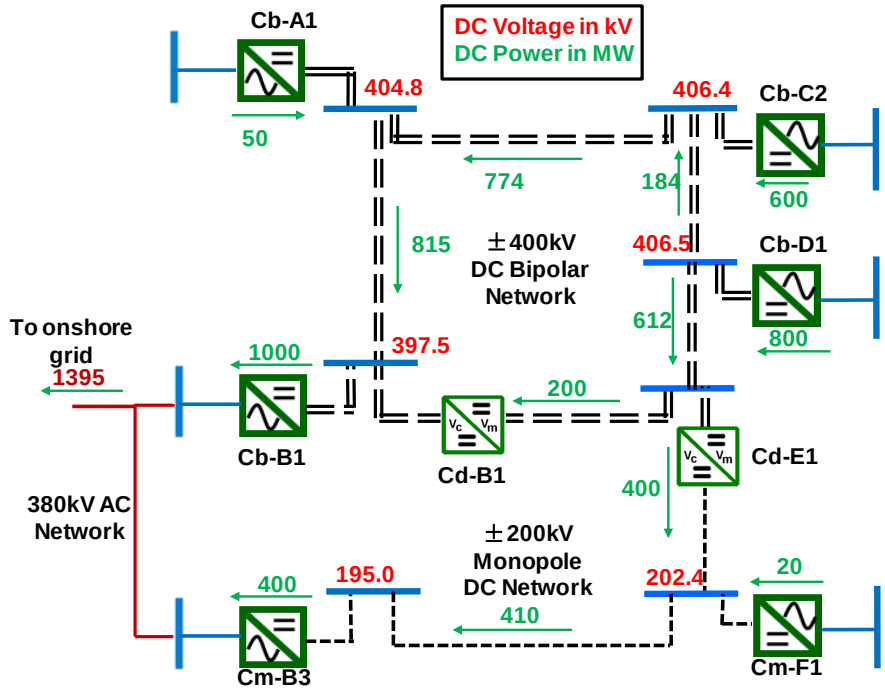

Figure 5.25: Load flow result with $P_{DC,Cd-B1}$=-200MW and $P_{DC,Cd-E1}$=-400MW

Chapter 6

Conclusions and Future Work

This chapter presents the conclusions of the thesis and suggests future work.

6.1 Conclusions

Voltage source converters based HVDC technology favours the concept of multi-terminal HVDC system due to the flexibility in the power control, black-start capability etc. However, existing HVDC connections, which are mainly point-to-point, are often operated at different voltages and with dissimilar configurations and therefore DC/DC converters will become necessary for their interconnection. In meshed MTDC grids, DC/DC converters can also be needed to control the power flow independently of the cable impedances due to the risk of cable overloading in specific network sections. This thesis has discussed the requirements for DC/DC converters in MTDC systems and was concluded that MTDC grid cannot rely on a single DC/DC converter topology. The choice of DC/DC converters varies for different systems based on various factors including voltage ratio, configuration of interconnected systems, need of galvanic separation, power rating etc.

A general overview of different DC/DC converters discussed in the literature was presented and then the attention was focused on two classes of DC/DC converters, i.e. DC/DC converters without galvanic separation and galvanically separated DC/DC converters.

A 4 four quadrant converter topology has been proposed as a viable solution for bidirectional power flow control in meshed MTDC grids with unified voltage rating. The selection was based on the converter's capability to operate in four quadrants of the IV curve and non-necessity of galvanic separation. The sizing of the components in the converter was calculated considering the voltage and current ripples. A cascaded control system using PI controllers and pulse width modulation (PWM)with inner loop as current control is recommended and implemented to obtain the control objective of power flow control. Simulation results has suggested good performance of controllers by tracking the power reference in all four quadrants of the IV curve.

An alternative solution for the power flow control in low ratio connection using Front-to-front DC/AC/DC converter has been also proposed. With 2 AC/DC converters, the control objective of regulating the active power flow through the HVDC line is realised by implementing vector control strategy in the converter performing power control, while using fixed modulation index, providing a voltage control for the other converter. Inner current controller parameters for the vector controller are derived using modulus optimum, while outer controller parameters are obtained using symmetrical optimum.

Transformer coupled DC/AC/DC converter has been proposed for a high ratio interconnection of two HVDC schemes. The transformer coupling provides the suitable voltage ratio in addition to the galvanic separation between two sides. The connection of the intermediate AC transformer varies according to the configuration(bipole or monopole) of two interconnecting HVDC schemes. Separate methods for interconnecting a bipolar HVDC scheme with monopolar scheme using 2-winding transformer and 3-winding transformer were proposed and a comparison was made with respect to the voltage and power rating of each component in the configuration. With the active power flow controller designed independently for each pole of the bipolar configuration, the capability of the converter to control the power flow, during a failure on one pole of the bipolar configuration was also demonstrated.

As the converters developed are intended to be implemented in a larger MTDC grid, dynamic average models of converters were also developed to obtain a continuous time invariant equivalent circuit of converter by averaging the effect of fast switching within a switching interval. This is useful both to reduce simulation time of large systems and for design of controllers.

A multi-terminal DC grid based on CIGRÉ B4 DC grid test system was modelled for verifying the performance of developed DC/DC converters. The result has shown how a properly designed DC/DC converter can be controlled to regulate the power flow in MTDC configuration in addition to the interconnection of two independent HVDC schemes.

6.2 Future Work

There are certain aspects of the DC/DC converters, which need to be further investigated. Suggestions for future work include:

- Simulation with switching model has introduced large harmonics in the system due to the high frequency switching. Therefore suitable filters have to be designed for eliminating the harmonics.
- The Front-to-front DC/AC/DC converters were implemented using two level converters. Due to the reduction in the average switching frequency per device resulting reduced harmonics, modular multi-level converters(MMC) are preferred over 2 level configuration. Therefore, the next step of analysis would be to implement the DC/AC/DC converter with MMC.
- Most of the existing HVDC schemes are operating with LCC technology, wherein power reversal is obtained through change in voltage polarity. In order to utilise

this existing grids, suitable DC/DC converters needs to be evaluated which could interconnect LCC based HVDC link with VSC based HVDC schemes.

- The failure of DC/DC converters in an MTDC grid could affect the stability of the system. Therefore, suitable analysis need to be carried out to verify the transient and dynamic stability.
- A laboratory set-up should be implemented to validate the simulation results obtained.

References

[1] The European offshore wind industry -key trends and statistics 2014, January 2015, EWEA website. http://www.ewea.org/fileadmin/files/library/publications/statistics/EWEA-Europ-ean-Offshore-Statistics-2014.pdf. Accessed: 2015-06-14.

[2] Wind energy scenarios for 2020, July 2014, EWEA website. http://www.ewea.org/fileadmin/files/library/publications/scenarios/EWEA-Wind-energy-scenarios-2020.pdf. Accessed: 2015-06-14.

[3] F. Wang, Yunqing Pei, D. Boroyevich, R. Burgos, and Khai Ngo. AC vs. DC distribution for off-shore power delivery. In *Industrial Electronics, 2008. IECON 2008. 34th Annual Conference of IEEE*, pages 2113–2118, Nov 2008.

[4] R. Majumder, C. Bartzsch, P. Kohnstam, E. Fullerton, A. Finn, and W. Galli. Magic Bus: High-Voltage DC on the New Power Transmission Highway. *Power and Energy Magazine, IEEE*, 10(6):39–49, Nov 2012.

[5] D. Van Hertem, M. Ghandhari, and M. Delimar. Technical limitations towards a SuperGrid - A European prospective. In *Energy Conference and Exhibition (EnergyCon), 2010 IEEE International*, pages 302–309, Dec 2010.

[6] Jiebei Zhu and C. Booth. Future multi-terminal HVDC transmission systems using Voltage source converters. In *Universities Power Engineering Conference (UPEC), 2010 45th International*, pages 1–6, Aug 2010.

[7] H. Stylen, K. Uhlen, A.R. rdal, and K. Sharifabadi. Laboratory demonstration of an offshore grid in the North Sea with DC droop control. In *Ecological Vehicles and Renewable Energies (EVER), 2014 Ninth International Conference on*, pages 1–8, March 2014.

[8] Yang Y. Jovcic D. Dennetire S. Jardini J. Vrana, T.K. and H Saad. HVDC and Power Electronics, The CIGRE B4 DC Grid Test System. //http://b4.cigre.org/Publications/Documentsrelated-to-the-development-of-HVDC-Grids. Accessed: 2015-06-14.

[9] HVDC Applications and Benifit History, Siemens website. http://www.energy.siemens.com/co/en/power-transmission/hvdc/applications-benefits/hvdc-history.htm. Accessed: 2015-06-14.

[10] E. W. Kimbark. *Direct Current Transmission*. Wiley, New York, vol. 1 edition, 1971.

[11] K. Meah and S. Ula. Comparative Evaluation of HVDC and HVAC transmission systems. In *Power Engineering Society General Meeting, 2007. IEEE*, pages 1–5, June 2007.

[12] Luig COLLA. Technical issues on the integration of long distance AC cables in HV and EHV networks. In *IEEE PES Insulated Conductors Committee Spring 2012 meeting - Seattle*, March 25-28 2012.

[13] High Voltage Direct Current Transmission Technology Proven Technology for Power Exchange, Siemens Power Transmission and Distribution, Siemens website. http://www.siemens.com/about/sustainability/pool/en/environmental-portfolio/products-solutions/powertransmission-distribution/hvdc_proven_technology.pdf. Accessed: 2015-06-14.

[14] Overview of Line Commutated Converter based HVDC, Cigre. http://b4.cigre.org/content/download/1971/25259/version/1/file/What+is+HVDCID10VER33.pdf. Accessed: 2015-06-14.

[15] Rajat Majumder Amirnaser Yazdani Nilanjan Chaudhuri, Balarko Chaudhuri. *Multi-terminal Direct-Current Grids: Modeling, Analysis, and Control*. John Wiley and Sons, New York, 2013.

[16] M.P. Bahrman and B.K. Johnson. The ABCs of HVDC transmission technologies. *Power and Energy Magazine, IEEE*, 5(2):32–44, March 2007.

[17] Lidong Zhang and L. Dofnas. A novel method to mitigate commutation failures in HVDC systems. In *Power System Technology, 2002. Proceedings. PowerCon 2002. International Conference on*, volume 1, pages 51–56 vol.1, Oct 2002.

[18] History of ABBs HVDC expertise, ABB website. http://www.abb.no/cawp/seitp202/7cfd9a3a7416a383c1256e8600406f4f.aspx. Accessed: 2015-06-14.

[19] HVDC Light, its time to connect, ABB website. //http://new.abb.com/docs/default-source/ewea-doc/hvdc-light.pdf?sfvrsn=2. Accessed: 2015-06-14.

[20] HVDC for beginners and beyond, ALSTOM website. //http://www.alstom.com/Global/Grid/Resources/Documents/Systems/HDVC%20for%20beginners%20and%20beyond%20Brochure%20GB.pdf. Accessed: 2015-06-14.

[21] D. R. Trainer C. D. Barker, C. C. Davidson and R. S. Whitehouse. Requirements of DC-DC Converter to facilitate large DC grids. In *CIGRE Session 2012*, 2012.

[22] F. Caricchi, F. Crescimbini, G. Noia, and D. Pirolo. Experimental study of a bidirectional DC-DC converter for the DC link voltage control and the regenerative braking in PM motor drives devoted to electrical vehicles. In *Applied Power Electronics Conference and Exposition, 1994. APEC '94. Conference Proceedings 1994., Ninth Annual*, pages 381–386 vol.1, Feb 1994.

[23] J. G. Oliveira M. Hedlund and H. Bernhoff. Sliding mode 4-quadrant DCDC converter for a flywheel application. In *Control Engineering Practice*, pages Volume 21, Issue 4, pp. 473–482., April 2013.

[24] C.P. Dick, A. Konig, and R.W. De Doncker. Comparison of Three-Phase DC-DC Converters vs. Single-Phase DC-DC Converters. In *Power Electronics and Drive Systems, 2007. PEDS '07. 7th International Conference on*, pages 217–224, Nov 2007.

[25] Rodrigo Teixeira Pinto. Survey on Available Multilevel Topologies for VSC-HVDC. In *TU Delft, DC systems, Energy conversion and Storage, Report 11*, Septemeber 2011.

[26] R. Marquardt. Modular Multilevel Converter: An universal concept for HVDC-Networks and extended DC-Bus-applications. In *Power Electronics Conference (IPEC), 2010 International*, pages 502–507, June 2010.

[27] J. Leuchter, P. Bauer, Petr Bojda, and V. Rerucha. Bi-directional DC-DC converters for supercapacitor based energy buffer for electrical gen-sets. In *Power Electronics and Applications, 2007 European Conference on*, pages 1–10, Sept 2007.

[28] T.M. Undeland N. Mohan and W.P. Robbins. *Power Electronics : Converters, Applications, and Design (Third edition)*. Wiley, 2003.

[29] R. W. Erickson. *Fundamentals of Power Electronics (First edition)*. Chapman and Hall, 1997.

[30] S. Chiniforoosh, J. Jatskevich, A. Yazdani, V. Sood, V. Dinavahi, J.A. Martinez, and A. Ramirez. Definitions and Applications of Dynamic Average Models for Analysis of Power Systems. *Power Delivery, IEEE Transactions on*, 25(4):2655–2669, Oct 2010.

[31] Ned Mohan. *Electric Drives: An Integrative Approach*. MNPERE, 2003.

[32] R. Vilanova and O. Arrieta. PID tuning for cascade control system design. In *Electrical and Computer Engineering, 2008. CCECE 2008. Canadian Conference on*, pages 001775–001778, May 2008.

[33] R. Revathy and N. Senthil Kumar. Design and evaluation of robust controller for AC-to-DC Boost converter. In *Computer, Communication and Electrical Technology (ICCCET), 2011 International Conference on*, pages 405–410, March 2011.

[34] I.H. Baciu, I. Ciocan, and S. Lungu. Modeling Transfer Function for Buck Power Converter. In *Electronics Technology, 30th International Spring Seminar on*, pages 541–544, May 2007.

[35] Electrical Rathore, A.K and National University of Singapore Computer Engineering. Small Signal Modelling of Boost Converter. `//http://www.ece.nus.edu.sg/stfpage/akr/ssmboost.pdf.` Accessed: 2015-06-14.

[36] Ruihua Song, Chao Zheng, Ruomei Li, and Zhou Xiaoxin. VSCs based HVDC and its control strategy. In *Transmission and Distribution Conference and Exhibition: Asia and Pacific, 2005 IEEE/PES*, pages 1–6, 2005.

[37] R.W. De Doncker and D.W. Novotny. The Universal field oriented controller. *Industry Applications, IEEE Transactions on*, 30(1):92–100, Jan 1994.

[38] S. D'Arco and J.A. Suul. Generalized implementations of piecewise linear control characteristics for multiterminal HVDC. In *Power Electronics, Electrical Drives, Automation and Motion (SPEEDAM), 2014 International Symposium on*, pages 66–72, June 2014.

[39] J. M. E. Vicente J. A. Cortez P. R. Laurentino . J. J. Rezek, C. A. D. Coelho. The Modulus Optimum (MO) Method Applied to Voltage Regulation Systems: Modeling, Tuning and Implementation. In *Proc. International Conference on Power System Transients, IPST01*, June 2001.

[40] J. A. Suul T. M. Undeland. C. Bajracharya, M. Molinas. Understanding of tuning techniques of converter controllers for VSC-HVDC. In *Nordic Workshop on Power and Industrial Electronics(NORPIE)*, June 2008.

[41] O. Aydin, A. Akdag, P. Stefanutti, and N. Hugo. Optimum controller design for a multilevel AC-DC converter system. In *Applied Power Electronics Conference and Exposition, 2005. APEC 2005. Twentieth Annual IEEE*, volume 3, pages 1660–1666 Vol. 3, March 2005.

[42] D. Jovcic. Bidirectional, High-Power DC transformer. *Power Delivery, IEEE Transactions on*, 24(4):2276–2283, Oct 2009.

[43] Pang Ting, Huang Shenghua, and Wang Shuanghong. A three phase ZVS bidirectional DC-DC converter. In *Vehicle Power and Propulsion Conference, 2008. VPPC '08. IEEE*, pages 1–6, Sept 2008.

[44] Working group B4-52. HVDC Feasibilty study. In *Cigre Tech Rep.*,, 2012.

[45] A.K. Theraja B.L. Theraja. *A Textbook of Electrical Technology: AC and DC Machines, Volume 2*. S Chand, 2006.

[46] Jun Liu, Licheng Sheng, Jianjiang Shi, Zhongchao Zhang, and Xiangning He. Design of High Voltage, High Power and High Frequency Transformer in LCC Resonant Converter. In *Applied Power Electronics Conference and Exposition, 2009. APEC 2009. Twenty-Fourth Annual IEEE*, pages 1034–1038, Feb 2009.

[47] Wei Shen, Fei Wang, D. Boroyevich, and C.W. Tipton. High-Density Nanocrystalline Core Transformer for High-Power High-Frequency Resonant Converter. *Industry Applications, IEEE Transactions on*, 44(1):213–222, Jan 2008.

[48] ABB Transformer,. http://www.constructionweekonline.com/article-22052-abb-wins-120m-saudi-transformers-deal/,.

[49] G. Bergna-Diaz. User guide for ProofGrids models in Matlab/Simulink, project memo AN 14.12.87 within the project Protection and Fault Handling in Offshore HVDC Grids,. http://www.sintef.no/Projectweb/ProOfGrids/, SINTEF Energy Research,December 2014.

Appendix A

Publications

A.1 IEEE TAP Energy Conference, June 2015

The first part of the work on 4Q converter is published in **Technological Advancements in Power Energy,IEEE International Conference, 2015** with the title "*Analysis of DC/DC converters in Multiterminal HVDC systems for large offshore wind farms*". The paper was presented at the conference by the first author on June 26th, 2015.

Analysis of DC/DC Converters in Multiterminal HVDC systems for large offshore wind farms

Shihabudheen K Kolparambath*, Jon Are Suul*,† and Elisabetta Tedeschi*
*Department of Electric Power Engineering, NTNU, Trondheim, Norway
†SINTEF Energy Research, Trondheim, Norway

***Abstract*—The development of far-offshore wind farms and other large-scale renewable energy sources at long distances from load centers will rely on HVDC transmission. Due to the capability for operation in isolated AC grids and integration into multi-terminal DC grids (MTDC), Voltage Source Converters (VSCs) are becoming the preferred technology for HVDC systems. However, most HVDC transmission schemes are currently constructed as point-to point connections, and there is not yet any clear standardization of voltage levels. Thus, DC/DC converters will become necessary if existing or emerging HVDC links should later be interconnected into MTDC configurations. DC/DC converters might also be needed for power flow control in meshed MTDC grids. In this paper, the general requirements for DC/DC converters in different MTDC grid configurations are briefly analyzed before particular attention is dedicated to converters without galvanic separation for power flow control in meshed MTDC grids. The control and operation of a 4-quadrant DC/DC converter for power flow control with voltage ratio close to unity is then analyzed and demonstrated by simulations in a 4-terminal configuration based on the Cigré DC grid test system.**

***Keywords*: Multiterminal, HVDC, DC/DC Converter, Power flow control, VSC**

I. Introduction

Utilization of energy from renewable sources like hydro, wind and solar is the only sustainable solution for meeting the increasing energy demand of a growing population while facing the challenges of global climatic changes. Recent energy statistics show a rapidly increasing utilisation of offshore wind. Until 2014, nearly 8 GW of installed capacity was achieved in Europe, but the total installations are expected to increase in a dramatic way to around 40 GW by 2020 [1]. However, HVAC transmission between offshore generation and onshore load centres is not suitable in case of long distances and wind farms located far offshore, due to the high cable charging capacitance, which reduces the active current capability of long ac cables. Thus, long distance HVAC transmission through subsea cables will lead to high cable losses and requirements for reactive power compensation [2]. These challenges can be avoided by HVDC systems, which can ensure higher transmission capacity, reduced losses and improved local system stability with no problem of reactive power control. For the same power transmission, previous studies show that the DC cable losses are nearly 30-50% less as compared to three phase AC system [3], although the losses and cost of the converter stations need to be taken into account when assessing the overall transmission scheme.

VSC-based HVDC systems can operate in weak and islanded AC systems and allow for DC power flow reversal without changing voltage polarity. Thus, VSC HVDC is a more flexible solution than conventional Line Commutated Converters (LCC) HVDC and is seen as the enabling technology for the implementation of multi-terminal HVDC grids. In this perspective, a future European Supergrid is envisioned as a VSC-based HVDC grid, interconnecting various European countries and neighbouring regions, while providing power corridors for North Sea wind power generation, solar power plants in North Africa and hydro generation in Norway. Such a HVDC transmission system will consist of a meshed DC grid with many connections between AC and DC systems [4].

Suitable converter topologies for interconnecting AC and DC systems, with various corresponding control philosophies, have already been analyzed [5]-[6]. However, a future HVDC grid is expected to emerge through a gradual development where point-to-point connections can later be connected into multi-terminal, meshed, configurations. If different HVDC links at different voltage levels should be connected, high power high voltage DC/DC conversion systems are required. Such DC/DC converters for HVDC applications are not as mature as for low voltage applications where a wide range of topologies are well established for suiting different voltage ratios and power ratings. Furthermore, the interconnection of HVDC systems, operating at different voltages with variable configurations cannot rely on a single DC/DC converter topology. This paper investigates DC/DC topologies for HVDC systems and focuses especially on those suitable for power flow control and interconnection in meshed systems operating with a common configuration (monopolar or bipolar) and with the same rated voltage. In particular, the design and control of a 4-quadrant DC/DC converter without galvanic insulation is investigated and a simulation model in Matlab/Simulink is developed. Such converter model is introduced in a 4-terminal HVDC ring configuration based on the CIGRÉ B4 DC grid test system, to evaluate and verify the performance for power flow control in a meshed HVDC grid.

II. DC/DC Converter for HVDC system

The selection of the DC/DC converter for a specific application depends on various factors, including power rating, voltage ratio, need of galvanic separation, fault blocking

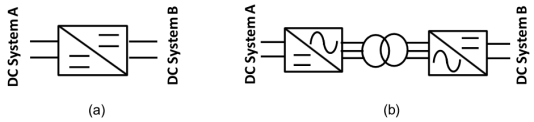

Fig. 1. DC/DC converter a)without galvanic separation and b)with galvanic separation

capability, quadrants of operation, etc. [7]. The steady-state power flow of a multiterminal HVDC grid with ring or meshed configuration will only depend on the resistance of the cables and on the control objectives of the different terminals. In such configurations, it might be necessary to introduce DC/DC converters to control the power flow in the system. Furthermore, DC/DC converters in DC system can also perform the function of a transformer in an AC system by allowing the exchange of power between systems operating at different voltages.

A. DC/DC Converter without galvanic separation

DC systems with the same topology (monopole or bipole) operating at similar voltage levels can be interconnected using a low ratio DC/DC converters without galvanic separation and operating in all the quadrants of V-I curve. This can be implemented using a dedicated DC/DC converter as shown in the Fig. 1a or through the connection of two front to front AC/DC VSCs. Several topologies including multilevel modular converters, resonance converters etc. are discussed in [7]-[8]. This paper, in the later sections, will specifically focus on an example of dedicated DC/DC converter.

B. DC/DC Converter with galvanic separation

Two DC systems operating at different voltages and/or with different configurations, i.e, one with monopole configuration and the other with bipole configuration, must be interconnected using DC/AC/DC topologies with transformer coupling which provides galvanic separation. The general schematic for such connection is shown in Fig. 1b. The transformer coupling helps blocking DC current flowing through AC connection and transferring the voltage stress from the converter to the coupling transformer [7]. The transformer could also be designed for frequencies higher than AC grid frequency to reduce the core size, thereby reducing the cost and volume.

III. Design, Modelling and Control of DC/DC Converter for low ratio connections

In this paper, design, modelling and control of a DC/DC converter topology used for low ratio connection is analysed in detail. Power flow control in a meshed MTDC grid might require operation in four quadrants of the I-V curve. Thus, 4Q converter topology as shown in Fig. 2 [9] will be suitable as long as galvanic separation is not needed. The converter is capable of transporting energy in forward and reverse directions and of stepping voltage up and down. The topology resembles a buck and boost converter when operating the four switches in certain manner. The operation of switches and diodes in different modes is shown in Table I and Table II,

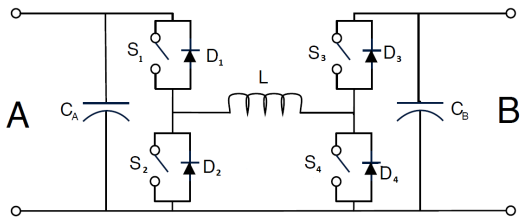

Fig. 2. Four Quadrant Converter

wherein A, 1 & 0 indicates status of the component, i.e. active, completely ON and completely OFF respectively.

A. Sizing of Components

The main components in the DC/DC converter are diodes, switch/IGBTs, inductors and capacitors. The sizing of diode and switch/IGBTs depends on many factors, including break-down voltage, withstand capability, continuous current, power rating etc., while inductor and capacitor are sized considering the current and voltage ripples and are different for each converter topology due to the difference in the operational mode. 4Q converter behaves as a buck/boost in relation to the operational modes of IGBT/switches and therefore sizing of components must be calculated taking into account both modes.

1) Inductor: The inductor is chosen such that ripple in the DC current is within the grid code acceptance limit. The calculation uses the standard formulas mentioned in [10]-[12]. Inductor size in buck mode is given by (1):

$$L = [(V_{in} - V_{out}).\frac{V_{out}}{V_{in}}.\frac{1}{f_{sw}}.\frac{1}{2\Delta I_L}] \quad (1)$$

where, ΔI_L is the ripple inductor current, V_{in} and V_{out} are the input and output voltage respectively, while f_{sw} represents the switching frequency. Eq. (2) can be used to compute the inductance in boost mode.

$$L = [V_{in}.\frac{V_{out} - V_{in}}{V_{out}}.\frac{1}{f_{sw}}.\frac{1}{2\Delta I_L}] \quad (2)$$

TABLE I
Operations of switches in different DC-DC modes

Voltage	Power direction	Mode	S1	S2	S3	S4
$V_A > V_B$	A $\rightarrow$ B	Buck	A	0	0	0
$V_B > V_A$	B $\rightarrow$ A	Buck	0	0	A	0
$V_A < V_B$	A $\rightarrow$ B	Boost	1	0	0	A
$V_B < V_A$	B $\rightarrow$ A	Boost	0	A	1	0

TABLE II
Operations of diodes in different DC-DC modes

Voltage	Power direction	Mode	D1	D2	D3	D4
$V_A > V_B$	A $\rightarrow$ B	Buck	0	A	1	0
$V_B > V_A$	B $\rightarrow$ A	Buck	1	0	0	A
$V_A < V_B$	A $\rightarrow$ B	Boost	0	0	A	0
$V_B < V_A$	B $\rightarrow$ A	Boost	A	0	0	0

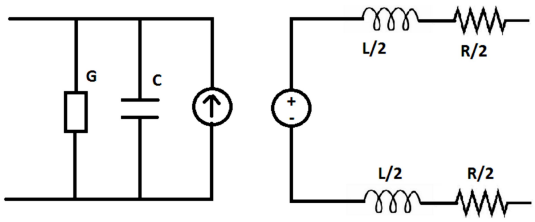

Fig. 3. Average Modelling of DC/DC Converter

2) Capacitor: The capacitors are required to maintain a regulated output voltage and the size of capacitor is a measure of the output voltage ripple. The computation is done using charge balance in the capacitor. In buck mode, the capacitance, C is given by (3):

$$C = \frac{1}{2}.\frac{1}{2f_{sw}}.\frac{V_{out}}{2L\Delta V_{out}}.\frac{(1-D)}{f_{sw}} \tag{3}$$

Capacitance in boost mode can be calculated using (4):

$$C = \frac{I_{out}D}{f_{sw}\Delta V_{out}} \tag{4}$$

ΔV_{out}, I_{out} and D represent the ripple in the voltage, output current and duty cycle, respectively. The results from buck and boost mode are then compared and maximum component value is considered for minimum current and voltage ripples.

B. Average Modelling of the converter

Dynamic average models of converters are usually developed to obtain a continuous time invariant equivalent circuit of converter by averaging the effect of fast switching within a switching interval [12]-[13]. This is useful both to reduce simulation time of large systems and for design of controllers. The DC/DC converter using AVM can be modelled as a current source behind a capacitor(C) and a voltage source behind an inductor(L), as it is shown in the Fig. 3, where R and G represent the parasitics associated with the circuit elements and losses.

C. Controllers

The objective of the converter is to control the power flow, without much variation in the voltage. Therefore the control variables are voltage and current. The controller uses a cascaded control system with inner loop as current control. The inner loop restricts the current through the inductor to a specified range. The bandwidth (speed of response) of a cascade controller increases towards the inner loop with current loop being the fastest and outer loop being the slowest [14]. The fast dynamics of the inner loop in the cascade control structure allow the attenuation of disturbances in faster rate and therefore reduce the possible effect, before the outer loop variable is affected [15]. The outer loops can be implemented in three possible ways, i.e., using current, voltage or power as the controlled variable. Since power is the parameter of interest, voltage and current are needed for the reference power to be calculated using (5).

$$P = VI \tag{5}$$

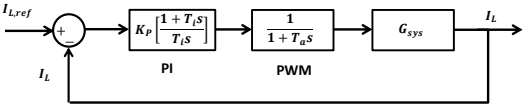

Fig. 4. Inner loop controller

Non linear control strategies with variable frequency methods like hysteresis control, sliding mode control etc. could be utilised as the control strategy to provide a fast transient response for the system, which is non linear due to the switching devices [16]. However, linear control technique using PI controllers and pulse width modulation (PWM) with fixed frequency allows more flexible control and is easy to implement while still providing good transient response.

1) Inner Loop Controller: The reference to the inner PI controller is the output from outer loop, with a limiting block (saturation) to restrict current to a pre-defined range. This current is calculated for the rated power of converter using Kirchhoff's voltage law keeping switch in ON state. This value also depends on the transmission line resistance. The transfer function for the PI regulator can be represented as (6):

$$G_1(s) = \frac{V_{conv}(s)}{I_{L,ref}(s) - I_L(s)} = Kp.\frac{1+T_is}{T_is} \tag{6}$$

where $T_i = K_p/K_i$, K_p and K_i being the gains of proportional and integral controller. The PWM converter can be considered as a first order system with a time delay, T_a. The corresponding transfer function can be written as (7):

$$G_2(s) = \frac{1}{1+T_as} \tag{7}$$

The control to output transfer function for the system differs according to the mode of operation. For the buck mode [17], it is given by (8):

$$G_{sys,buck}(s) = \frac{V_0}{D(1+\frac{sL}{R}s+s^2(LC))} \tag{8}$$

The small signal transfer function when the system is operated in boost mode [18] is given by (9):

$$G_{sys,boost}(s) = \frac{(1-D)V_0 - (LI_L)s}{LCs^2+\frac{L}{R}s+(1-D)^2} \tag{9}$$

The complete block diagram representation for inner loop is shown in Fig. 4.

2) Outer Loop Controller: The output loop controller could be either Power, Voltage or Current. Fig. 5 shows three alternative ways of implementing the controller in Simulink. V_{ref} and I_{ref} can be calculated using the DC power equation of (5) for the given power reference. The controllers are designed for 2% overshoot and 0.3s settling time.

D. Simulation Model of the DC/DC converter

A 2000MW, 380 to 420kV converter according to Fig. 1a with Power controller in the the outer loop was simulated in MATLAB Simulink, using SimPowerSystems toolbox. Table III shows the DC/DC converter parameters used for the

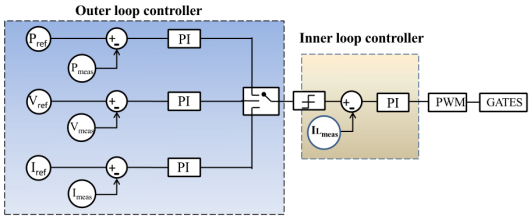

Fig. 5. Cascaded controller strategies for 4Q Converter

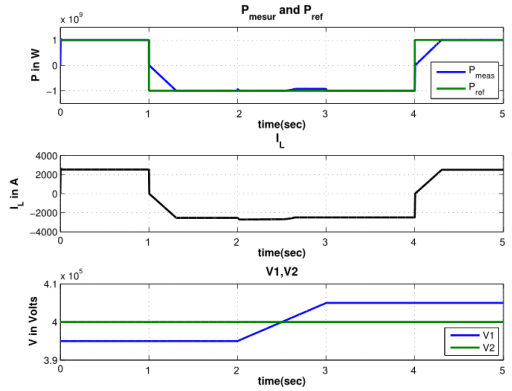

Fig. 6. Output response with Power(outer) and Current(inner) control loop

simulation, calculated as described in section III.A. The variables of interest including, input and output voltage and current, inductor current etc. are measured. The switching of IGBTs depends on the power and voltage values and the corresponding logic for the operating mode is developed using logic gates. Simulation is carried out to verify the controller performance when the DC/DC converter is operating in all the four quadrants. Initial power reference for the outer loop is set at 0.5pu in boost mode and then changed to -0.5pu to verify the bi-directionality. The above conditions are then simulated for buck mode from t=2.5s. The power and related current and voltage waveforms are shown in Fig. 6. The results suggest good performance of controllers by tracking the reference in all four modes with an acceptable degree of error. The current limiter limits the inductor current always below the maximum value. The simulation have also been performed with current controller in both outer and inner loops. The results almost match those obtained with previous controller and are hence not reported.

IV. Meshed MTDC Grid System

The proposed DC/DC converter is incorporated in the DCS3 system, a subsystem of CIGRÉ B4 HVDC Grid [19] to verify its performance. The DCS3 system is a symmetrical bipole configuration network comprising four AC/DC converters. The

TABLE III
DC/DC converter design parameters

Parameters	L	$C1$	$C2$	f_{sw}
Values	$34mH$	$10\mu F$	$10\mu F$	$1kHz$

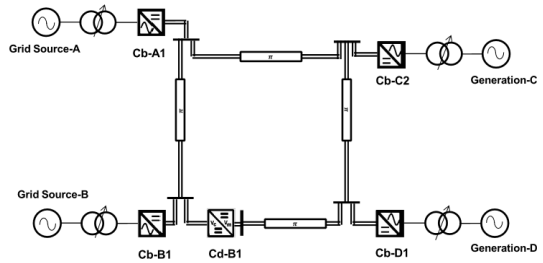

Fig. 7. DCS3 subsystem

schematic of DCS3 subsystem is shown in Fig. 7, where DC lines are modelled in pi configuration. The DC cable parameters used for simulation are shown in Table IV. The AC/DC converters impose control strategies with either PQ or V_{DC} regulator in the outer loop and current regulator in the inner loop using PI controller. The outer loop regulates PQ or V_{DC} reference by calculating the active and reactive current reference for the inner loop, while the inner current controller calculates the required AC voltage reference for the PWM [20]. A phase-locked loop (PLL) is utilised for synchronization of control voltage to the AC grid voltage.

A case scenario is analysed where, the operating point of the Cb-D1 AC/DC converter is varied from 100MW($\rightarrow$ AC grid) to 350MW($\rightarrow$ DC grid) at t=5s. Simulation is carried out first without DC/DC converter and then incorporating it into the system. The AC/DC converters only control the power delivered to its DC side of the converter. The proportion of power flowing through lines connected to it depends on the resistance of the line and hence there is no control of line power flow. The load flow result obtained after simulation for the case(Cb-D1:350MW $\rightarrow$ DC grid) is shown in Fig. 9. As a second case, the Cd-B1 DC/DC converter is enabled with a setpoint of 150MW from D to B until t=4s, reduce to 50MW and reverse the power direction and deliver 200MW at t=7s. The power flow through the cable B1-D1 is now controlled using the converter according to the reference value. Fig. 10 illustrates the performance of the converter by tracking the

TABLE IV
DC Cable Parameters[19]

Cable ID	**Length** (km)	**R** (Ω)	**L** (mH)	**C** (μF)
A1-B1	400	3.80	844.8	76.24
A1-C2	200	1.90	422.4	38.12
C2-D1	300	2.85	633.6	57.18
B1-D1	400	3.80	844.8	76.24

TABLE V
Load flow result in MW

Cable ID	**Without DC/DC Converter**	**With DC/DC Converter** P_{set}**=150MW**	**With DC/DC Converter** P_{set}**=200MW**
A1-B1	184 (B1$\rightarrow$A1)	148 (B1$\rightarrow$A1)	202 (A1$\rightarrow$B1)
A1-C2	745 (C2$\rightarrow$A1)	779 (C2$\rightarrow$A1)	1130 (C2$\rightarrow$A1)
C2-D1	398 (D1$\rightarrow$C2)	432 (D1$\rightarrow$C2)	783 (D1$\rightarrow$C2)
B1-D1	186 (D1$\rightarrow$B1)	150 (D1$\rightarrow$B1)	200 (B1$\rightarrow$D1)

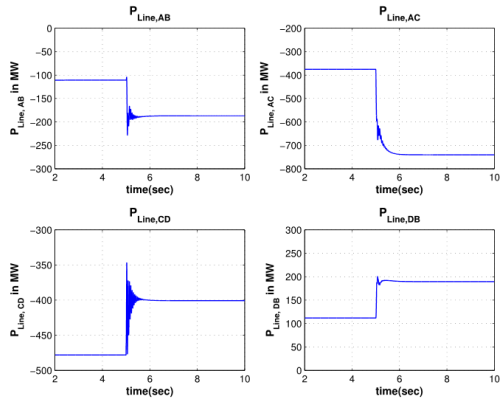

Fig. 8. Power flowing through DC lines without DC/DC converter

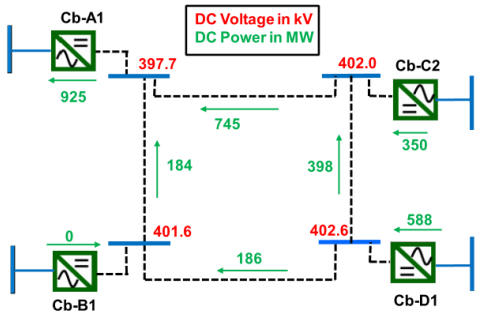

Fig. 9. Load flow result without DC/DC converter

set reference. The power control in line DB affects the power flow through other lines as expected since the case scenario of four AC/DC converters determines the total power in the DC network, which is still the same as without DC/DC converter. The power measured at the DC side of the AC/DC converter is shown in Fig. 11. It can be observed that the DC power of each AC/DC converter remains the same irrespective of changing the power at DC/DC converter, although with some ripples during the power change. The converter DC voltages are also analysed to verify compliance with their operational limit. Results are plotted in Fig. 12. The current flowing through the inductor of DC/DC converter is shown in Fig. 13, where the current is regulated using the inner loop of the controller and always limiting the current within the allowed range. The load flow results for two cases with DC/DC converter are shown in Fig. 14 and Table V. Load flow results show the performance of both AC/DC converters and DC/DC converter. The V_{DC} at Cb-A1 is maintained at 397.7kV, while real power delivered from Cb-C2 and Cb-D1 is regulated to the set value for both the cases discussed.

V. Conclusion

Future MTDC transmission systems might emerge through interconnection of point-to-point HVDC links. Such a development will require high power high voltage DC/DC converters for interconnecting systems with different DC voltages or

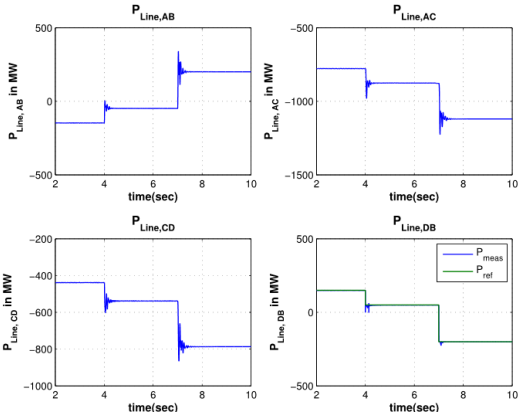

Fig. 10. Power flowing through DC lines with DC/DC converter

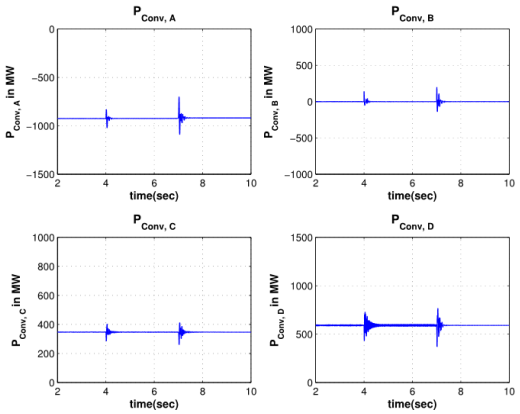

Fig. 11. DC Power output at AC/DC converter

grounding configurations. In meshed MTDC grids, DC/DC converters can also be needed to control the power flow independently of the cable impedances. This paper has discussed the requirements for DC/DC converters in MTDC systems and has identified the four quadrant converter topology as a viable solution for bidirectional power flow control in meshed MTDC grids with unified voltage rating. Moreover, the paper has shown how a properly designed DC-DC converter can be controlled to regulate the power flow in a 4-terminal MTDC ring configuration based on the Cigré DC grid test system.

Acknowledgment

The authors would like to thank Dr. Yongtao Yang, DNV GL for the support provided to this work, and Dr. G Bergna-Diaz for providing the simulation models [20].

References

[1] The European offshore wind industry -key trends and statistics 2014, January 2015, [Online]. Available: http://http://www.ewea.org/fileadmin/files/library/publications/statistics/EWEA-European-Offshore-Statistics-2014.pdf.

[2] F. Wang, P. Yunqing, D. Boroyevich, R. Burgos and N. Khai, "Ac vs. dc distribution for off-shore power delivery," in *34th Annual IEEE Conf. of Industrial Electronics* 2008, pp. 2113-2118.

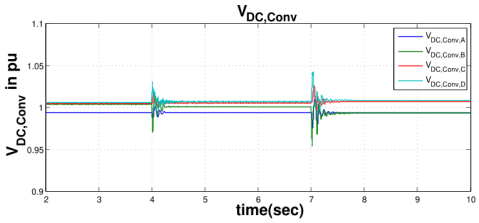

Fig. 12. DC Voltages of AC/DC Converter in pu

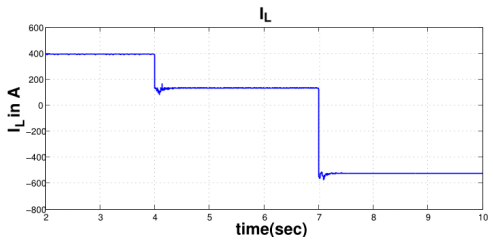

Fig. 13. Current through the inductor of 4Q Converter

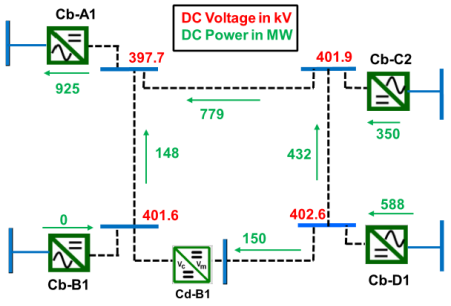

(a)

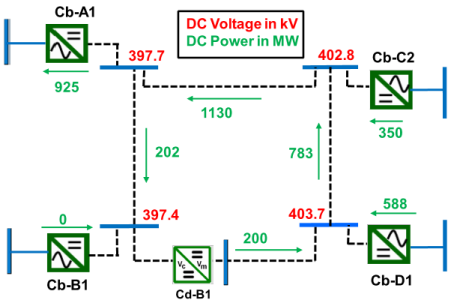

(b)

Fig. 14. Load flow result with DC/DC converter with a)$Pset = 150MW$ and b)$Pset = -200MW$

[3] R. Majumder, C. Bartzsch, P. Kohnstam, E. Fullerton, A. Finn and W. Galli, "Magic bus: High-voltage DC on the new power transmission highway," in *IEEE Power Energy Mag*. 2012, vol. 10, no. 6, pp. 39-49.

[4] D. V. Hertem, M. Ghandhari and M. Delimar, "Technical limitations towards a supergrid- A european prospective," in *Proc. IEEE Int. Energy Conf. Exhib.*, 2010 pp. 302-309.

[5] J. Zhu and C. Booth, "Future multi-terminal HVDC transmission systems using Voltage source converters," in *Universities Power Engineering Conference (UPEC)*, 2010 45th International, vol., no., pp. 1-6, Aug. 31 2010- Sept. 3 2010.

[6] Stylen, H.; Uhlen, K.; rdal, A.R.; Sharifabadi, K., "Laboratory demonstration of an offshore grid in the North Sea with DC droop control," in *Ecological Vehicles and Renewable Energies (EVER), 2014 Ninth International Conference on* , vol., no., pp.1,8, 25-27 March 2014.

[7] C. D. Barker, C. C. Davidson, D. R. Trainer, and R. S. Whitehouse, "Requirements of DC-DC Converters to facilitate large DC Grids," in *Cigre Session 2012*, 2012.

[8] C. E. Sheridan, M. M. C. Merlin and T. C. Green "Assessment of DC/DC converters for use in DC nodes for offshore grids," in *Proc. ACDC. 10th IET Int. Conf. AC DC Power Transmiss.*, pp. 1-6 2012.

[9] M. Hedlund, J. G. Oliveira and H. Bernhoff, "Sliding mode 4-quadrant DCDC converter for a flywheel application," *Control Engineering Practice*, Volume 21, Issue 4, April 2013, pp. 473-482.

[10] J. Leuchter, P. Bauer, P. Bojda and V. Rerucha, "Bi-directional DC-DC Converters for Supercapacitor Based Energy Butfer For Electrical GEN-SETS," in *Proceedings of the 12th European Conference on Power Electronics and Applications(EPE 2007)*. Aalborg, 2007, pp. 1-10.

[11] N. Mohan, T. M. Undeland and W. P. Robbins, *Power Electronics: Converters, Applications, and Design*, (Third edition), Wiley Publications, 2003.

[12] R. W. Erickson, *Fundamentals of Power Electronics*, (First edition), New York: Chapman & Hall, May 1997, 791 pages.

[13] S. Chiniforoosh, J. Jatskevic, A. Yazdani, V. Sood ,V. Dinavahi ,J. A. Martinez and A. Ramirez, "Definitions and applications of dynamic average models for analysis of power systems," in *IEEE Trans. Power Del.*, vol. 25, no. 4, pp. 2655-2669 2010.

[14] N. Mohan, *Electric Drives: An Integrative Approach*, Minneapolis, MN: MNPERE, 2003.

[15] R. Vilanova and O. Arrieta, "PID tuning for cascade control system design," in *Electrical and Computer Engineering, 2008. CCECE 2008. Canadian Conference on* , vol., no., pp. 001775-001778, 4-7 May 2008.

[16] Revathy, R.; Senthil Kumar, N., "Design and evaluation of robust controller for AC-to-DC Boost converter," in *Computer, Communication and Electrical Technology (ICCCET), 2011 International Conference on* , vol., no., pp.405,410, 18-19 March 2011.

[17] I. H. Baciu, I. Ciocan, and S. Lungu, "Modeling Transfer Function for Buck Power Converter," in *30th International Spring Seminar on Electronics Technology*, May 2007, pp. 541-544.

[18] A. K. Rathore, Small Signal Modelling of Boost Converter, [Online]. Available: http://www.ece.nus.edu.sg/stfpage/akr/ssmboost.pdf.

[19] Vrana, T.K., Yang, Y., Jovcic, D., Dennetire, S., Jardini, J., Saad, H (B4 57 and B4 58), "The CIGRE B4 DC Grid Test System", HVDC and Power Electronics, Available: http://b4.cigre.org/Publications/Documents-related-to-the-development-of-HVDC-Grids.

[20] G. Bergna-Diaz, "User Guide for ProOfGrids Models in Matlab/Simulink," project memo AN 14.12.87 within the project "Protection and Fault Handling in Offshore HVDC Grids," http://www.sintef.no/Projectweb/ProOfGrids/, SINTEF Energy Research, December 2014

A.2 IEEE Southern Power Electronics Conference

The second part of the work on DC/DC converters with galvanic separation is submitted in **Southern Power Electronics Conference, IEEE, 2015** with the title "*DC/DC Converters for interconnecting independent HVDC systems into Multiterminal DC grids*". The submitted paper is attached.

DC/DC CONVERTERS FOR INTERCONNECTING INDEPENDENT HVDC SYSTEMS INTO MULTITERMINAL DC GRIDS

ABSTRACT

The development of offshore wind farms, the integration of other large scale renewables and the need to transmit high amounts of power over large distances will result in increasing number of HVDC systems into the power network. Voltage source converters (VSC) based HVDC technology favours the concept of multi-terminal HVDC system (MTDC) due to the flexibility in the power control, black-start capability etc. However, existing HVDC connections, which are mainly point-to-point, are often operated at different voltages and with dissimilar configurations and therefore DC/DC converters will become necessary for their interconnection and for the control of power flow in meshed MTDC grids. The goal of this paper is to summarize the requirements for DC-DC converters in HVDC applications and focus on the modelling and control of high voltage ratio solutions, proving their applicability in a subsystem of the CIGRE B4 HVDC test system.

I. INTRODUCTION

The offshore energy installations are growing exponentially, especially in Europe, where a cumulative installed capacity of 8GW was reached in 2014 [1]. This, coupled with deregulated energy markets, has resulted in more attention towards VSC based HVDC system that can eventually evolve in the interconnection of existing point-to-point HVDC connections operating with different voltages and different configurations. Additionally, the need for power flow control when there is a risk of cable overloading in specific network sections, require the introduction of DC/DC converters. However, DC/DC converters for high voltage high power applications are not as developed as for low power applications and also cannot rely on a single topology. This paper reviews converter topologies for HVDC applications and examines design, modelling and control of solutions suitable for interconnecting two systems with high voltage ratio and interconnection of dissimilar configurations (monopolar and bipolar). Finally different DC/DC configurations are introduced in the simulation model of CIGRE B4 HVDC grid system to verify their functionality.

II. DC/DC CONVERTER FOR HVDC SYSTEM

The choice of DC/DC converters for interconnecting two HVDC systems for a specific application depends on various factors including voltage ratio, configuration of interconnected systems, need of galvanic separation, power rating etc. [2]. A general overview of DC/DC converters listed in the literature is given in the Table. 1. A more detailed comparison will be included in the final paper.

Table 1: Overview of DC/DC Converters

Voltage ratio	Topology	Comments
$\frac{V_{\{DC,HV\ side\}}}{V_{\{DC,LV\ side\}}} \leq 1.2$ (for power flow control)	4Q Converter[3] $\frac{V_{\{DC,A\}}}{V_{\{DC,B\}}} \leq \pm 1.2$	Dedicated DC/DC converter, No galvanic separation
	Bidirectional Boost converter [4]	
	Front-Front DC/AC/DC Converter[5]	Mostly modular multi-level converter(MMC)
$\frac{V_{\{DC,HV\ side\}}}{V_{\{DC,LV\ side\}}} \geq 1.2$	Resonant DC/DC Converter[6]-[7]	Soft switching
	Transformer coupled DC/AC/DC Converter[2]-[8]	Galvanic separation, MMC

This paper focuses on galvanically isolated DC/DC converters intended for interconnecting systems operating with different voltages and different configurations. i.e., monopolar and bipolar.

III. DC/DC CONVERTER WITH GALVANIC SEPARATION

Like AC systems operating with different voltages use a transformer for interconnection, DC/DC converters with transformer coupling can be utilised in a DC system for the exchange of power between two systems operating at different voltages. Coupling through transformer blocks a direct path between two DC sides, thereby preventing propagation of faults from one side to the other and

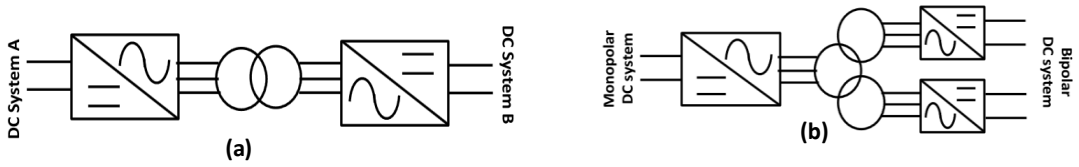

Figure 1: Transformer coupled DC/AC/DC converters interconnecting systems with (a) different voltage (b) dissimilar configuration

helps in avoiding short circuit condition [2]. One advantage of the scheme is that the transformer could be designed for higher frequency to reduce the core size. The schematics of DC-AC-DC

converter for interconnecting systems with different voltage and different configurations are shown in Fig. 1.a and 1.b, respectively.

A. CONTROLLERS

The models in Fig. 1 consist of different AC/DC converters. The control objective of regulating the active power flow through the HVDC line could be realised by implementing vector control strategy [9] in the converter performing power control, while using fixed modulation index [10] for the voltage controlled one as shown in Fig. 2. The scheme in Fig. 2(a) allows independent control of the power flow in each pole of bipolar configuration. Further details will be included in the final paper.

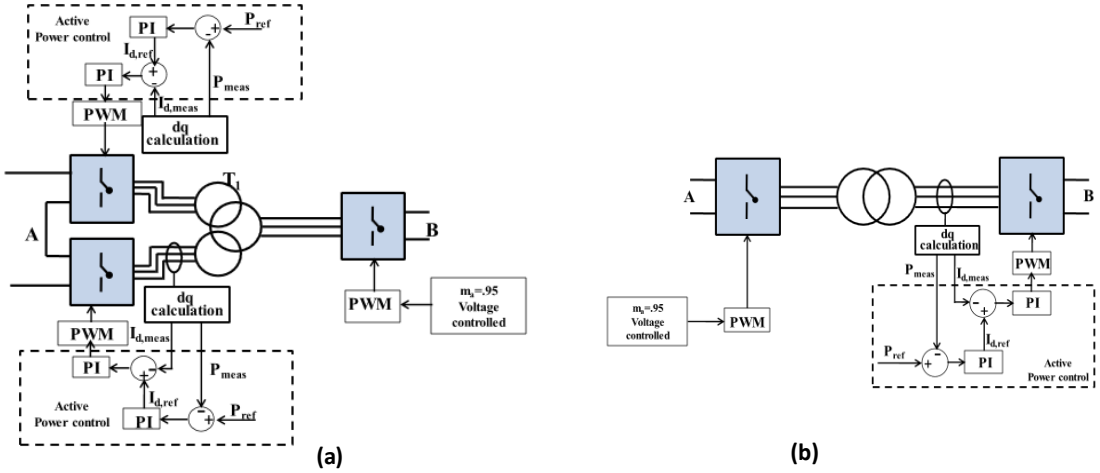

Figure 2: Control strategy for DC/AC/DC Converter interconnecting systems with (a) dissimilar configuration (b) different voltages

The controller gains for outer power loop and inner current loop regulator for the vector controller are calculated using modulus optimum and symmetric optimum criteria, respectively [11]. The outer loop controllers calculate the active current reference, $I_{d,ref}$ and reactive current reference, $I_{q,ref}$ for the inner loop, while inner loop calculates the AC voltage reference for PWM generator. PLL is used for the synchronisation of the control voltage to the AC grid voltage.

B. RESULTS

A 2000MW, ±400kV (Bipolar)/±200kV (Symmetric monopolar) converter (Fig. 2.a) was implemented in MATLAB Simulink, using Sim-PowerSystems toolbox to verify the proper operation of controllers designed. A transformer coupled DC/AC/DC converter in addition to interconnection of

independent HVDC systems also provides the flexibility of power control. The results of a case, where the power reference is changed from -500MW to 300MW at t=2.5 sec is plotted in the Fig. 3. It is evident that DC voltage remains constant, while DC current changes according to the setting. In the final paper, control and operation of a system as in Fig. 2.b will be also presented.

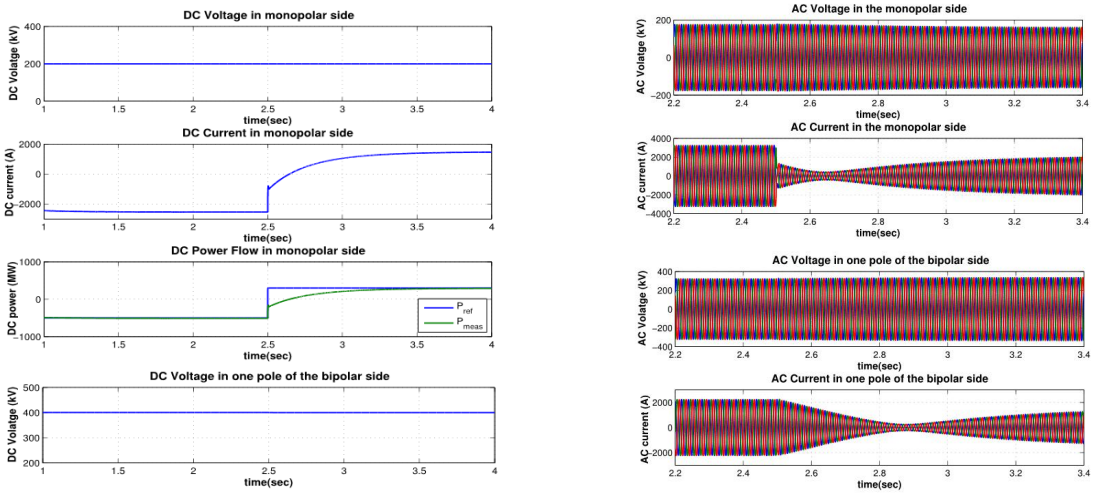

Figure 3: Output response for transformer coupled DC/AC/DC Converter

IV. MTDC GRID SYSTEM

After the standalone verification of the DC/DC converter performance, it is incorporated in a Meshed HVDC system, a subsystem of CIGRE B4 HVDC grid [12], together with a non-isolated solution already studied in [3]. The schematic is shown in the Fig. 4, where DC lines are modelled in pi configuration. The system consists of a Bipolar ±400kV DC network and a Symmetric Monopole ±200kV DC network. DC/DC converter Cd-E1 interconnects the bipolar system with monopole, while Cd-B1 is placed in the cable B1-E to control the cable power flow. The 6 AC/DC converters in the system impose the control strategies with either PQ or V_{DC} regulator in the outer loop and current in the inner loop. Various case scenarios are simulated to verify the functionality of both AC/DC and DC/DC converters. An example of an

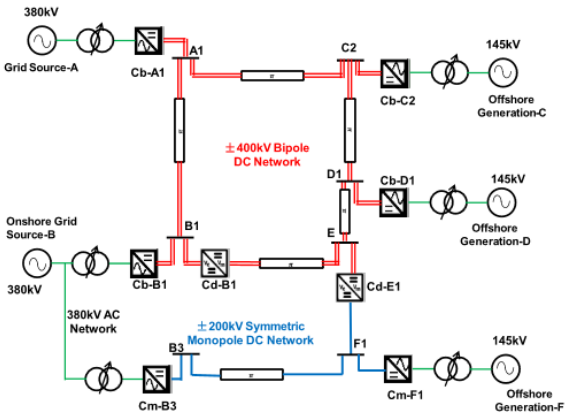

Figure 4: CIGRE B4 MTDC Test grid

analysed case scenario is shown in the Table II and the simulation results are summarised in Fig. 5. Fig. 5 shows that each AC/DC converter in the system defines the power delivered to the grid and does not have any control over the cable power flow. Cd-B1 when implemented using 4Q converter [3] defines the power flowing through the cables, while Cd-E1 interconnects two systems of different configurations and voltages and also provides the additional flexibility of power control from one system into another. Additional results on the system operations will be included in the final paper.

Converter	Set point
Cb-A1	$V_{DC} = 404.8\text{kV}$
Cb-B1	$P_{set} = 1000\text{MW}$
Cb-C2	$P_{set} = -600\text{MW}$
Cb-D1	$P_{set} = -800\text{MW}$
Cm-F1	$V_{DC} = 200.4\text{kV}$
Cm-B3	$P_{set} = 400\text{MW}$
Cd-B1	$\boldsymbol{P_{set} = 300\text{MW}}$
Cd-E1	$\boldsymbol{P_{set} = 400\text{MW}}$

Table II: An example case scenario

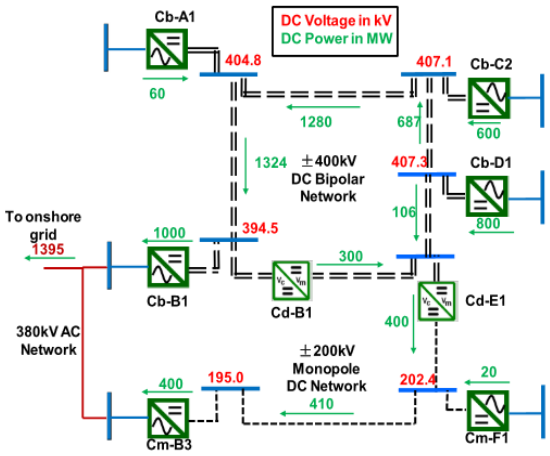

Figure 5: Simulation result for the case given in Table II

V. CONCLUSION and FUTURE WORK

DC/DC converters are necessary in the future MTDC grid to interconnect subsystems with different DC voltages or grounding configurations. The goal of this paper is to investigate, model and design DC/DC converter topologies with a system level perspective for application in multi-terminal HVDC systems. The validity of the approach is demonstrated in the CIGRE MTDC test system.

The final paper will cover detailed design of converters in Fig. 1 including tuning of controllers, average modelling, analysis of converter parameters and various cases with different parameter settings of both AC/DC and DC/DC converters of CIGRE B4 system.

REFERENCES

[1] The European offshore wind industry -key trends and statistics 2014, January 2015, [Online].Available: http://www.ewea.org/fileadmin/files/library/publications/statistics/EWEA-Europ-ean -Offshore-Statistics-2014.pdf

[2] C. D. Barker, C. C. Davidson, D. R. Trainer, and R. S. Whitehouse, "Requirements of DC-DC Converters to facilitate large DC Grids," in *Cigre Session* 2012, 2012.

[3] S.K. Kolparambath, J. A. Suul, E. Tedeschi," Analysis of DC/DC converters in multi-terminal HVDC systems for large offshore windfarms," in *IEEE conference in Technological advancements in Power & Energy*, 2015.

[4] Font, J.; Martinez, L., "Modelling and analysis of a bidirectional boost converter with output filter," *Electrotechnical Conference, 1991. Proceedings., 6th Mediterranean* , vol., no., pp.1380,1383 vol.2, 22-24 May 1991

[5] R. Feldman , M. Tomasini , E. Amankwah , J. Clare , P. Wheeler , D. Trainer and R. Whitehouse "A hybrid modular multilevel voltage source converter for HVDC power transmission", *IEEE Trans Ind. Appl.*, vol. 49, no. 4, pp.1577 -1588 2013

[6] D. Jovcic "Bidirectional, high-power dc transformer", *IEEE Trans. Power Del.*, no. 4, pp.2276 -2283 2009

[7] Pang Ting; Huang Shenghua; Wang Shuanghong, "A three phase ZVS bidirectional DC-DC converter," *Vehicle Power and Propulsion Conference, 2008. VPPC '08. IEEE* , vol., no., pp.1,6, 3-5 Sept. 2008

[8] C. E. Sheridan, M. M. C. Merlin and T. C. Green "Assessment of DC/DC converters for use in DC nodes for offshore grids," in Proc. *ACDC. 10th IET Int. Conf. AC DC Power Transmiss.*, pp. 1-6 2012.

[9] S. D'Arco, J. A. Suul, "Generalized Implementation of Piecewise Linear Control Characteristics for Multiterminal HVDC" in Proceedings of the *22nd International Symposium on Power Electronics, Electrical Drives, Automation and Motion, SPEEDAM 2014*, Ischia, Italy, 18-20 June 2014, pp- 66-72

[10] N. Mohan, T. M. Undeland and W. P. Robbins, *Power Electronics: Converters, Applications, and Design*, (Third edition), Wiley Publications, 2003.

[11] C. Bajracharya, M. Molinas, J. A. Suul, T. M. Undeland, "Understanding of tuning techniques of converter controllers for VSC-HVDC," *Nordic Workshop on Power and Industrial Electronics(NORPIE)*, June 9-11, 2008.

[12] B4 57 and B4 58, "The CIGRE B4 DC Grid Test System", HVDC and Power Electronics, Available: http://b4.cigre.org/Publications/Documentsrelated- to-the-development-of-HVDC-Grids.

Appendix B

Transformations

abc to dq-Park Transformation

$$\begin{bmatrix} d \\ q \\ 0 \end{bmatrix} = \frac{2}{3} \begin{bmatrix} cos(\omega t) & cos(\omega t - \frac{2\pi}{3}) & cos(\omega t + \frac{2\pi}{3}) \\ -sin(\omega t) & -sin(\omega t - \frac{2\pi}{3}) & -sin(\omega t + \frac{2\pi}{3}) \\ \frac{1}{2} & \frac{1}{2} & \frac{1}{2} \end{bmatrix} \begin{bmatrix} a \\ b \\ c \end{bmatrix}$$

dq to abc-Inverse Park Transformation

$$\begin{bmatrix} a \\ b \\ c \end{bmatrix} = \begin{bmatrix} cos(\omega t) & -sin(\omega t) & 1 \\ cos(\omega t - \frac{2\pi}{3}) & -sin(\omega t - \frac{2\pi}{3}) & 1 \\ cos(\omega t + \frac{2\pi}{3}) & -sin(\omega t + \frac{2\pi}{3}) & 1 \end{bmatrix} \begin{bmatrix} d \\ q \\ 0 \end{bmatrix}$$

Appendix C

Simulink Model & Matlab Code

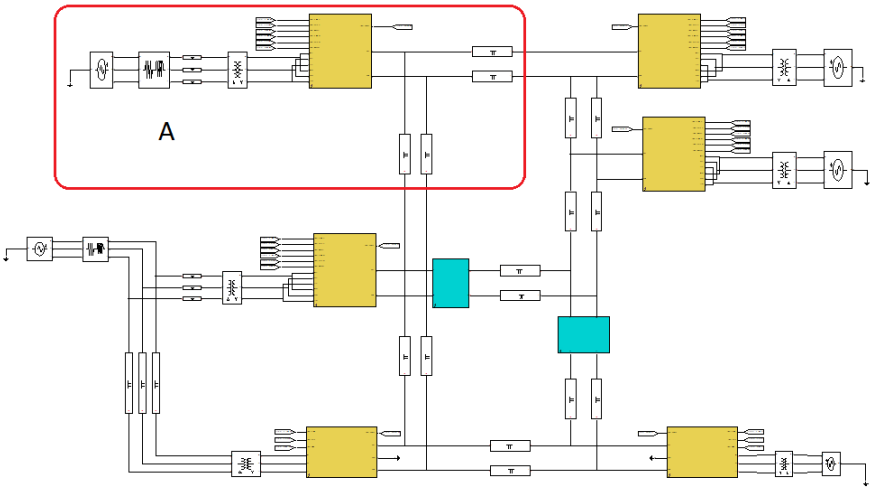

Figure C.1: *Simulink Model of part of CIGRÉ B4 HVDC system*

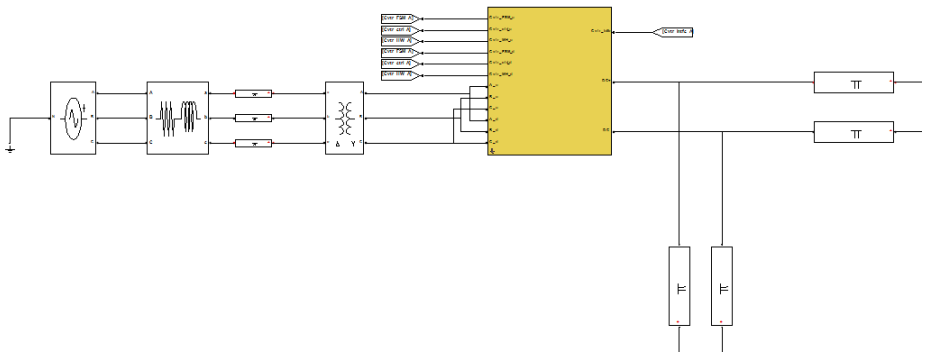

Figure C.2: *Expanded view of section A in C.1*

```
function varargout = ScenarioTemplate(varargin)

%#codegen
Ts = 0;
savemat = 1;
if nargin>=2
    savemat = varargin{2};
elseif nargin>=1
    Ts = varargin{1};
end

nCvtr_ref = 16; % # number of references for each converter
nEl_mod_ctrl_ref = 10; % number of additional events
nSec_ctrl_ref = 16; % number of additional events

% definition of ref index
idx.enable_cvtr_intfc=1;
idx.enable_SVPWM_intfc=2;
idx.enable_PLL_intfc=3;
idx.enable_Vdc_ctrl_intfc=4;
idx.enable_PQ_ctrl_intfc=5;
idx.f_sw_ref=6;
idx.f_ref_PLL=7;
idx.Id_ref=8;
idx.Iq_ref=9;
idx.P_ref=10;
%%
idx.Q_ref=11;
idx.Vdc_ref=12;
idx.cntcr_ctrl_intfc=13;
idx.enable_ICalibration_intfc=14;
idx.enable_VdcCalibration_intfc=15;
idx.enable_VCalibration_intfc=16;

% definition of Events index
idxE.SW1 = 1;
idxE.Fault1 = 2;

% definition of ref index
idxSC.Vdc_ref_max_A=1;
idxSC.Vdc_ref_min_A=2;
idxSC.droop_gain_A=3;
idxSC.Idc_ref_A=4;
idxSC.Vdc_ref_max_B=5;
idxSC.Vdc_ref_min_B=6;
idxSC.droop_gain_B=7;
idxSC.Idc_ref_B=8;
idxSC.Vdc_ref_max_C=9;
idxSC.Vdc_ref_min_C=10;
idxSC.droop_gain_C=11;
idxSC.Idc_ref_C=12;
idxSC.Vdc_ref_max_D=13;
idxSC.Vdc_ref_min_D=14;
idxSC.droop_gain_D=15;
idxSC.Idc_ref_D=16;
```

```
ts_ConvA = timeseries('ts_ConvA');
ts_ConvA = setinterpmethod(ts_ConvA, 'zoh');
ts_ConvB = timeseries('ts_ConvB');
ts_ConvB = setinterpmethod(ts_ConvB, 'zoh');
ts_ConvC = timeseries('ts_ConvC');
ts_ConvC = setinterpmethod(ts_ConvC, 'zoh');
ts_ConvD = timeseries('ts_ConvD');
ts_ConvD = setinterpmethod(ts_ConvD, 'zoh');
ts_ConvF = timeseries('ts_ConvF');
ts_ConvF = setinterpmethod(ts_ConvF, 'zoh');
ts_ConvG = timeseries('ts_ConvG');
ts_ConvG = setinterpmethod(ts_ConvG, 'zoh');
ts_ConvH = timeseries('ts_ConvH');
ts_ConvH = setinterpmethod(ts_ConvH, 'zoh');
ts_ConvJ = timeseries('ts_ConvJ');
ts_ConvJ = setinterpmethod(ts_ConvJ, 'zoh');
ts_ConvK = timeseries('ts_ConvK');
ts_ConvK = setinterpmethod(ts_ConvK, 'zoh');
ts_Events = timeseries('ts_Events');
ts_Events = setinterpmethod(ts_Events, 'zoh');
ts_Secondary_control = timeseries('ts_Secondary_control');
ts_Secondary_control = setinterpmethod(ts_Secondary_control, 'zoh');

%% Initialization
f_sw_ref = 5000;

sA.data = zeros(1,nCvtr_ref); % Default initialization is zero.
sA.time = 0;
sA.data(idx.f_sw_ref) = f_sw_ref; % Initialize required variables.
sA.data(idx.f_ref_PLL) = 50;
ts_ConvA = addsample(ts_ConvA,sA);

sB.data = zeros(1,nCvtr_ref);
sB.time = 0;
sB.data(idx.f_sw_ref) = f_sw_ref;
sB.data(idx.f_ref_PLL) = 50;
ts_ConvB = addsample(ts_ConvB,sB);

sC.data = zeros(1,nCvtr_ref);
sC.time = 0;
sC.data(idx.f_sw_ref) = f_sw_ref;
sC.data(idx.f_ref_PLL) = 50;
ts_ConvC = addsample(ts_ConvC,sC);

sD.data = zeros(1,nCvtr_ref);
sD.time = 0;
sD.data(idx.f_sw_ref) = f_sw_ref;
sD.data(idx.f_ref_PLL) = 50;
ts_ConvD = addsample(ts_ConvD,sD);

sF.data = zeros(1,nCvtr_ref);
sF.time = 0;
sF.data(idx.f_sw_ref) = f_sw_ref;
sF.data(idx.f_ref_PLL) = 50;
ts_ConvF = addsample(ts_ConvF,sF);
```

```
sG.data = zeros(1,nCvtr_ref);
sG.time = 0;
sG.data(idx.f_sw_ref) = f_sw_ref;
sG.data(idx.f_ref_PLL) = 150;
ts_ConvG = addsample(ts_ConvG,sG);

sH.data = zeros(1,nCvtr_ref);
sH.time = 0;
sH.data(idx.f_sw_ref) = f_sw_ref;
sH.data(idx.f_ref_PLL) = 150;
ts_ConvH = addsample(ts_ConvH,sH);

sJ.data = zeros(1,nCvtr_ref);
sJ.time = 0;
sJ.data(idx.f_sw_ref) = f_sw_ref;
sJ.data(idx.f_ref_PLL) = 50;
ts_ConvJ = addsample(ts_ConvJ,sJ);

sK.data = zeros(1,nCvtr_ref);
sK.time = 0;
sK.data(idx.f_sw_ref) = f_sw_ref;
sK.data(idx.f_ref_PLL) = 50;
ts_ConvK = addsample(ts_ConvK,sK);

sE.data = zeros(1,nEl_mod_ctrl_ref);
sE.time = 0;
ts_Events = addsample(ts_Events,sE);

sSC.data = zeros(1,nSec_ctrl_ref);
sSC.time = 0;
sSC.data(idxSC.Vdc_ref_max_A) = 1.1;
sSC.data(idxSC.Vdc_ref_min_A) = 1.1;
sSC.data(idxSC.droop_gain_A) = 0;
sSC.data(idxSC.Idc_ref_A) = 0;
sSC.data(idxSC.Vdc_ref_max_B) = 1.12;
sSC.data(idxSC.Vdc_ref_min_B) = 1.08;
sSC.data(idxSC.droop_gain_B) = 0;
sSC.data(idxSC.Idc_ref_B) = .8;
sSC.data(idxSC.Vdc_ref_max_C) = 1.14;
sSC.data(idxSC.Vdc_ref_min_C) = 1.06;
sSC.data(idxSC.droop_gain_C) = 0;
sSC.data(idxSC.Idc_ref_C) = .6;
sSC.data(idxSC.Vdc_ref_max_D) = 1.16;
sSC.data(idxSC.Vdc_ref_min_D) = 1.04;
sSC.data(idxSC.droop_gain_D) = 0;
sSC.data(idxSC.Idc_ref_D) = .7;

ts_Secondary_control = addsample(ts_Secondary_control,sSC);

% Events Definitions
% 1) set the new time:          sX.time = newtime
% 2) update the required data:  sX.data(index) = newvalue
% 3) add the sample:            ts_ConvX = addsample(ts_ConvX,sX);
```

```
%% Converter A1
% definition of event 1 A1
sA.time = 0.01;
sA.data(idx.enable_SVPWM_intfc) = 1;
sA.data(idx.enable_PLL_intfc) = 1;
sA.data(idx.enable_Vdc_ctrl_intfc) = 1;
sA.data(idx.Vdc_ref) = 404.8*1e3;
sA.data(idx.cntcr_ctrl_intfc) = 1;
ts_ConvA = addsample(ts_ConvA,sA);

% definition of event 2 A1
sA.time = 0.3;
sA.data(idx.enable_cvtr_intfc) = 1;
ts_ConvA = addsample(ts_ConvA,sA);


%% Converter B1
% definition of event 1 B1
sB.time = 0.01;
sB.data(idx.enable_SVPWM_intfc) = 1;
sB.data(idx.enable_PLL_intfc) = 1;
sB.data(idx.enable_PQ_ctrl_intfc) = 1;
sB.data(idx.P_ref)=1000e6;
sB.data(idx.Q_ref)=0;
sB.data(idx.cntcr_ctrl_intfc) = 1;
ts_ConvB = addsample(ts_ConvB,sB);

% definition of event 2 B1
sB.time = 0.35;
sB.data(idx.enable_cvtr_intfc) = 1;
ts_ConvB = addsample(ts_ConvB,sB);


%% Converter C2
% definition of event 1 C2
sC.time = 0.01;
sC.data(idx.enable_SVPWM_intfc) = 1;
sC.data(idx.enable_PLL_intfc) = 1;
sC.data(idx.enable_PQ_ctrl_intfc) = 1;
sC.data(idx.P_ref)=-600e6;
sC.data(idx.Q_ref)=0;
sC.data(idx.cntcr_ctrl_intfc) = 1;
ts_ConvC = addsample(ts_ConvC,sC);

% definition of event 2 C2
sC.time = .25;
sC.data(idx.enable_cvtr_intfc) = 1;
ts_ConvC = addsample(ts_ConvC,sC);


%% Converter D1
% definition of event 1 D1
sD.time = 0.01;
sD.data(idx.enable_SVPWM_intfc) = 1;
sD.data(idx.enable_PLL_intfc) = 1;
```

```
sD.data(idx.enable_PQ_ctrl_intfc) = 1;
sD.data(idx.P_ref)=-800e6;
sD.data(idx.Q_ref)=0;
sD.data(idx.cntcr_ctrl_intfc) = 1;
ts_ConvD = addsample(ts_ConvD,sD);

% definition of event 2 D1
sD.time = 0.2;
sD.data(idx.enable_cvtr_intfc) = 1;
ts_ConvD = addsample(ts_ConvD,sD);


%% Converter F1
% definition of event 1 F1
sF.time = 0.01;
sF.data(idx.enable_SVPWM_intfc) = 1;
sF.data(idx.enable_PLL_intfc) = 1;
sF.data(idx.enable_Vdc_ctrl_intfc) = 1;
sF.data(idx.Vdc_ref) = 204.6e3;
ts_ConvF = addsample(ts_ConvF,sF);

% definition of event 2 F1
sF.time = 0.45;
sF.data(idx.enable_cvtr_intfc) = 1;
ts_ConvF = addsample(ts_ConvF,sF);


%% Converter B3
% definition of event 1 B3
sJ.time = 0.01;
sJ.data(idx.enable_SVPWM_intfc) = 1;
sJ.data(idx.enable_PLL_intfc) = 1;
sJ.data(idx.enable_PQ_ctrl_intfc) = 1;
sJ.data(idx.P_ref)=400e6;
sJ.data(idx.Q_ref)=0;
sJ.data(idx.cntcr_ctrl_intfc) = 1;
ts_ConvJ = addsample(ts_ConvJ,sJ);

% definition of event 2 B3
sJ.time = 0.5;
sJ.data(idx.enable_cvtr_intfc) = 1;
ts_ConvJ = addsample(ts_ConvJ,sJ);


%% Events
% definition of event 1 E
sE.time = 0.01;
sE.data(idxE.SW1) = 1; % close breaker 1
ts_Events = addsample(ts_Events,sE);

%% END

% resample timeseries using uniform time with timestep Ts, start Tstart and
end Tend
if Ts>0
```

```
    time = 0:Ts:ts_ConvA.Time(end);
    ts_ConvA = resample(ts_ConvA,time,'zoh');
    time = 0:Ts:ts_ConvB.Time(end);
    ts_ConvB = resample(ts_ConvB,time,'zoh');
    time = 0:Ts:ts_ConvC.Time(end);
    ts_ConvC = resample(ts_ConvC,time,'zoh');
    time = 0:Ts:ts_ConvD.Time(end);
    ts_ConvD = resample(ts_ConvD,time,'zoh');
    time = 0:Ts:ts_ConvF.Time(end);
    ts_ConvF = resample(ts_ConvF,time,'zoh');
    time = 0:Ts:ts_ConvG.Time(end);
    ts_ConvG = resample(ts_ConvG,time,'zoh');
    time = 0:Ts:ts_ConvH.Time(end);
    ts_ConvH = resample(ts_ConvH,time,'zoh');
    time = 0:Ts:ts_ConvJ.Time(end);
    ts_ConvJ = resample(ts_ConvJ,time,'zoh');
    time = 0:Ts:ts_ConvK.Time(end);
    ts_ConvK = resample(ts_ConvK,time,'zoh');
    time = 0:Ts:ts_Events.Time(end);
    ts_Events = resample(ts_Events,time,'zoh');
    time = 0:Ts:ts_Secondary_control.Time(end);
    ts_Secondary_control = resample(ts_Secondary_control,time,'zoh');
end

if savemat==1
    % save ts to mat files
    mtx_A = [ts_ConvA.Time, ts_ConvA.Data];
    mtx_B = [ts_ConvB.Time, ts_ConvB.Data];
    mtx_C = [ts_ConvC.Time, ts_ConvC.Data];
    mtx_D = [ts_ConvD.Time, ts_ConvD.Data];
    mtx_F = [ts_ConvF.Time, ts_ConvF.Data];
    mtx_G = [ts_ConvG.Time, ts_ConvG.Data];
    mtx_H = [ts_ConvH.Time, ts_ConvH.Data];
    mtx_J = [ts_ConvJ.Time, ts_ConvJ.Data];
    mtx_K = [ts_ConvK.Time, ts_ConvK.Data];
    mtx_E = [ts_Events.Time, ts_Events.Data];
    mtx_SC = [ts_Secondary_control.Time, ts_Secondary_control.Data];

    mtx_AA = mtx_A'; %#ok<NASGU>
    mtx_BB = mtx_B'; %#ok<NASGU>
    mtx_CC = mtx_C'; %#ok<NASGU>
    mtx_DD = mtx_D'; %#ok<NASGU>
    mtx_FF = mtx_F'; %#ok<NASGU>
    mtx_GG = mtx_G'; %#ok<NASGU>
    mtx_HH = mtx_H'; %#ok<NASGU>
    mtx_JJ = mtx_J'; %#ok<NASGU>
    mtx_KK = mtx_K'; %#ok<NASGU>
    mtx_EE = mtx_E'; %#ok<NASGU>
    mtx_SCSC = mtx_SC'; %#ok<NASGU>

    save('Scenario_ConvA.mat','mtx_AA','-v4');
    save('Scenario_ConvB.mat','mtx_BB','-v4');
    save('Scenario_ConvC.mat','mtx_CC','-v4');
    save('Scenario_ConvD.mat','mtx_DD','-v4');
    save('Scenario_ConvF.mat','mtx_FF','-v4');
    save('Scenario_ConvG.mat','mtx_GG','-v4');
```

```
    save('Scenario_ConvH.mat','mtx_HH','-v4');
    save('Scenario_ConvJ.mat','mtx_JJ','-v4');
    save('Scenario_ConvK.mat','mtx_KK','-v4');
    save('Scenario_Events.mat','mtx_EE','-v4');
    save('Scenario_Secondary_control.mat','mtx_SCSC','-v4');

    varargout = [];
else
    varargout = {ts_ConvA ts_ConvB ts_ConvC ts_ConvD ts_ConvF ts_ConvG
ts_ConvH ts_ConvJ ts_ConvK ts_Events ts_Secondary_control idx idxE idxSC};
%#ok<EMCA>
end
```